Force Amplitude Modulation of Tongue and Hand Movements

By

Angela M. Dietsch

Submitted to the graduate degree program in the Department of Speech-Language-Hearing: Sciences and Disorders and the Graduate Faculty of the University of Kansas in partial fulfillment of the requirements for the degree of Doctor of Philosophy.

_____
Jeffrey P. Searl, Ph.D., Chairperson

Committee members*

_____
Jeffrey M. Burns, M.D., M.S. *

_____
Carmen M. Cirstea, M.D., Ph.D. *

_____
Susan T. Jackson, Ph.D. *

_____
John A. Stanford, Ph.D. *

Date Defended: August 23, 2011

The Dissertation Committee for Angela M. Dietsch

certifies that this is the approved version of the following dissertation:

Force Amplitude Modulation of Tongue and Hand Movements

_____

Jeffrey P. Searl, Ph.D., Chairperson

Date approved: August 23, 2011

Force Amplitude Modulation of Tongue and Hand Movements

Angela M. Dietsch

Abstract.

Rapid, precise movements of the hand and tongue are necessary to complete a wide range of tasks in everyday life. However, the understanding of normal neural control of force production is limited, particularly for the tongue. Functional neuroimaging studies of incremental hand pressure production in healthy adults revealed scaled activations in the basal ganglia, but no imaging studies of tongue force regulation have been reported. The purposes of this study were (1) to identify the neural substrates controlling tongue force for speech and nonspeech tasks, (2) to determine which activations scaled to the magnitude of force produced, and (3) to assess whether positional modifications influenced maximum pressures and accuracy of pressure target matching for hand and tongue movements. Healthy older adults compressed small plastic bulbs in the oral cavity (for speech and nonspeech tasks) and in the hand at specified fractions of maximum voluntary contraction while magnetic resonance images were acquired. Volume of interest analysis at individual and group levels outlined a network of neural substrates controlling tongue speech and nonspeech movements. Repeated measures analysis revealed differences in percentage signal change and activation volume across task and effort level in some brain regions. Actual pressures and the accuracy of pressure matching were influenced by effort level in all tasks and body position in the hand squeeze task. The current results can serve as a basis of comparison for tongue movement control in individuals with neurological disease. Group differences in motor control mechanisms may help explain differential response of limb and tongue movements to medical interventions (as occurs in Parkinson disease) and ultimately may lead to more focused intervention for dysarthria in several conditions such as PD.

ACKNOWLEDGEMENTS

The process of preparing this dissertation has been an extraordinary journey both professionally and personally. Of the many people who have been enormously helpful along the way, I am especially thankful to my advisor, Dr. Jeff Searl, whose patience and mentorship throughout my doctoral program has been invaluable. I could not have hoped for a better model of scientific discipline, inspired teaching, and professional/personal life balance.

I am indebted to my committee members Drs. Carmen Cirstea, Jeff Burns, John Stanford, and Susan Jackson for their support and expertise. They challenged me to accept nothing but my best efforts at every stage of the dissertation process. In addition, Dr. Cirstea generously shared equipment and MR expertise that were vital to data collection and analysis.

Very special recognition goes to Dr. Ed Auer, Jr. who invested many hours training me in the intricacies of MRI research design and analysis, and to Dr. Bill Brooks who sponsored scanner time for this study and provided insightful feedback to refine my scientific writing skills.

I warmly acknowledge the faculty and staff in the department of Hearing & Speech and at the Hoglund Brain Imaging Center for their generosity in sharing their technical abilities, knowledge, and moral support. I fully appreciate how lucky I have been to work amongst friends who coordinated many details and tolerated my interminable questions with grace and cheer.

Profound appreciation goes to the network of friends and family who have saved me many times over with encouraging messages and babysitting time. At long last, I have come to accept that I cannot do everything myself, and I am so grateful for the safety net they provide. I cannot imagine how we would have survived without their help. My parents' absolute faith that this project would eventually be completed was a bright light on some dark nights.

I wasn't a mother when this study began, but Ellena has turned me into one along the way. I am so glad that she is here now, and there is nothing in my life, related to this dissertation or not, for which I am more grateful. While she has been a tremendous inspiration to me, many of the long work hours would have been much more joyfully spent with her. I can only hope that she will understand and forgive those lost moments as her own intensely inquisitive nature continues to develop.

TABLE OF CONTENTS

LIST OF TABLES

LIST OF FIGURES

LIST OF ABBREVIATIONS

%SC	percent signal change
2D	two-dimensional
A1	primary auditory cortex
ANOVA	analysis of variance
BG	basal ganglia
BOLD	blood-oxygen-level-dependent
CB	cerebellum
CBF	cerebral blood flow
CBV	cerebral blood volume
CVA	clustered volume acquisition
DA	dopamine/dopaminergic
fMRI	functional magnetic resonance imaging
GABA	gamma-Aminobutyric acid
GLM	general linear model
GPe	globus pallidus externa
GPi	globus pallidus interna
HDR	hemodynamic response
IWPD	individuals with Parkinson disease
kPa	kilopascals
M1	primary motor cortex
MR/MRI	magnetic resonance/magnetic resonance imaging
MVC	maximum voluntary contraction

N	Newton
PD	Parkinson disease
PET	positron emission tomography
PMA	premotor area
P_{max}	maximum pressure
psi	pounds/inch^2
RFX	random effects analysis
ROI	region(s) of interest
S1	primary somatosensory cortex
SA	somatosensory association area
SMA	supplementary motor area
SNc	substantia nigra pars compacta
SNr	substantia nigra reticulate
SNR	signal-to-noise ratio
SOE	sense of effort
SPM	statistical parametric map
STS	sparse temporal sampling
TE	echo time
TR	repetition time
V1	primary visual cortex
V3	visual association area
VA	ventroanterior nucleus of thalamus
VL	ventral lateral nucleus of thalamus

VOI	volumes of interest
VPl	lateral ventroposterior nucleus of thalamus
VPm	medial ventroposterior nucleus of thalamus

1.0 INTRODUCTION

To complete everyday tasks for self-care and communication, thousands of rapid, precisely controlled movements are performed reliably and regularly by manual and orolingual musculature. In humans, articulators must be able to traverse exact distances at sufficient speeds to produce intelligible speech, and even slight imprecision in movement is perceived as abnormal by listeners (Carroll & Sanchez-Ramos, 2011; Kent, Duffy, Slama, Kent, & Clift, 2001; Vul, Harris, Winkielman, & Pashler, 2009). Beyond absolute strength, the fine control of force is necessary to accelerate and decelerate the articulators for precise contacts and releases. Similar exactitude is required in manual tasks such as grasping objects or opening a door. Motor control theory offers a framework for our understanding of how the central nervous system and muscles interact to perform such movements (Feldman, 2008; Latash, Levin, Scholz, & Schoner, 2010; Warren, 2006), and the behavioral characteristics of force regulation have been studied in healthy humans as well as those with movement disorders such as Parkinson disease (Crow & Ship, 1996; Robin, Goel, Somodi, & Luschei, 1992; Solomon, Robin, & Luschei, 2000). Lesion studies in animal models using comparable skilled behaviors have allowed investigators to infer some basic information about the neurological correlates of force regulation (Bethel-Brown, Morris, & Stanford, 2011; Ciucci & Connor, 2009; Skitek, Fowler, & Tessel, 1999).

Functional neuroimaging offers opportunities to define more precisely the neurological bases that regulate force for hand and orolingual movements. To date, limited studies focusing on manual grip behaviors have noted that basal ganglia (BG) activations consistently appear to scale in correlation to incremental hand pressure production (Spraker, Yu, Corcos, & Vaillancourt, 2007; Sterr et al., 2009; Vaillancourt, Mayka, Thulborn, & Corcos, 2004; Ward, Swayne, & Newton, 2008; Wasson, Prodoehl, Coombes, Corcos, & Vaillancourt, 2010). This

suggests that the BG might have a key role in the force modulation of hand movements. However, no imaging studies of tongue force regulation have been reported, and only early preliminary data regarding brainstem involvement in tongue control is available (Estep, 2009). Control of tongue movements is supported by a more extensive cortico-pallido-bulbar network than hand movements (Allison, Meador, Loring, Figueroa, & Wright, 2000; Riecker et al., 2005), so lingual force modulation may be regulated by different mechanisms in the BG and other areas compared to hand force control. The current study aims to distinguish the neural networks controlling force production for both the tongue and the hand in healthy older adults.

Once a better understanding of the neural mechanisms underlying normal speech movements is acquired, subsequent lines of investigation can aggressively probe how and why Parkinson disease (PD) and other movement disorders differentially affect limb and tongue movements. Defining normal control circuitry in the proposed study will serve as the basis for comparison in future investigations of BG disease processes with a goal of refining and/or designing targeted interventions to improve the speech of individuals with PD (IWPD).

2.0 BACKGROUND AND SIGNIFICANCE

2.1 *Human Force Regulation in Normal Conditions*

2.1.1 Manual Force Control

The relationship between targeted and actual force and pressure production in the hand movements of healthy humans has been studied as part of force control. Maximum pressure (P_{max}) of hand squeeze in young adults has been documented in the range of 140-170 kilopascals (kPa; Crow & Ship, 1996; Luschei, 2009; Robin, et al., 1992). A statistically significant reduction in P_{max} has been reported by age 60 years, with an average P_{max} range of 127-137 kPa in several studies using the same hand squeeze device (Crow & Ship, 1996; O'Day, Frank, Montgomery, Nichols, & McDade, 2005; Solomon, et al., 2000). Somodi, Robin, and Luschei (1995) compared perceived and actual pressures generated at various target percentages of subjects' P_{max} for subjects 17 to 50 years of age. They noted that subjects were more accurate at the extremes of their pressure range. That is, when asked to produce 10% or 90% of their P_{max} they generally were able to do so with high accuracy. In contrast, subjects were less accurate in producing targeted pressures in the mid portion of their hand pressure range. A study by Lafargue and colleagues of eight healthy adults ranging in age from 36-81 years revealed that estimations of the effort required to produce a target pressure were strongly correlated to the actual pressures generated (Lafargue, D'Amico, Thobois, Broussolle, & Sirigu, 2008). Healthy adults exhibit remarkable precision in the amount of pressure produced during specific tasks across the lifespan although some changes in maximum hand pressure generation and control are noted with healthy older adults.

2.1.2 Orolingual Force Control

2.1.2.1 Nonspeech tasks. Control of orolingual movements for nonspeech tasks (e.g., pressing, tip elevation, swallowing) has proven different from that of hand control in a number of respects. One main difference is in the basic strength of articulators relative to the hand. Average P_{max} for lingual press tasks as measured by compression of a polymer air-filled bulb during anterior tongue elevation is typically documented in the range of 65-75 kPa for healthy adults 20-40 years of age (Crow & Ship, 1996; Luschei, 2009; Solomon & Munson, 2004), less than half of hand P_{max}. Maximum lingual pressures begin to decline by age 80, a full two decades later than significant reductions in P_{max} for the hand (Crow & Ship, 1996; Youmans, Youmans, & Stierwalt, 2009). The relative preservation of tongue strength may be due to differences in the types of muscle fiber inherent to tongue versus hand muscles, to the relatively consistent demands of tongue activity across the lifespan, and to other as-yet-undefined factors. Both lingual P_{max} and tongue-to-palate pressure during swallowing appear to decrease with advanced age. Because both decrease, older individuals use a percentage of the maximum range during swallowing that is similar to younger speakers. Proportionally, older subjects are still working at approximately the same point within their physiological range as younger subjects, thus maintaining a similar percentage of reserve lingual strength for swallowing throughout the lifespan (Youmans, et al., 2009).

In addition to differences in maximum pressure produced by the tongue and hand, accuracy of pressure generation between the two structures may differ. Somodi et al. (1995) asked subjects to protrude the tongue at specified percentages of their lingual P_{max}; the actual lingual pressure generated was measured and compared to the requested level to assess accuracy of pressure generation. They found that subjects were more accurate in producing targeted

pressures at the extremes of their lingual P_{max} range. The authors speculated that because speech occurs at a relatively low percentage of maximum tongue pressure (15-20%) and a high sense of effort is required at the upper margins of tongue strength, calibration may be enhanced at these extremes (Somodi, et al., 1995). This finding for the tongue was similar to what Somodi et al. reported for the hand, although there was greater discrepancy between targeted and actual pressures for the tongue compared to the hand. This led the authors to conclude that the tongue was less sensitive in terms of force regulation than the hand. This may reflect the relatively smaller cortical representation of the orolingual structures compared to the hand in the human homunculus (Somodi, et al., 1995).

2.1.2.2 Speech tasks. Lingual force and pressure during speech has been less thoroughly investigated than during nonspeech tasks for various reasons. First, speech is a low-effort, low-force task and so measurement of lingual P_{max} has not been of significant interest to investigators. Although the maximum force of the tongue is approximately 15-22 newtons (N), only about 2 N of force are estimated to be necessary to produce normal speech (Kent, Kent, & Rosenbek, 1987). Luschei (1991) argued that such measures are taken as the articulatory movements are being terminated at the contact point, and thus underestimate the amount of tongue strength necessary for stabilization and quick initiation of articulatory movements. A second reason for lack of information about lingual force control during speech relates to technical difficulties in obtaining measures during speech. Intra-oral placement of force transducers with appropriate physical and response characteristics has been challenging because of the delicate nature of articulatory movements that are easily perturbed. This has forced investigators to measure contact pressures between the tongue and palate or between the lips during articulation that Luschei accurately described as only reflecting one portion of movement during consonant or

vowel production (i.e., at contact point termination). Using contact point pressure measurements, Searl (2007) and Gozee, Murdoch and Theodoros (2002) reported that during individual consonant production, normal adults generated ~8% of labial P_{max}, which is consistent with the speech force estimates projected by Kent et al (1987).

The limited magnitude of articulatory contact pressure that has been reported for non-disordered speakers is consistent with the general perception of speech as non-effortful by the talker. Healthy adults consistently rated everyday speech as requiring 'no particular effort' on a direct magnitude estimation scale (Solomon & Robin, 2005), indicating that they do not have conscious awareness of any force requirements during typical speech. Only when individuals are asked to exceed typical speech demands (e.g., loud, prolonged voice use) has a sense of effort been reported (Kelchner, Toner, & Lee, 2006; Laukkanen, Ilomaki, Leppanen, & Vilkman, 2008). The orolingual muscles appear to be well designed for the low-force, high-repetition demands of speech.

2.1.3 Role of Visual Feedback in Force Control

A significant body of research has shown that force control is more accurate when real-time visual feedback is provided (Baweja, Patel, Martinkewiz, Vu, & Christou, 2009; Gentil & Tournier, 1998; Luschei, 1991; Robin, Somodi, & Luschei, 1991; Solomon, Drager, & Luschei, 2002). This appears to be true for the hand as well as the tongue. In studies using the same device for sustained tongue and hand presses, healthy young adults 19-40 years of age were able to match and maintain pressures for over three times the duration when visual feedback was provided compared to pressures obtained without visual feedback (Robin, et al., 1991; Solomon, et al., 2002). Similarly, subjects performing a sustained pressure task displayed nearly twice the deviation from target finger pressure when visual feedback was removed (Baweja, et al., 2009).

Although these findings are not necessarily surprising, Slifkin and peers' (2000) study of finger force control suggested that there are limits in the central nervous system's ability to fine-tune the accuracy of manual force regulation. They found that while the motor system appears to generate target-matching corrections approximately once per second, the accuracy peaked when visual feedback was provided at 6.4 Hz and did not improve with more rapid feedback. Further, in a functional magnetic resonance imaging (fMRI) study, force production was actually less accurate and visuomotor network activations were elevated when feedback was graphed at a greater frequency with more detail (Sterr, et al., 2009). These data underscore that force production is more accurate when visual feedback is available, but too much information can overwhelm the system and become detrimental to the overall accuracy of force production.

2.1.4 Motor Control Theory, Sense of Effort, and Motivation in Force Control

Theories of motor control have attempted to explain how the central nervous system regulates movement in a neuromuscular system with many more degrees of freedom than are needed for a particular task (Latash, et al., 2010). Behavior patterns are learned as the agent gains awareness of both its environment and the impact of its movement on the environment (Feldman, 2008). The force, rate, and trajectory of the pattern are adjusted in reference to the particular target rather than the starting point, and afferent feedback is used to further refine the movement and expand the pattern (Feldman, 2008). The uncontrolled manifold theory postulates that task-relevant direction in joints and muscles are relatively confined by the motor plan, but the plan allows other factors to vary. For example, the flexion of the fingers and angle of the wrist may be dictated in a hand squeeze task, but the motor plan does not place particular requirements on the relative position of the elbow joint or rotation of the arm. Those components are allowed to adjust as needed to minimize the relative effort of the task and to maintain as much equilibrium

as possible in joints while still completing the target behavior (Latash, et al., 2010). With practice, the motor plan becomes more stable and requires less effort to execute.

To be effective, the "normal" motor plan must also be flexible enough to accommodate a variety of internal and external factors (Warren, 2006). Some of these factors are invariable, like the threshold position within a joint that determines whether a particular muscle is active or inactive. Others, such as neuromuscular disease, may change over time but are consistent enough to be accommodated as the motor plan is repeated within the new parameters (Latash, et al., 2010). Differences in intrinsic factors such as tissue histology may influence how a particular motor plan is executed in one body part versus another, especially with regard to endurance and relative effort across tasks. The tongue, for example, has a disproportionately greater number of type IIA fibers compared to the hand, whose muscles contain predominantly fatigue-resistant type I fibers (Gentil & Tournier, 1998; Kent, 2004; Wohlert & Smith, 1998). A series of studies by Solomon and colleagues revealed that the time constant for sustained fractions of P_{max} was less for the tongue than for the hand across all subjects (Solomon, 2000, 2004; Solomon, et al., 2002; Solomon, Robin, Mitchinson, VanDaele, & Luschei, 1996). In other words, they found that the lingual musculature fatigued more quickly than the hand during a comparable squeeze task, and that subjects experienced an increased perception of effort in attempting to maintain the tongue contraction compared to that of the hand. The orolingual system appears to be taxed more quickly at higher percentages of P_{max}, and centrally-generated motor signals have proportionally less speed and amplitude as the system fatigues (Bennett, van Lieshout, & Steele, 2007). The motor control paradigm integrates many variables into a schema that can adapt to these factors and perform consistently.

Despite their relative stability, motor control plans are being executed by living organisms, so fatigue and motivation also can influence pressure and force control. The term 'behavioral economics' refers to the cost-reward balance that drives activity choices in humans and animals (Salamone, 2009). The perceived effort of executing a particular motor program is weighed against the motivation to achieve the associated benefit or reward. Within the neurological system, the cortico-striato-pallidal loop and the neurotransmitter dopamine (DA) in particular appear to have specific roles in regulating effort-related decisions (Nunes et al., 2010; Salamone et al., 2009). In humans, researchers can assess not just performance, but also the internal perception of effort associated with various tasks. Sense of effort (SOE) appears to be a combination of (1) intrinsic physical and cognitive factors such as muscle fatigue, baseline strength, and attention, and (2) extrinsic task demands including required speed, external force, momentum, and perception of task difficulty (Dickerson, Martin, & Chaffin, 2007; Feldman, 2008). Differences in BG circuitry for distinct body regions, such as hand versus tongue movements, are not yet understood adequately to explain their role in these endurance and SOE variances.

The DA pathways also have been shown to play a role in learning new motor behaviors (Salamone, Correa, Farrar, Nunes, & Pardo, 2009). Conscious learning of a force task (i.e. developing and stabilizing a motor plan) required increased activation of brain areas such as the posterior insula, anterior cingulate cortex, and somatosensory areas that were less involved in kinematic learning or simple force production (de Graaf et al., 2004). The taxing of additional resources also may increase the overall SOE involved in such "learning" to reproduce a specific force (de Graaf, et al., 2004). The amount of effort (and thus pressure) one is willing to exert may be more influenced by the behavioral economics of the DA pathways than by the challenges

of a particular experimental task (Dickerson, et al., 2007; Feldman, 2008; Salamone, Correa, et al., 2009). Furthermore, the emerging importance of these pathways in regulating effort and force informs the understanding of the clinical effects of conditions such as PD.

2.2 *Relevant Neural Networks in Force Control*

2.2.1 Neural Bases of Manual Force Regulation

To date, neuroimaging research regarding force regulation in humans has focused on hand movements. fMRI studies have provided critical data regarding the neural areas and circuits responsible for generating and regulating these hand gestures. The BG, key cortical areas (such as the primary motor cortex and somatosensory cortex), thalamus, and cerebellum are organized somatotopically. Multiple pathways function in parallel to initiate and refine voluntary movements with specific rate and force parameters, and to inhibit involuntary movements that might interfere with the intended outcome (Figure 1 outlines these pathways). Different tasks elicit slightly different activation patterns; only, areas that show increased activation in multiple studies are included in this summary (Keisker, Hepp-Reymond, Blickenstorfer, Meyer, & Kollias, 2009; Spraker, et al., 2007; Sterr, et al., 2009; Vaillancourt, et al., 2004; Ward, et al., 2008; Wasson, et al., 2010).

2.2.1.1 Basal Ganglia. The basal ganglia are a group of subcortical nuclei located at the base of the forebrain and are part of the cortico-striato-pallido-thalamo-cortical pathway (Kandel, Schwartz, & Jessell, 2000; Mink, 2003). Within this complex feed-forward loop for action selection and motor control, the BG use two channels to regulate inhibitory control over movements. The striatum (composed of the caudate nucleus, putamen, and ventral striatum) receives excitatory glutaminergic input from the cerebral cortex as well as excitatory and

inhibitory DA input from the substantia nigra pars compacta (SNc). Some information is routed via "direct" inhibitory gamma-Aminobutyric acid (GABA) channels to the internal segment of the globus pallidus (GPi) and substantia nigra reticulata (SNr; Hikosaka, 2007). A second "indirect" pathway within the BG sends inhibitory GABAergic signals from the striatum into the external segment of the globus pallidus (GPe). Then the subthalamic nucleus (STN) combines the GPe's inhibitory GABAergic input with excitatory glutaminergic inputs from the cortex and thalamus, eventually providing excitatory input to the GPi and SNr. The GPi and SNr integrate the excitatory input from the indirect pathway with the inhibitory signals from the direct pathway, ultimately resulting in inhibitory signals to the ventrolateral thalamus (see Section 2.2.1.3). Disruptions to the BG system can affect both voluntary and involuntary movements. For example, decreased DA input to the striatum because of SNc destruction in PD causes inhibition of the direct pathway (which facilitates movement) and excitation of the indirect pathway (which inhibits movement), resulting in symptoms of hypokinesis and rigidity (Ho, Iansek, Marigliani, Bradshaw, & Gates, 1998; Ramig, Fox, & Sapir, 2008). Damage at the level of the striatum, as with Huntington disease and other disorders, has opposite effects on the direct and indirect pathways and yields symptoms of hyperkinesis and chorea (Benjamin, 1997; Giannakopoulou, Armata, Mitsacos, Shashidharan, & Giompres, 2010). Additionally, Lafargue and colleagues theorized that PD disrupts the integration of afferent and efferent information within the cortical-BG loop that is crucial for internal SOE, force regulation, and timing (Lafargue, et al., 2008). In previous fMRI studies of hand movement, BG areas of activation include the GPi, GPe, STN, caudate nucleus, and putamen (Keisker, et al., 2009; Spraker, et al., 2007; Sterr, et al., 2009; Vaillancourt, et al., 2004; Ward, et al., 2008; Wasson, et al., 2010).

Figure 1. *Overview of Key Feed-Forward Loops in Motor Processing.* The two tracts operate simultaneously to contribute to the regulation of motor behaviors. The cortico-striato-pallido-thalamo-cortical tract appears to be primarily concerned with force regulation, whereas the cortico-ponto-cerebello-dentato-thalamo-cortical tract is implicated in the control of rate. Laterality notes refer to a right hand squeeze, though information about speech processing is also included. Line weights reflect relative contributions. CB = cerebellum, M1 = primary motor cortex, PMA = premotor cortex, S1 = primary somatosensory cortex, SA = somatosensory association cortex, SMA = supplementary motor cortex, SNc = substantia nigra pars compacta SNr = substantia nigra reticulata VL = ventral lateral nucleus of thalamus, VPm = medial ventroposterior nucleus of thalamus

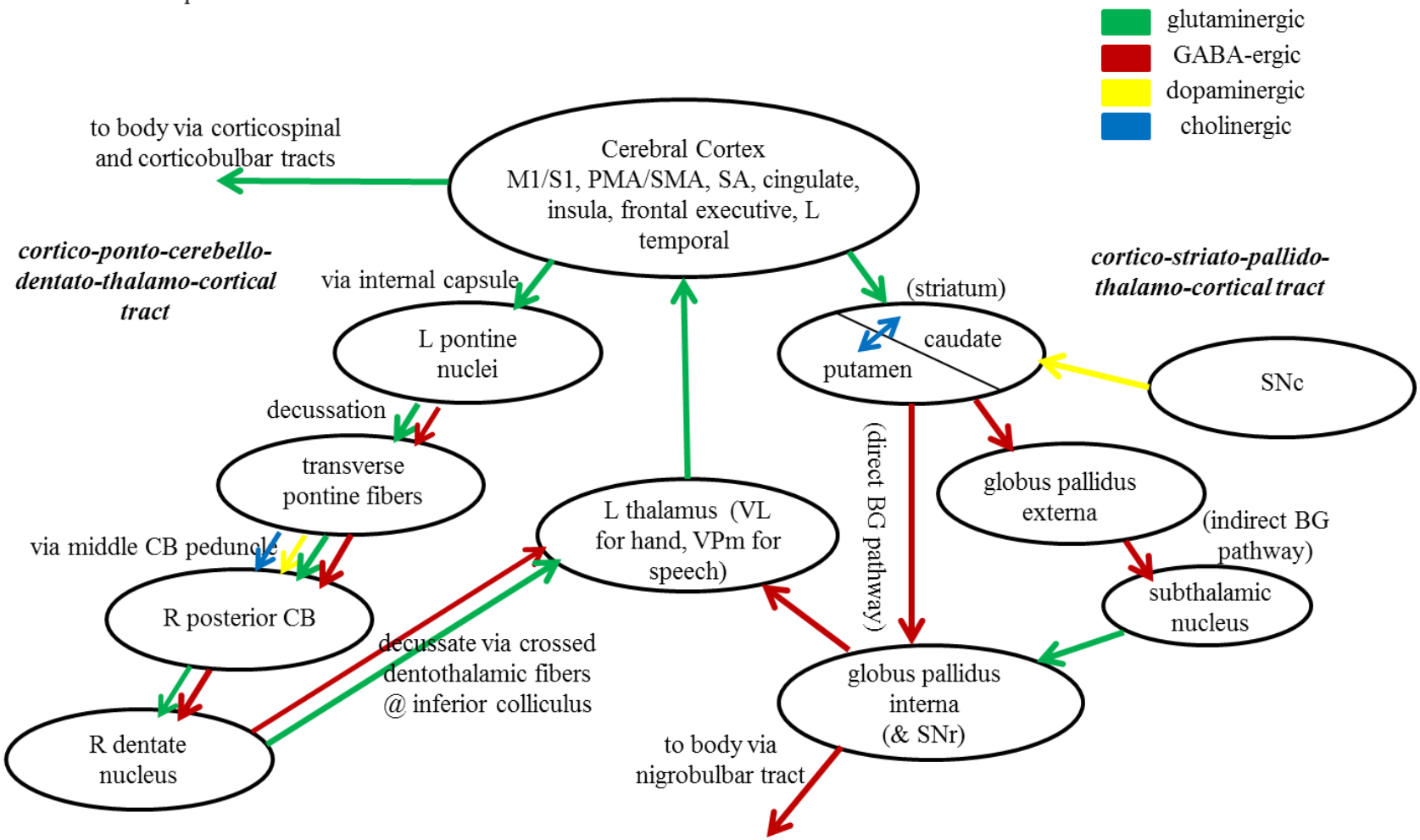

2.2.1.2 Cerebral cortex. Areas within the bilateral frontal, temporal, and parietal lobes communicate with each other to plan, initiate, execute, and refine voluntary movements (Kandel, et al., 2000). Integration of perceptual information from the body is an important component in these processes. In previous fMRI studies of finger tapping and hand gripping at various rates and effort levels, activations contralateral to the tested hand were identified in the ventral and dorsolateral premotor cortex (PMA), primary motor area (M1), somatosensory cortex (S1), pre-supplementary motor area (preSMA), insula, and supplementary motor areas (SMA) as well as portions of the parietal lobe of that hemisphere (Ehrsson et al., 2000; Keisker, et al., 2009; Kuhtz-Buschbeck, Ehrsson, & Forssberg, 2001; Spraker, et al., 2007; Sterr, et al., 2009; Vaillancourt, et al., 2004; Ward, et al., 2008; Wasson, et al., 2010). The insula, active in some studies of hand force, appears to be involved in the perception of exertion (Fink, Frackowiak, Pietrzyk, & Passingham, 1997; Williamson, McColl, Mathews, Ginsburg, & Mitchell, 1999; Williamson et al., 2001). The supramarginal gyrus in the parietal lobe has a role in proprioception (Bodegard et al., 2003; de Vries et al., 2009).

2.2.1.3 Thalamus. The thalamus is situated between the cerebral cortex and the brainstem. It integrates inhibitory signals from the BG, sensory feedback from the body, and cerebellar inputs in preparation for movement (Kandel, et al., 2000). Although the thalamus was originally thought to serve simply as a relay station, more recent studies suggest a complex system of filtering so that only selective excitatory signals are relayed to the cortex (Lam & Sherman, 2010; Min, 2010; Wang, Webber, & Stanley, 2010). Within the thalamus, nuclei activated during hand movements include the ventrolateral (VL), ventroanterior (VA), lateral ventroposterior (VPl), medial ventroposterior (VPm), and centromedial nuclei (Ehrsson, et al., 2000; Spraker, et al., 2007; Vaillancourt, et al., 2004; Wasson, et al., 2010). The VL nucleus receives input

primarily from the dentate nucleus of the cerebellum, and projects to premotor and primary motor areas of the cortex. The VA nucleus receives input from the BG and projects to the premotor and supplemental motor areas. The VPl and VPm nuclei receive somatosensory input from the spinothalamic and trigeminothalamic tracts, respectively, and project to the inferior portion of the postcentral gyrus.

2.2.1.4 Cerebellum. The cerebellum (CB) is located inferior to the cerebral cortex and posterior to the brainstem. While the CB does not initiate movement, it appears to have important roles in stabilizing posture and muscle tone (anterior lobes, I-V) and coordinating and refining motor activity (posterior lobes, VI-X) via its connections to the brainstem and cerebral cortex (Kandel, et al., 2000). Multiple areas of the CB including lobules V, VI, and VII and the dentate nucleus are activated during various manual force tasks (Keisker, et al., 2009; Vaillancourt, et al., 2004; Ward, et al., 2008; Wasson, et al., 2010).

Only some of the above-noted areas in the BG, cortex, thalamus, and CB exhibit *scaled* levels of activation with changes in grip force. Increased grip strength was frequently coupled with increased blood-oxygen-level dependent (BOLD) activation in most areas, but regions that integrate sensorimotor feedback with motor signaling sometimes showed greater activation levels during more precise gentle grip tasks. Changes in force amplitude have been associated with scaled alterations in BOLD signaling in M1, S1, SMA, GPi, STN, VL, VA, VPl, VPm, and CB (Keisker, et al., 2009; Spraker, et al., 2007; Ward, et al., 2008; Wasson, et al., 2010).

2.2.2 Neural Bases of Orofacial and Lingual Movements

Neuroimaging studies of a variety of oral movements and speech production have helped to delineate the neural networks that control orolingual tasks. Tasks such as sucking, whistling, syllable repetition, and multisyllabic utterances have been compared to breathing to elucidate

functional control areas for such tasks (Bohland & Guenther, 2006; Dresel et al., 2005; Estep, 2009; Riecker, et al., 2005; Simonyan, Ostuni, Ludlow, & Horwitz, 2009; Soros et al., 2006; Wise, Greene, Buchel, & Scott, 1999). Orofacial movements typically are represented in both hemispheres, presumably due to the midline location and bilateral innervation tracts of the relevant structures (Muellbacher, Artner, & Mamoli, 1999; Murphy et al., 1997; Riecker, et al., 2005), although some studies suggest a left lateralization effect in speech tasks (Ghosh, Tourville, & Guenther, 2008; Malandraki, Sutton, Perlman, & Karampinos, 2009; Simonyan, et al., 2009). Some differences in activation have been noted in nonspeech versus speech tasks, but many areas are implicated in both types of behavior.

2.2.2.1 Basal Ganglia. Functional imaging studies of orofacial movements and speech tasks have consistently shown increased BOLD signaling in the GPe and putamen. Activation in the caudate nuclei was detected only for multisyllabic word production compared to vowel production, consistent with its assumed role in higher-level motor control and learning (Bohland & Guenther, 2006; Dresel, et al., 2005; Estep, 2009; Riecker, et al., 2005; Simonyan, et al., 2009; Soros, et al., 2006; Wise, et al., 1999). Studies of individuals with and without neurological disorders such as PD support an alteration in normal behavioral economics when the BG system is disrupted (Nunes, et al., 2010; Salamone, Farrar, et al., 2009). Generally, healthy adults and individuals with PD have comparable lingual P_{max} and contact pressures for speech, but IWPD report a greater SOE compared to their healthy peers (McAuliffe, Ward, Murdoch, & Farrell, 2005; Solomon & Robin, 2005; Somodi, et al., 1995). The increased BOLD activations during more complex speech tasks coupled with the increased sense of speech effort reported by individuals with BG disorders reinforce that the BG has a role in modulating the effort "cost" of motor activities.

2.2.2.2 Cerebral cortex. Bilateral activations have been consistently noted across orolingual tasks in M1, PMA, S1, the secondary somatosensory cortex , SMA, cingulate motor area, and insula (associated with self-awareness of movements). Training effects in the SMA have been noted after one hour of tongue protrusion tasks (Arima et al., 2011). Activations in the occipital and right temporal lobes (visual and auditory cortices, respectively) were attributed to processing of the visual prompts, auditory self-monitoring, and phonological processing during overt whistling/speech tasks (Bohland & Guenther, 2006; Chang, Kenney, Loucks, Poletto, & Ludlow, 2009; Dresel, et al., 2005; Estep, 2009; Riecker, et al., 2005; Simonyan, et al., 2009; Soros, et al., 2006; Wise, et al., 1999).

2.2.2.3 Thalamus. The VL, VPm (topographically associated with orofacial musculature), and the medial dorsal (believed to play a role in memory) nuclei are activated during oromotor tasks (Bohland & Guenther, 2006; Dresel, et al., 2005; Estep, 2009; Riecker, et al., 2005; Simonyan, et al., 2009; Soros, et al., 2006).

2.2.2.4 Amygdala. The amygdalae are nuclei located in the medial aspect of the temporal lobe. Part of the limbic system, they are involved in emotional learning and memory and also serve as relay stations for impulses for the facial and trigeminal nerves. Bilateral amygdala activation was described only during whistling tasks (Dresel, et al., 2005).

2.2.2.5 Cerebellum. Activations were noted in lateral and rostral paravermal areas typically associated with tongue and lip movements including lobules VI, VIII, and IX. BOLD signal was increased during multisyllabic utterances compared to monosyllables or simple oral movements (Bohland & Guenther, 2006; Dresel, et al., 2005; Estep, 2009; Riecker, et al., 2005; Simonyan, et al., 2009; Soros, et al., 2006; Wise, et al., 1999).

2.2.2.6 Brainstem. The brainstem contains the nuclei of cranial nerves III-XII as well as multiple

central pattern generators. Respectively, these areas are responsible for motor and sensory innervation to orofacial (and other) musculature, and for the regulation of respiration and other automated orofacial movements. The red nucleus in the rostral midbrain is thought to be involved in motor coordination, postural control, and somatosensory processing. Although many neuroimaging studies have not included the brainstem as part of the scanning field, activations have been detected in the pontomedullary junction (cranial nerve nuclei) and the midbrain (Dresel, et al., 2005; Estep, 2009; Simonyan, et al., 2009; Soros, et al., 2006; Wise, et al., 1999).

Since there are no published neuroimaging studies of force regulation in orolingual musculature to date, it is unclear which regions may exhibit scaled activation during such tasks. Based on evidence from hand movement studies, modulated activations in portions of the PMA/SMA, M1, S1, thalamus, BG, and CB that are normally involved in orolingual movements (as described above) might be expected.

2.3 *Functional Imaging and Orolingual Movements*

2.3.1 Challenges Inherent to Imaging of Orolingual Movements

Functional MRI is a useful tool for assessing the neurological networks that underlie motor behaviors, despite certain limitations. For example, a certain degree of variability in the fMRI signal is caused by subtle shifts in the scanner's electronics and static magnetic field. Additional noise can be attributed to physiological factors such as respiration, cardiac activity, and head or body movements. These types of noise are common to all MR image acquisition. Another source of MR noise is susceptibility effects, wherein spurious movement of tissue or air outside the area being scanned disrupts the magnetic field within the region to be imaged (Gracco, Tremblay, & Pike, 2005). Susceptibility can create movement artifacts that mimic

BOLD activation and/or that mask true BOLD signals, increasing the risk of both Type I and Type II errors (Mehta, Grabowski, Razavi, Eaton, & Bolinger, 2006; Soltysik & Hyde, 2008).

Orolingual movements for speech and swallowing can contaminate data beyond the noise that is inherent to virtually all MR imaging. Orolingual movements have been shown to cause areas of signal warping, especially in the more anterior and inferior areas of the brain such as the frontal and temporal lobes. The magnitude of this interference has been measured at 5-100% of the BOLD signal itself (Birn, Bandettini, Cox, & Shaker, 1999). Although some noise problems can be managed with scan preparation and processing corrections, susceptibility effects are difficult to correct using post-hoc procedures.

To avoid the confounding factors associated with speech movements, early fMRI speech investigators tended to use "silent" speech tasks rather than overt speech (Birn, et al., 1999; Birn, Cox, & Bandettini, 2004; Huang, Carr, & Cao, 2002). Although some theorized that actual speech production would generally equate to the BOLD signal identified in "silent" speech plus activations in the motor cortex, positron emission tomography (PET) scanning studies revealed that overt speech involved more complex neural interactions (Birn, et al., 1999; Huang, et al., 2002). In addition to increased motor cortex activations, overt speech tasks involve auditory and somatosensory feedback loops and a number of subcortical regions (Chang, Kenney, Loucks, & Ludlow, 2009). Since covert or imagined execution during fMRI is inadequate to delineate the full network responsible for motor tasks, researchers have tested a number of options to control for the signal noise resulting from orolingual movements.

2.3.2 Prospective Options for Overcoming Motion Artifact

Careful positioning, training, and online movement tracking can limit the amount of movement that occurs during all types of MR scanning. Depending on voxel size, small amounts

of translational and rotational head movement are typically considered acceptable because they do not exceed voxel boundaries and can be corrected during data processing (Field, Yen, Burdette, & Elster, 2000; Kemeny, Ye, Birn, & Braun, 2005; Mehta, Verber, Wieser, Schmit, & Schindler-Ivens, 2009). Head restraints such as foam padding, memory foam pillows, and straps may be employed during MR scans to reduce head movements (Brown et al., 2009; Gracco, et al., 2005; Mehta, et al., 2009; Soros et al., 2008). Pre-scan training sessions have proven useful to familiarize participants with the positioning, confined space, and target behaviors of the scanning protocol in hopes of decreasing extraneous motion (Brown, et al., 2009; Huang, et al., 2002; Mehta, et al., 2009). Subject preparation offers practical and effective strategies for limiting the small head movements that are common during neuroimaging procedures.

Design approaches to address susceptibility artifacts were adapted from strategies to better assess auditory neurophysiology. Subjects in MR regularly wear earplugs to attenuate scanner noise levels to tolerable levels, but the loud clicks and beeps associated with moments of image acquisition in a traditional block design contaminated all subsequent volumes of the auditory pathway imaging attempts (Edmister, Talavage, Ledden, & Weisskoff, 1999; Hall et al., 1999; Okada & Nakai, 2003). Investigators found that these disturbances could be avoided with an event-related paradigm, which exploits the lag in hemodynamic response (HDR) to auditory stimuli (Birn, et al., 1999). Clustered volume acquisition (CVA) confines the collection of multiple images to the end of a brief stimulus block, allowing the HDR to the intended stimulus to have peaked by the time of the first volume while avoiding any HDR to the associated scanner noise (Edmister, et al., 1999). Sparse temporal sampling (STS) acquires a single brain volume at the beginning of each 12-second (for example) block. This image effectively captures the HDR to the previous epoch's stimulus or rest condition. The length of each block must be calculated to

capture the peak of the HDR. Like CVA, this method has proven effective at eliminating scanner noise interference since the image acquisition occurs before any HDR to the scanner noise peaks. The STS data have been associated with greater effect size, signal intensity, and signal-to-noise ratio (SNR) than CVA. This is because each volume captures only peak BOLD activation, and the timing differences in echo time and repetition time (TE and TR, respectively) allow complete relaxation of the spins between each volume (Hall, et al., 1999; Okada & Nakai, 2003; Zaehle et al., 2007). Compared to CVA, however, STS yields significantly fewer volumes in the same total scan time, which limits STS's statistical power (Nebel et al., 2005; Okada & Nakai, 2003; Zaehle, et al., 2007). Early testing of oral motor tasks compared continuous image acquisition during blocks of activity versus a single performance of the target activity, and found that the single trial model avoided motion susceptibility problems for all speech, swallowing, lingual, and jaw movements tested (Birn, et al., 1999). These studies were the foundation for effective neuroimaging of orolingual behaviors.

Sparse temporal sampling is now commonly used to minimize movement artifact and auditory pathway confounds in studies of speech production and speech processing, though researchers continue to investigate methods for refining imaging techniques and extending task duration (Chang, Kenney, Loucks, & Ludlow, 2009; Gracco, et al., 2005; Soros, et al., 2006). Examination of simple and complex speech tasks and visual tasks has led investigators to use an optimal duration of approximately 5 seconds between the stimulus cue and the middle of image acquisition in order to capture peak HDR (Nebel, et al., 2005; Soros, et al., 2006). Voxel size and slice orientation for fMRI of vowel production was explored by Soltysik and Hyde (2008), who identified that 2 x 2 x 3 mm voxels yielded the highest true-positive ratio of BOLD activation.

This data provided important parameters for designing study protocols that maximize both signal detection and efficiency.

2.3.3 Retrospective Options for Overcoming Motion Artifact

Pre-processing of the fMRI data may include a number of steps to correct for motion noise. Coregistration involves the realignment of successive images to a reference image, usually the first volume of the series (Huang, et al., 2002; Huettel, Song, & McCarthy, 2004). To perform the coregistration function, most fMRI software packages offer algorithms that assume a two-dimensional (2D) rigid-body transformation, meaning that the size and shape of the two 2D slices to be realigned are identical (Costagli, Waggoner, Ueno, Tanaka, & Cheng, 2009; Riecker, Kassubek, Groschel, Grodd, & Ackermann, 2006; Soros, et al., 2008). In addition to coregistration, spatial interpolation is used to estimate BOLD intensity at a location that was not originally sampled, such as for reconstructing data after the coregistration has been completed (Huettel, et al., 2004). Filtering removes any low frequency scanner drift or artifact from respirations or cardiac activity. Spatial interpolation and filtering functions are included in most fMRI processing software packages. One study compared various orderings of multiple correction strategies and asserted that realignment coregistration followed by filtering and then interpolation algorithms was most effective at minimizing movement artifact while preserving data integrity (Jones, Bandettini, & Birn, 2008). Spatial smoothing is another component of motion correction, in which the intensity of a particular voxel is statistically distributed to adjacent voxels. Smoothing decreases the number of independent comparisons required in analysis, increasing both SNR and power but also decreasing the anatomical precision of the resulting image (Huang, et al., 2002; Huettel, et al., 2004; Lindquist, 2008; Zaehle, et al., 2007). Functional-structural coregistration and normalization procedures map the fMRI data onto a

structural scan of the subject's brain, and then to standardized brain space so that it can be compared to other subjects (Huang, et al., 2002; Huettel, et al., 2004). All of these preprocessing strategies provide some degree of motion correction, but at a cost with regard to the spatial and temporal resolution of the final fMRI images.

After preprocessing, statistical analysis is completed for individual subjects' and/or grouped data. During this stage, the time course statistics for each voxel are compiled into an HDR tracing. Then this tracing is compared to a model of the expected HDR signal from an active voxel, which is derived from the study design. The fMRI software evaluates how well the actual HDR shape matches the expected model using one of several statistical options (such as the general linear model), and the resulting value represents the intensity level that is reflected in color fMRI maps.

2.4 *Aging and Functional Magnetic Resonance Imaging*

Much of the extant fMRI literature has utilized young adults as subjects, presumably because it is a readily available population on university campuses where this type of research is most common. However, given the long range objectives of this line of research on tongue force in PD and other neurological diseases, the age of the subjects (controls as well as experimental) must be considered. Well-documented age-related changes in the brain have been detected as early as age 40 and could have an impact on fMRI signals (Lu et al., 2004; Raz et al., 2005) . A brief review of the important age changes that may be of importance is offered here.

2.4.1 Challenges Inherent to Imaging in Normal Aging and Disease

Research has confirmed a variety of structural and functional changes in the brain that are associated with age. Gray matter, which is comprised of the outermost layers of neurons where

neural processing occurs, has been shown to decrease in volume with age (Bangen et al., 2009; Honea et al., 2009; Raz, et al., 2005). Since BOLD signaling is an indirect measure in that it reflects changes in blood flow to regions of increased neural activity, any differences in CBF influence BOLD signaling (Bangen, et al., 2009; Huettel, et al., 2004; Leenders et al., 1990). PET studies have shown declines in CBF, cerebral blood volume (CBV), and cerebral metabolic rates with advancing age (Leenders, et al., 1990; Marchal et al., 1992; Martin, Friston, Colebatch, & Frackowiak, 1991). Atherosclerosis, a narrowing and stiffening of blood vessels that occurs more often in older individuals, may contribute to the changes in CBF and CBV because small decreases in the compliance and diameter of the blood vessels lead to dramatic increases in the resistance to flow rate. Diseases that are common in aging, such as diabetes, hypertension, and hyperlipidemia, increase the risk for occlusive vascular disorders. Since they are not neurologically based, these diseases are not typically part of the exclusion criteria for neuroimaging studies and thus inadvertently may be a factor in the CBF and CBV reductions that are often reported (Cools, Miyakawa, Sheridan, & D'Esposito, 2010; D'Esposito, Deouell, & Gazzaley, 2003; Hughes, Barker, Owen, & Rowe, 2010). In aggregate, these age-related differences point to disparate metabolic demands and hemodynamic responsiveness between older and younger brains. Additionally, factors such as exercise and general brain chemistry may create additional variability within a similar-aged subject pool even when specific disease processes are not a factor. For example, older adults who exercised regularly appeared to mitigate atrophy in the temporal and parietal cortices, and had greater CBF than those who did not (Colcombe et al., 2003; Honea, et al., 2009; Pereira et al., 2007). These changes directly affect the relationship between neuronal activity and the HDR that underlies BOLD signaling.

Functional MRI data reflect age-related neurovascular changes in several general trends. Healthy older subjects typically exhibit decreased intensity of BOLD signal in active voxels compared to younger subjects (Rajah & D'Esposito, 2005; Riecker et al., 2003). This could be an artifact of the lower SNR that has been consistently reported in older subjects, in that it is more difficult to detect a statistically significant signal in a noisy image background (D'Esposito, Zarahn, Aguirre, & Rypma, 1999; Rajah & D'Esposito, 2005; Riecker, et al., 2003). Another area of age-related neurovascular change is related to the volume of BOLD activation during tasks. Spatial extent of activation is frequently diminished in older subjects, but activation patterns sometimes reflect additional areas of BOLD signal compared to younger subjects (D'Esposito, et al., 1999; Malandraki, et al., 2009; Riecker, et al., 2003). There are several theories behind these equivocal patterns. The dedifferentiation theory postulates that decreased neurotransmission causes a reduction in SNR and detection of fewer distinct regions of neural activity, but the theory does not account for any increases in activation volume. The shifts also could reflect decreased lateralization of functions, wherein the role of one cortical area lessens and its contralateral compliment becomes more active. The functional compensation theory is an expansion of this idea, suggesting that areas of increased activation are attempting to compensate for areas of decreased activation elsewhere in the brain (Buckner, Snyder, Sanders, Raichle, & Morris, 2000; Hughes, et al., 2010; Rajah & D'Esposito, 2005). Results of a recent finger tapping study indicated that aged individuals who exhibited more widespread bilateral activations in the motor areas had the quickest reaction times, tending to support the compensation theory (Hughes, et al., 2010). While further investigation of these proposals is warranted, a multitude of age-related differences in signal patterns increases the difficulty of completing fMRI research in older individuals.

2.4.2 Strategies for Overcoming Aging Confounds

A number of options have been explored for separating true activation differences from these age-related changes in neurovascular coupling. Simple design considerations can reduce the disparities. Imaging studies of neurological disease or trauma have commonly used healthy young adults as controls, likely due to convenience factors at university-based research facilities. Instead, comparison of subjects to age-matched controls highlight the activation differences caused by the pathology of interest while minimizing the effects of age-related changes (D'Esposito, et al., 2003). Imaging of the default mode network when the subject is at rest allows imagers to subsequently subtract this baseline state from activations on all intervention tasks so that changes in activation, rather than main effects, are being compared between groups (Koch et al., 2010). Finally, discrepancies in gray matter volume could skew direct comparisons in activation volume. Such disparity accounted for nearly one-third of the difference in activation volume in a recent study by Kannurpatti, Motes, Rypma, and Biswal (2010). To correct for this variance, the authors scaled all activation volumes to the mean gray matter volume across all subjects prior to comparing BOLD activation patterns. Through prudent design and analysis strategies, the confounding effects of age-related changes can be minimized in neuroimaging studies.

2.5 *Significance and Specific Aims of Current Study*

2.5.1 Significance

The overall goal of the present study is to identify the neural mechanisms underlying speech and nonspeech orolingual activity, particularly the role of the BG in modulating the force amplitude of tongue movements in healthy controls. This study provides foundational knowledge

for understanding the role of the BG and other brain areas in modulating the force amplitude of tongue movements during speech and nonspeech activity. Results of the study will help to define the neural mechanisms underlying speech production and to inform hypotheses about the impact of neurological insults on regulation and execution of tongue movements. Additionally, results from non-disordered adults in the proposed study will provide a basis for comparison in future studies of populations with BG-based disorders that affect orolingual movements for speech. For example, current understanding of the underlying neuropathology is inadequate to explain speech symptoms of PD effectively; alterations in ability to modulate the force of tongue movements in PD may be a primary contributor to articulatory alterations that can be detected perceptually, acoustically, or kinematically although this has yet to be demonstrated empirically. The age range of healthy subjects in the current study was selected because it corresponds to a significant portion of the age range of IWPD. In the future, this design protocol may be applied to subjects with PD. Information about the differences between healthy and diseased neural controls for regulating tongue movements could be useful for developing interventions to improve the speech of individuals with PD. A more detailed understanding of speech force regulation in PD could, for example, allow for more informed positioning of deep brain stimulator probes into regions most relevant for speech or to the development of pharmacologic interventions that more specifically act within regions of the BG that are heavily involved in speech force or effort regulation.

2.5.2 Specific Aims

Specific Aim #1: Describe the neural substrates involved in the control of tongue and hand force for speech and nonspeech tasks in healthy subjects 40-60 years of age. Neuroimaging data for an

age range similar to a significant portion of IWPD have been limited to date, and functional connectivity of the networks supporting such tasks has not been fully described in the literature.

Hypothesis (H_{1A}): Hand force during hand squeeze tasks is regulated by a network of neural structures including basal ganglia, primary sensorimotor cortex, premotor and supplementary motor areas, insula, cingulate, thalamus, and cerebellum.

Hypothesis (H_{1B}): Tongue force during speech and nonspeech tasks is regulated by neural structures including basal ganglia, primary sensorimotor cortex, premotor and supplementary motor areas, insula, cingulate, thalamus, and cerebellum.

Specific Aim #2: Determine neural areas with scaled magnitude of activation across multiple levels of force production for hand and tongue (nonspeech and speech) movements in healthy subjects aged 40-60 years.

Hypothesis (H_{2A}): The intensity and volume of activation in the basal ganglia, primary semsorimotor cortex, thalamus, and cerebellum will correlate positively to the magnitude of force exerted during incremental hand movements by healthy subjects.

Hypothesis (H_{2B}): The intensity and volume of activation in the basal ganglia primary sensorimotor cortex, thalamus, and cerebellum will correlate positively to the magnitude of force exerted during incremental tongue movements by healthy subjects.

Exploratory Aim: To compare the impact of upright versus supine positioning on magnitude and accuracy of force generation in healthy subjects. Pressure generation by the hand and tongue has been reported in a number of studies with subjects in an upright position, but no published research regarding tongue and hand force in the supine position required for functional

neuroimaging has been identified. These data will clarify whether changes in the posture of the body, which might influence the position of the tongue within the oral cavity, also affect tongue pressures. Such information is of importance for designing and interpreting fMRI studies involving speech and tongue movements in both normal and disordered individuals.

Hypothesis (H_{Ex}): Individuals will demonstrate similar patterns of target force production in upright and supine positions.

3.0 METHODS

3.1 *Participants*

Twelve right-handed (based on the Edinburgh Handedness Inventory (Oldfield, 1971), average score +85.6) healthy adults between 40 and 60 years of age (mean age 51.4 years; females 52.9, males 49.4 years) were enrolled from volunteer pools at the University of Kansas Medical Center via recruitment posters and e-mails within the community. This range was selected because it corresponds to a large portion of the age range of IWPD, a population that is likely to be targeted using a similar study protocol in future years. The subject pool included seven females and five males. Participants were screened to ensure (i) functional hearing and English proficiency for conversational exchanges and (ii) normal speech and oral motor function (per self-report and investigator observation). Potential subjects were excluded for: (i) MRI contra-indications such as implanted metals or claustrophobia as per the screening form used at Hoglund Brain Imaging Center; (ii) prior surgery on the brain, hand, or vocal tract (other than routine dental procedures); and (iii) central or peripheral nervous system disease or injury that might perturb hand, speech, or voice function.

All subjects provided written informed consent to participate in the study after reviewing verbal and written details regarding the purpose, duration, and nature of the study. The study was approved by the Human Subjects Committee at the University of Kansas Medical Center (HSC #12105).

3.2 *Instrumentation*

Air-filled polymer bulbs (Iowa Oral Performance Instrument; IOPI Medical, Washington) designed specifically to measure tongue-palate and hand-squeeze pressures during force tasks

were utilized. The tongue bulb was placed lengthwise in midline on the anterior hard palate of the oral cavity just posterior to the alveolar ridge, at the typical point of contact for the speech sound tested, /t/. The incisors rested lightly on the attached tubing to stabilize the jaw. The hand bulb was placed in the palm of the right hand of each subject, with fingers wrapped around the bulb but not pressing into it, as per manufacturer's specifications (Luschei, 2009). The IOPI has been tested and utilized in a number of studies investigating tongue function for speech purposes as well as hand data for comparative purposes (Hewitt et al., 2008; Potter & Short, 2009; Solomon, et al., 2002; Solomon & Robin, 2005; Solomon, et al., 2000). The tongue bulb measures 3 x 1.5 x 1 cm whereas the hand bulb is a 10-mL spherical water-filled rubber syringe bulb surrounding a 1-mL air-filled bulb (Solomon & Robin, 2005). The bulbs were connected to a custom-designed pressure transducer via 65 feet of 1.67 mm ID polyethylene tubing. This length of tubing was necessary in order to house the transducer outside the magnetic field, but created a relatively large volume of "dead space" within the closed bulb-tubing-transducer system. To enable measurement of small pressure changes in this system, three cubic centimeters of air were injected to create baseline pressures of approximately one pound/inch^2 (psi). The transducer recorded pneumatic pressure values (psi to the nearest thousandth) from the hand and tongue bulbs during the target tasks. Input from the transducer was transmitted to a computer running LabVIEW software (LabVIEW 7.1, National Instruments), which recorded the pressure data over time and integrated pressure feedback into the graphic display being viewed by the participant in the scanner. Figure 2 illustrates the layout of the study equipment.

This visual feedback was provided to subjects in the scanner using a standard projector/mirror configuration. Subjects were fitted with magnet-compatible corrective lenses as needed to ensure adequate visual acuity for viewing stimuli and feedback. Subjects wore

Figure 2. *Illustration of Scanner Suite and Study Equipment*. During the scanning session, the subject lies on the scanner bed and is inserted into the scanner bore from the top of the head to the shoulders. Polyethylene tubing runs from air-filled hand/tongue bulb through a port in the scanner room, then above the ceiling to a pressure transducer located in the control room . The transducer streams data to the devoted laptop, where it is integrated into the visual feedback being projected into the scanner by the LabVIEW program. Drawing is not to scale.

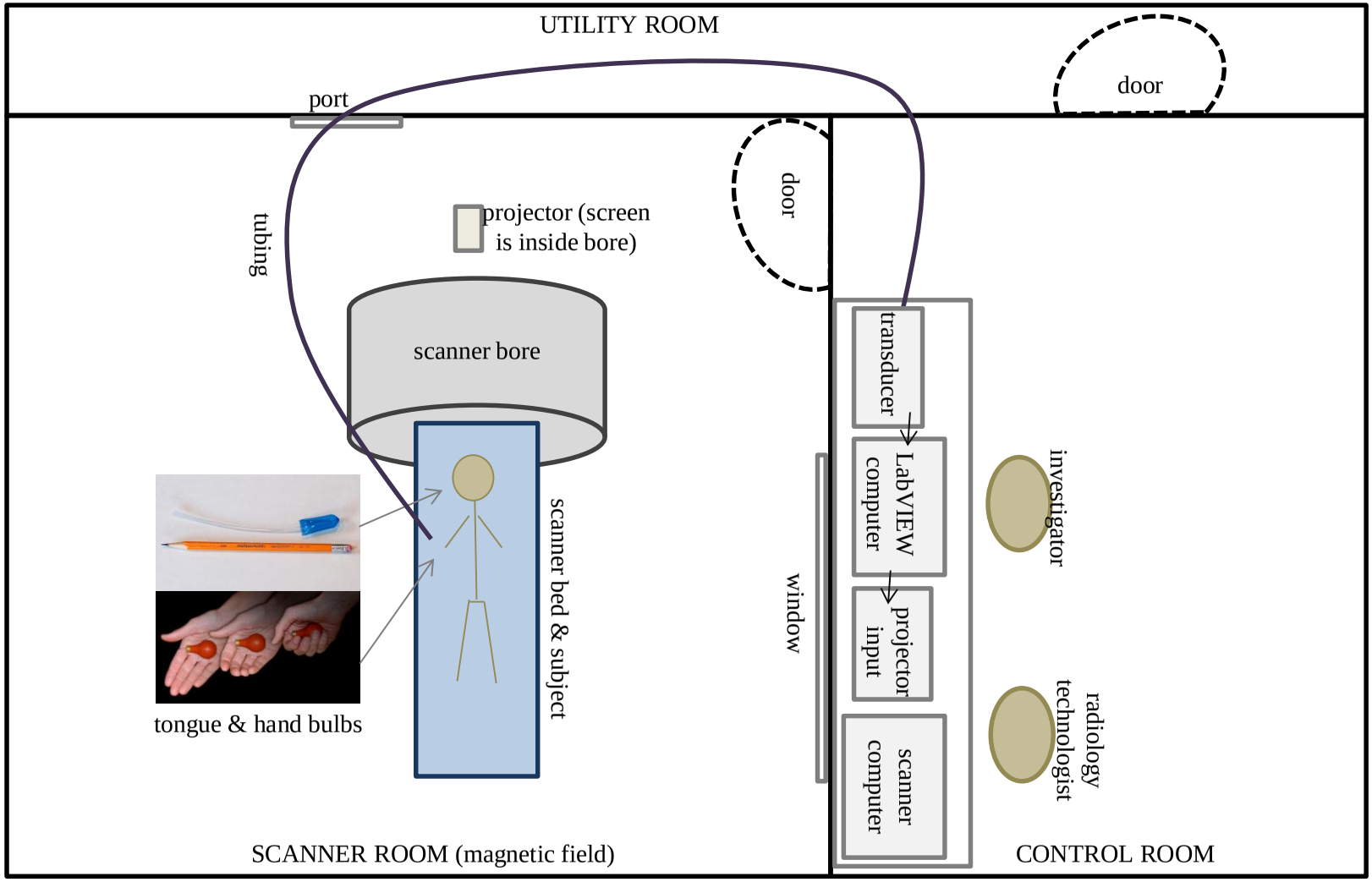

circumaural headphones with an attached microphone to allow two-way communication between the participant and investigators, and to protect the participants from scanner noise.

3.3 *Overview of Study Design and Procedures*

In the present study, fMRI was used to determine the cortical and subcortical regions involved in controlling force production for hand and orolingual movements. Targeted behaviors included hand squeeze, tongue-to-palate press, and repetition of the unvoiced phoneme /t/. These behaviors were selected because the hand squeeze task mimics those utilized in neuroimaging studies of incremental force production (Spraker, et al., 2007; Ward, et al., 2008). Further, there is a substantial pool of behavioral data for both hand and tongue press tasks in healthy subjects (Solomon & Robin, 2005; Solomon, et al., 2000; Solomon, Robin, Mitchinson, VanDaele, & Luschei, 1996), but no published neuroimaging studies regarding force control for these orolingual movements were identified. The phoneme /t/ was selected for the speech repetition task because its contact point corresponds to the optimal placement for the IOPI device, its unvoiced nature minimizes auditory feedback and sensorimotor activations associated with vocal cord vibration, and previous neuroimaging studies using repetitions of this phoneme offer comparative data (Estep, 2009; Soros, et al., 2006).

Subjects underwent six fMRI runs in a multifactorial, repeated-measures design. This allowed each subject to serve as his/her own control and reduced the impact of between-subject variability. Controlling for this variability is especially important in older adults because of age-related changes in neurovascular coupling (D'Esposito, et al., 2003), and because of potential differences in task performance (Ward, et al., 2008). Within each run, a single behavior (hand squeeze, tongue press, or phoneme repetition) was cued to prevent subject confusion and to

allow the same pressure transducer configuration to be utilized for all pressure data collection. Five repetitions of a single effort level (25%, 50%, or 75% of maximum voluntary contraction; MVC) were blocked together to facilitate accuracy of task performance. These effort level blocks were randomized across runs and subjects, controlling for order effects at both individual- and group-level analyses (additional information in Section 3.3.3).

3.3.1 Practice Sessions

Immediately prior to MRI scanning, subjects completed a training session outside the scanner room to (i) ensure task compliance; (ii) minimize learning effects within the scanner session; and (iii) obtain maximum voluntary contraction (MVC) values for each of the three tasks in both upright and supine positions (necessary for the Exploratory Aim). The oral and hand bulbs were placed as previously described. Prior to the start of the respective task trial, the subject was instructed as follows to ensure accurate task performance compared to similar studies: 1) hand squeeze - "Squeeze the bulb as hard as you can with your fist. Don't use your fingertips to press into the bulb;" 2) nonspeech tongue press - "Press forward and up against the bulb as hard as you can with the front part of your tongue;" and 3) speech - "Say /t/ over and over using as much effort as you can." Each of these instructions was followed by the general instruction: "Keep pressing [or repeating in the case of the /t/ production] until the screen tells you to stop." (Luschei, 2009; Solomon & Robin, 2005; Solomon, et al., 2000; Solomon, et al., 1996). For each task, the highest pressure produced over three trials was used as the MVC for all subsequent stimuli within LabVIEW (Solomon & Robin, 2005; Solomon, et al., 2000). The subjects completed one upright practice run for each of the three target behaviors performed during the fMRI. Verbal instructions prior to this component of training were slightly modified from those above, such as: "Press forward and up against the bulb *half* as hard as you can with

the front part of your tongue," for the 50% MVC segment (Solomon & Robin, 2005; Somodi, et al., 1995). Coinciding with these verbal instructions, the stimulus cues that were later projected into the MRI Session were viewed directly on the computer monitor during the practice session (Figure 4). The importance of remaining still within the scanning environment was emphasized during this practice session.

3.3.2 MRI Sessions

With assistance from the radiology technician, participants were positioned supine in the scanner bed. Pillows, padding, blankets, and Velcro straps were utilized to restrict limb and head movements and maximize participant comfort. The headphones (and corrective lenses, when necessary) were fitted and checked for function. After the scanner bed was positioned in the scanner, the stimulus projection was checked for comfortable viewing and subjects were re-instructed regarding the need to remain still throughout the testing. Between runs, subjects were provided with verbal encouragement and updates regarding anticipated timeframes for each component of testing. Visual prompts for the requested behaviors, target force levels, and rest were provided via the projection-mirror display. Stimulus blocks were randomized for effort level, but only one behavior was implemented within each run. Subjects were cued to perform target tasks at fractions of the supine MVC obtained during the practice session. Immediate visual feedback of actual force production was provided through the projection system.

Using a 3 Tesla Siemens Allegra scanner, the MR protocol includes (1) a whole-brain T_1-weighted structural scan [3D-MPRAGE, repetition time = 2300 ms, echo time = 3 ms, 1 x 1 x 1 mm^3 voxels, 208 slices]; (2) functional MR using sparse temporal scanning to control for movement [ten-second blocks including three seconds of data acquisition followed by seven seconds of compression, BOLD, repetition time = 10000 ms with 7000 ms delay, echo time = 30

ms, 3.75 x 3.75 x 3 mm^3 voxels and 0.5 mm gap, interslice time = 78 ms]. The LabVIEW stimulus/recording software was synchronized with the scanner sequence to ensure capture of peak HDR (Handwerker, Ollinger, & D'Esposito, 2004), and for accurate tracking of the randomized behavioral tasks. Total time in the scanner was approximately one hour per subject.

3.3.3 Stimulus Presentation

Two runs of each of the three target behaviors (hand squeeze, tongue press, and phoneme repetition) were completed. Each run contained six blocks of target behaviors, two at each level of effort (25%, 50%, and 75% of MVC). Each randomized block included five repetitions of a ten-second epoch. The epoch was comprised of three seconds of data acquisition followed by seven seconds for the behavior task (see Figure 3).

The visual cues provided to the subject included two horizontal bars representing pressure, and color-coded words to signal subjects to “Get Ready,” “Go,” and “Rest” at the timing increments described above and graphed below. The desired percentage of MVC was marked on the lower horizontal bar, and the upper bar filled from left to right to reflect the amount of pressure being produced by the subject. During the three-second periods of image acquisition, the “Rest” cue remained on the screen (see Figure 4).

Figure 3. *Overview of Time Segments in One Functional Run.* One behavioral task was performed per run, with two blocks of each effort level in randomized order. The visual prompts provided to the subjects are shown in quotations.

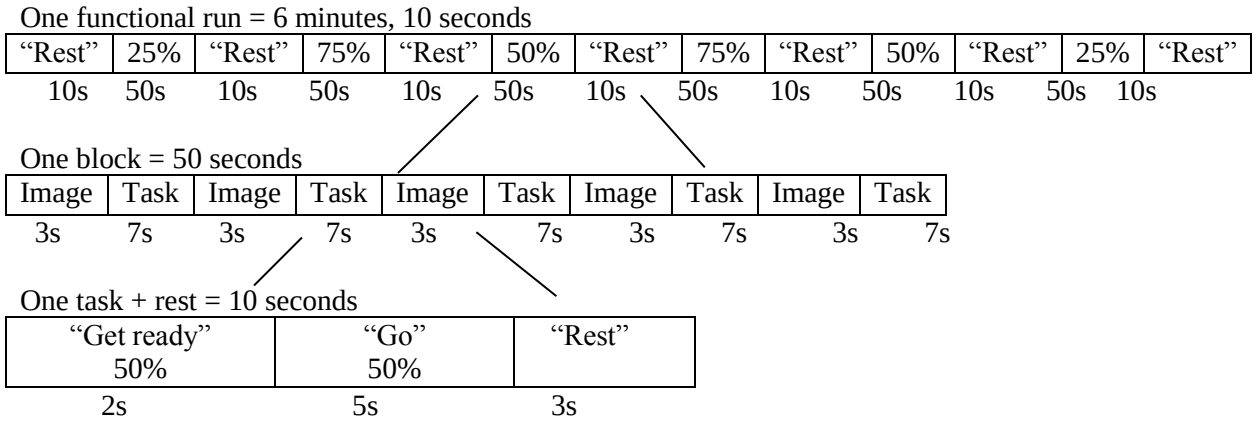

Figure 4. *Screen View of Stimulus Software.* The verbal cue varied from "rest" to "get ready" to "go" according to the time segments in the sequence. The upper bar filled from left to right, displaying the pressure being exerted by the subject. The lower bar reflected the target pressure for the current block.

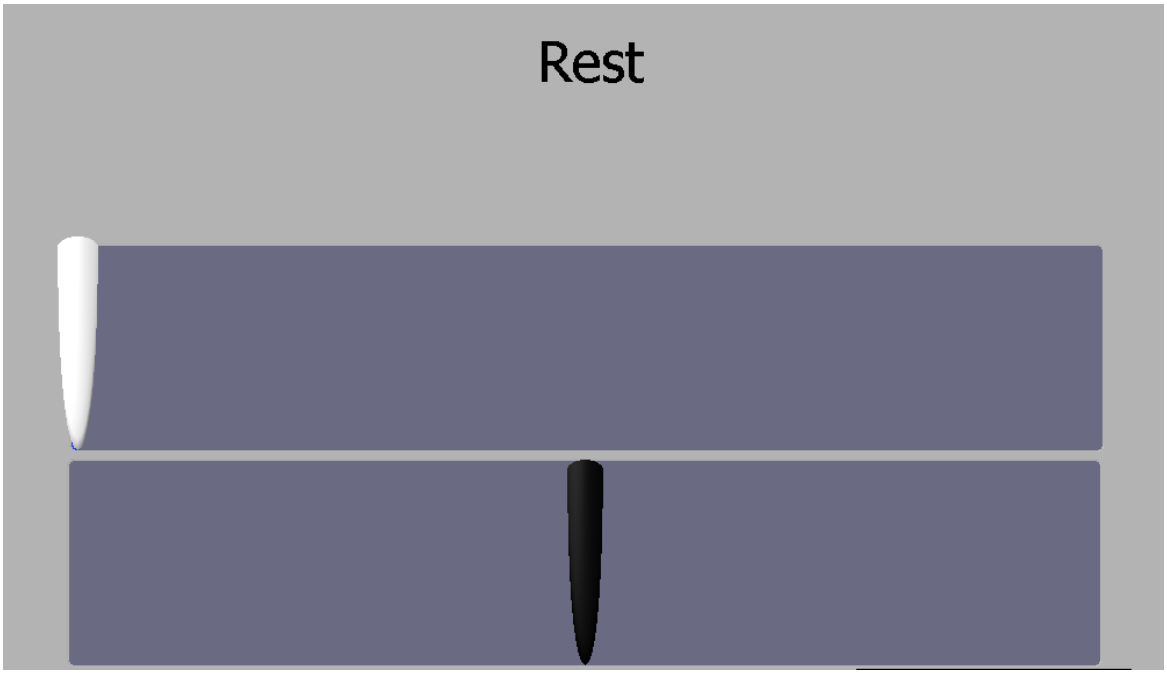

3.4 *Neuroimaging Data*

3.4.1 Processing

3.4.1.1 Preprocessing. Standard MR data processing was completed via BrainVoyager software (BrainVoyager QX 2.1.1.1542, Brain Innovation, Netherlands). Raw data were converted from DICOM format to a BrainVoyager-compatible format, and images were reconstructed from k-space. Images were screened for magnet and motion artifact prior to additional processing.

Anatomical data were isovoxel-formatted to 1 x 1 x 1 mm^3, converted to BrainVoyager standard sagittal orientation, and transformed into standardized Talairach space (Talairach & Tornoux, 1988) to allow comparisons at group level and between individual subjects (Figure 5).

Preprocessing of functional data included motion correction across six parameters (translation and rotation in each of three dimensions). Within each subject, the first volume of the first functional run of a behavior was used as the reference volume for both runs of that task. Other preprocessing steps such as temporal and spatial smoothing were avoided in order to preserve resolution for the small anatomical regions of interest (ROI) and sparse temporal sampling design (Benjamin, 1982). Movement translations and rotations during and between functional runs were assessed for shifts beyond the 3 mm voxel size in order to control for the effects of motion artifact.

3.4.1.2 Contrasts for General Linear Model. Similar to the analysis methods used by Riecker and colleagues (2006; 2005), two models of anticipated HDR patterns were created for each participant based on the randomized task sequence for each run. One protocol compared a single active vs. rest contrast, with all levels of the behavior collapsed into the active condition (25% MVC + 50% MVC + 75% MVC > rest). The other model treated each effort level as a separate condition compared to rest, producing three separate contrasts (25% MVC > rest; 50% MVC >

Figure 5. *Anatomical Images of Representative Brain.* In the upper series, a brain is shown in native space. In the lower series, the same brain image has been transformed into standard Talairach space. This transformed image served as the representative brain to which all group-level functional models were mapped.

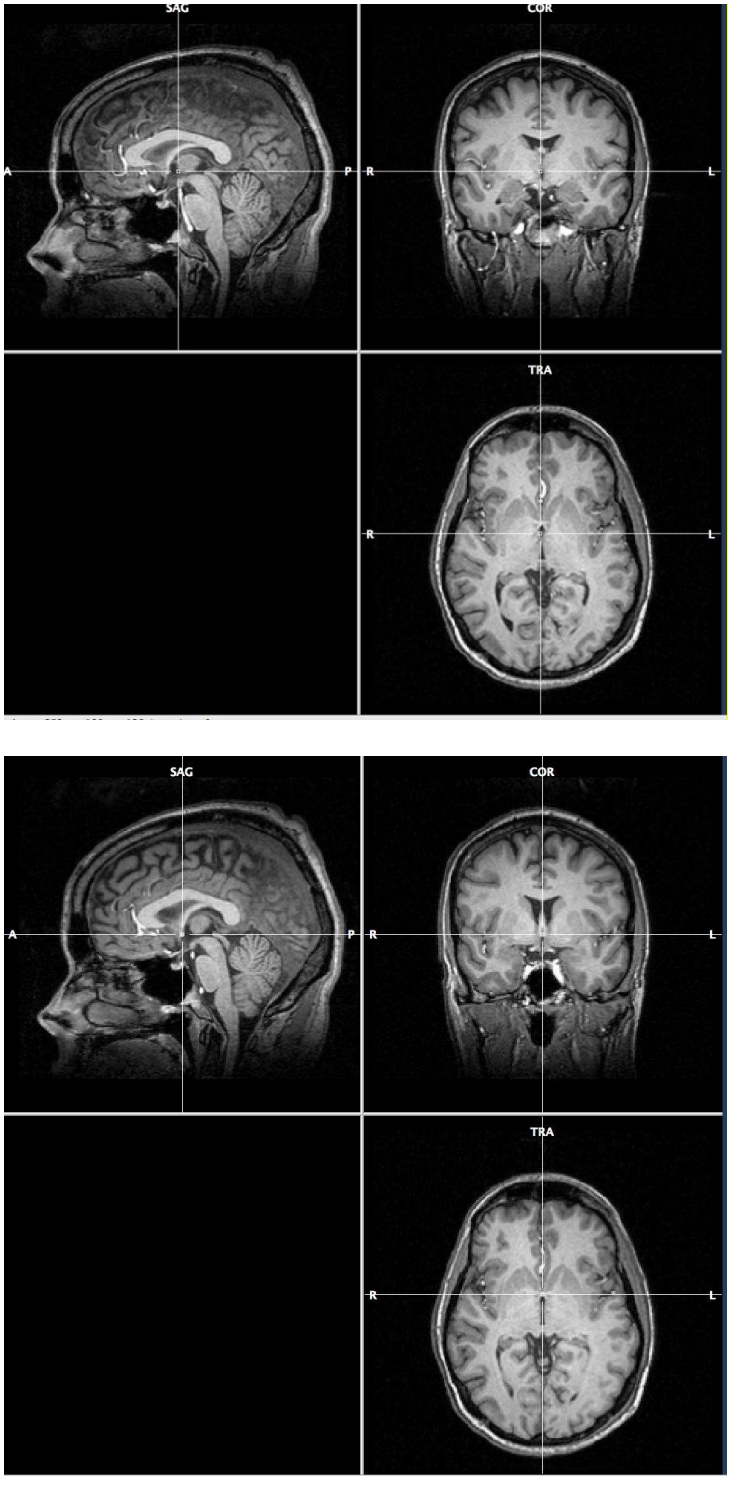

rest; 75% MVC > rest). A separate set of predictors was created for each functional run in order to accommodate the randomized sequence of effort levels within the presentation blocks. Each protocol was linked to the functional data separately, resulting in two different sets of activation statistics for each subject (unscaled and scaled) for each functional run. Each dataset was aligned with that subject's raw anatomical scan and reviewed for quality to ensure that the functional map overlapped brain tissue but not bone or cerebrospinal fluid across all planes and that there were no artifacts from motion or scanner incongruities. Then the functional data were aligned to the Talairach-transformed anatomical image using the same quality checks to allow further individual and group analyses.

3.4.2 Analysis

3.4.2.1 Group Analysis: Part I. The unscaled (active vs. rest) datasets from all subjects for a single task were combined in a multi-subject random effects general linear model (RFX GLM; 25% MVC + 50% MVC + 75% MVC > rest). RFX GLM is the standard for group-level fMRI analysis because it accounts for between-subject variability, increasing the reliability of results and allowing inferences about the population from which the sample was obtained (Friston, Holmes, Price, Buchel, & Worsley, 1999). In this analysis, the actual HDR was compared to the anticipated HDR (based on the active > rest model created for each run) for each voxel within an individual's brain volume through a series of analyses of variance (ANOVA). The resulting estimated beta weights were averaged across subjects for task and condition, and these averages were compared to the model through another GLM using one-sample t-tests for each voxel. This unscaled GLM model was superimposed onto a representative Talairach-transformed anatomical scan from one subject (Figure 5, previously referenced). A statistical parametric map (SPM) of the entire image volume was constructed to summarize the results, with the magnitude of the t-

statistics presented via color coding.

Threshold selection for SPM construction and methods of corrections for multiple comparisons have been widely debated in the literature but there is currently no consensus on best strategies (Amerman & Parnell, 1990; Lieberman & Cunningham, 2009; Poldrack & Mumford, 2009; Vul & Kanwisher, 2010). For this study, a minimum cluster threshold of five voxels and $p = 0.005$ was used for SPM mapping without further family-wise correction. This method allowed preservation of power while avoiding the risk of both Type I and Type II errors. Specifically, the probability of multiple contiguous voxels exceeding the $p = 0.005$ threshold due to random error is remote, minimizing false positive (Type I error) risk (Forman et al., 1995; Liss, Weismer, & Rosenbek, 1990). At the same time, this strategy avoids pitfalls such as biasing results toward the null hypothesis and failing to detect more subtle or complex effects of brain activity (Type II error), as occurs with the use of anatomical ROIs or Bonferroni-type corrections (Caruso, McClowry, & Max, 1997; Liss, et al., 1990). The specific p-value and minimum cluster size were selected because this combination of parameters has been shown to control for Type I errors more efficiently than a $p = 0.001$ restriction alone (Liss, et al., 1990; Torre & Barlow, 2009), while allowing detection of activations in expected areas based on previous literature despite the limited power of the dataset (Ackermann, 2008; Ackermann & Riecker, 2004; Keisker, et al., 2009; Riecker, et al., 2005; Spraker, et al., 2007).

The location and size of each area of shared activation in the resulting SPM was identified for comparison to the anticipated areas of activation for each task (H_{1A} and H_{1B}). A volumes of interest (VOI) mask was created from these grouped unscaled data at the detection parameters described above. The advantages of using VOIs from the functional mask rather than anatomically-drawn ROIs are (i) all task-relevant brain activations are evaluated instead of

limiting analysis to pre-selected areas; (ii) determination of appropriate anatomical correlates to functional brain regions has widely varying reliability across different brain areas; (iii) since VOIs include only commonly active voxels, the signal-to-noise ratio and outcome data are not diluted by the inclusion of adjacent inactive areas that may be part of a pre-drawn ROI; and (iv) drawing of anatomical ROIs based on landmarks is somewhat subjective given the wide variability in brain anatomy across subjects. The main limitations of the VOI approach are (i) some areas that are not relevant to the behavioral task of interest are likely to be included, such as the visual cortex in this study; and (ii) some general regions of activation may not be included in the VOI mask even though portions of them are active across subjects. The variability in both anatomical and functional brain regions across subjects is such that within the primary motor cortex, the area associated with right thumb movement in one subject may be slightly different from that area in another person. When their functional data are combined, there may not be adequate statistical power for either of the small individual areas within the motor cortex to exceed detection parameters for the VOI mask.

3.4.2.2 Individual Analysis. A fixed effect GLM approach was used to collapse the two functional runs of each behavior into a single dataset. Fixed effects analysis is more sensitive in detecting differences between the anticipated and actual HDR models, but its results are limited only to the subjects tested with no ability to make inferences about the general population (Friston, et al., 1999). Since the design of this study included RFX analyses before and after this fixed effects component, such inferences about its results are appropriate. Each subject's scaled functional dataset (aligned to his/her own Talairach-transformed anatomical image) was set to the same minimum cluster and p-value thresholds as described above and the group VOI mask was applied. Outcome data included percent signal change and spatial extent of activation.

Percent signal change (%SC) reflects the average change in BOLD signal intensity across all of the voxels in the VOI during the specified active condition compared to the baseline rest condition. Spatial extent of activation reflects the number of voxels within the VOI whose %SC exceeded the threshold chosen by the researcher. Although the two measures are related to each other, the relationship is indirect. To illustrate this, consider two subjects who have relatively similar increases in the %SC for a given VOI. One might have a small spatial extent of very intense BOLD activation that skews the overall average for the region, whereas the other has a larger spatial extent of voxels whose activations just exceed the intensity threshold. In this study, the reported values for each outcome represent the overlap between the individual's functional activations and the VOI from the group mask. These data were extracted for all three effort/contrast levels (25% MVC > rest; 50% MVC > rest; 75% MVC > rest) for each task within each subject.

3.4.2.3 Group Analysis: Part II. The data from the individual analysis were imported to SPSS (IBM Corporation, New York), combined, checked for normal distribution and equal variances, and transformed as necessary to meet these assumptions (see Figure 6). Repeated measures ANOVA were conducted for each VOI, outcome measure, and task, using subject as a random factor and effort level as a fixed factor to determine if scaling occurred (H_{2A} and H_{2B}). Additionally, activations were correlated across all VOIs to define functional connectivity of the regions.

Figure 6. *Raw and Transformed Data for VOI Analysis.* Spatial extent of activation data (tongue VOI 11) reveal skewed data that fail to meet assumptions of normality in the upper image. In the lower image, a square root transformation has been applied and the residuals approximate a normal distribution. The transformed data were used in subsequent statistical analyses.

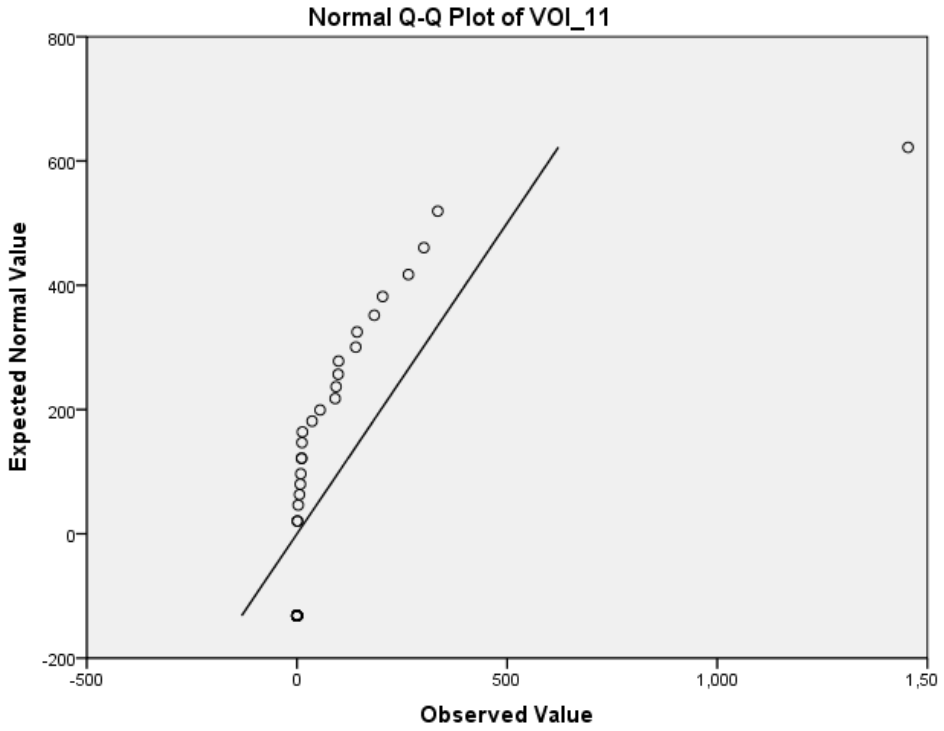

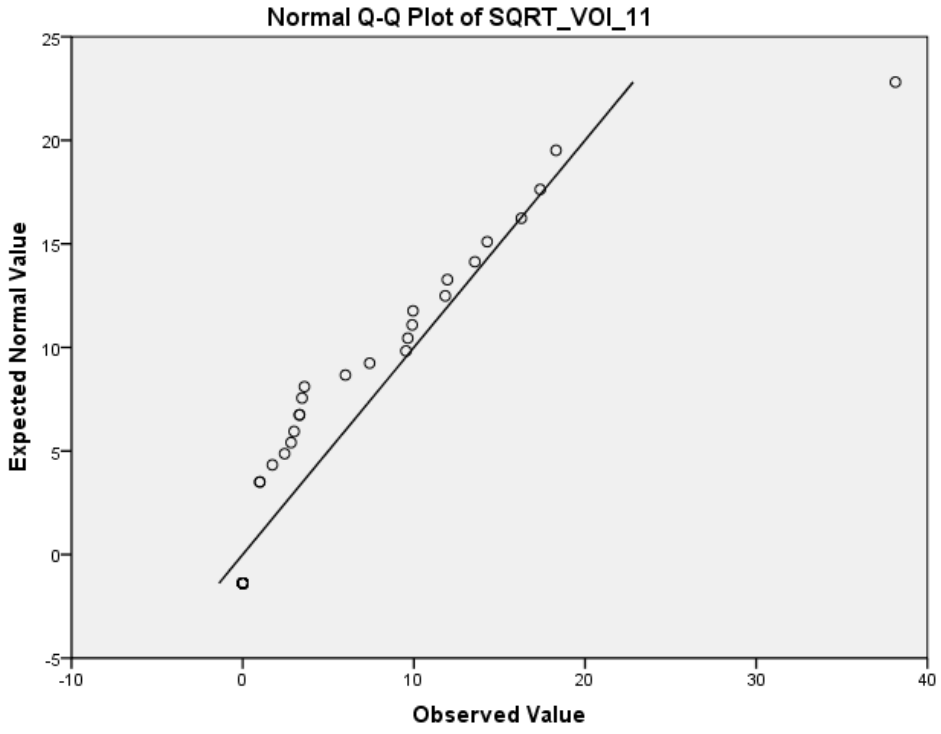

3.5 *Behavioral Data Processing & Analysis*

Values from the pressure transducer were logged by the LabVIEW software at a frequency of 10 Hz. Mean pressures were calculated with an Awk script (Bell Labs, New Jersey) that averaged pressure values across all ten of the five-second "go" blocks for each effort level within each run. Since each subject participated in two supine runs, the two means for each effort level were then averaged to yield a single value for each percent of MVC. These calculations yielded a mean actual pressure for each subject at each effort level in each position. Target pressures for each effort level were derived as percentages of the highest obtained MVC for each task and position. These values were imported to SPSS for further analysis.

As with the imaging data, assumptions of normal distribution and equal variances were confirmed before further analysis. Two-way repeated measures ANOVA with the actual pressure data for each task were used to compare pressures across effort levels (25%, 50%, 75%, and MVC), and positions (upright and supine). Task-specific three-way repeated measures ANOVA compared actual pressures to the calculated targets across fixed factors of effort level (25%, 50%, 75%) and position with subject as a random factor to inform the understanding of the relationship between generated pressures and SOE (H_{Ex}).

4.0 RESULTS

Each subject completed two functional runs of each of the three behavioral tasks. In over 90% of runs, movements were less than 1.5 mm across each of the six motion parameters. In three cases, shifts of greater than 3 mm were noted in one of the six parameters. Since these larger movements occurred between (rather than within) runs, motion correction resulted in no appreciable image shifts upon subsequent cine-loop review. Data for one run of the hand task in one subject were corrupted by stimulus software malfunction and was therefore excluded from further analysis.

4.1 *Neuroimaging Data*

4.1.1 Group Analysis: Part I

The RFX GLM created by collapsing all single-subject unscaled (active vs. rest) functional datasets resulted in one group activation map for each behavior. Creation of these group activation maps and identification of VOIs addressed Specific Aim #1 (H_{1A} and H_{1B}). The results are reported at uncorrected statistical thresholds and are discussed as preliminary findings because of the small size of the study (N = 12) and the associated limitations in statistical power.

4.1.1.1 Hand Squeeze. The group RFX GLM for the right hand squeeze task resulted in seventeen areas of activation shown in Table 1 and Figure 7. Consistent regions of activation across subjects included bilateral somatosensory and insular cortices, bilateral cerebellum, right putamen, left thalamus, left posterior cingulate cortex, and several areas within the visual cortex. All activations were positive except those in the left primary visual cortex (V1), the left somatosensory association cortex (SA), and the left visual association cortex (V3; clusters 7, 9, and 10). VOIs within the visual cortex are included in the results, but those activations were

assumed to be related to the processing of the continuous visual feedback. As such, they are not the focus of this study's findings or discussion. Of note, SPM thresholds detected a small area of shared activation within the right M1 but none in the left M1.

Table 1. *Volumes of Interest for Right Hand Squeeze.* Group mask at $p = 0.005$, minimum cluster size 5 voxels. BA = Brodmann's area, CB = cerebellum, M1 = primary motor cortex, S1 = primary somatosensory cortex, SA = somatosensory association cortex, V1 = primary visual cortex, V3 = visual association cortex, VL = ventral lateral nucleus of thalamus

Cluster	Location	BA	Talairach Coordinates	# Voxels
1	R S1	2	48 -27 31	192
2	R occipital	--	43 -63 1	580
3	R insular cortex	13	36 1 11	246
4	R anterior CB	--	21 -49 -20	1289
5	R M1	4	33 -15 51	307
6	R putamen	--	25 -3 9	150
7	L V1	17	-2 -80 13	3336
8	L posterior cingulate	31	-5 -18 48	1002
9	L SA	7	-3 -62 46	274
10	L V3	18	-9 -93 18	251
11	L VL	--	-21 -10 17	161
12	L ant CB	--	-22 -56 -21	257
13	L S1	3	-24 -33 69	161
14	L V3	18	-26 -87 4	247
15	L supramarginal	40	-38 -31 48	4278
16	L insular cortex	13	-38 -1 9	574
17	L V3	19	-44 -71 -7	258

Figure 7. *Glass Brain of Hand Squeeze Volumes of Interest.* View from left side (upper) and top (lower) of brain illustrating the seventeen VOIs resulting from the group active > rest contrast at $p = 0.005$ and minimum cluster size 5 voxels.

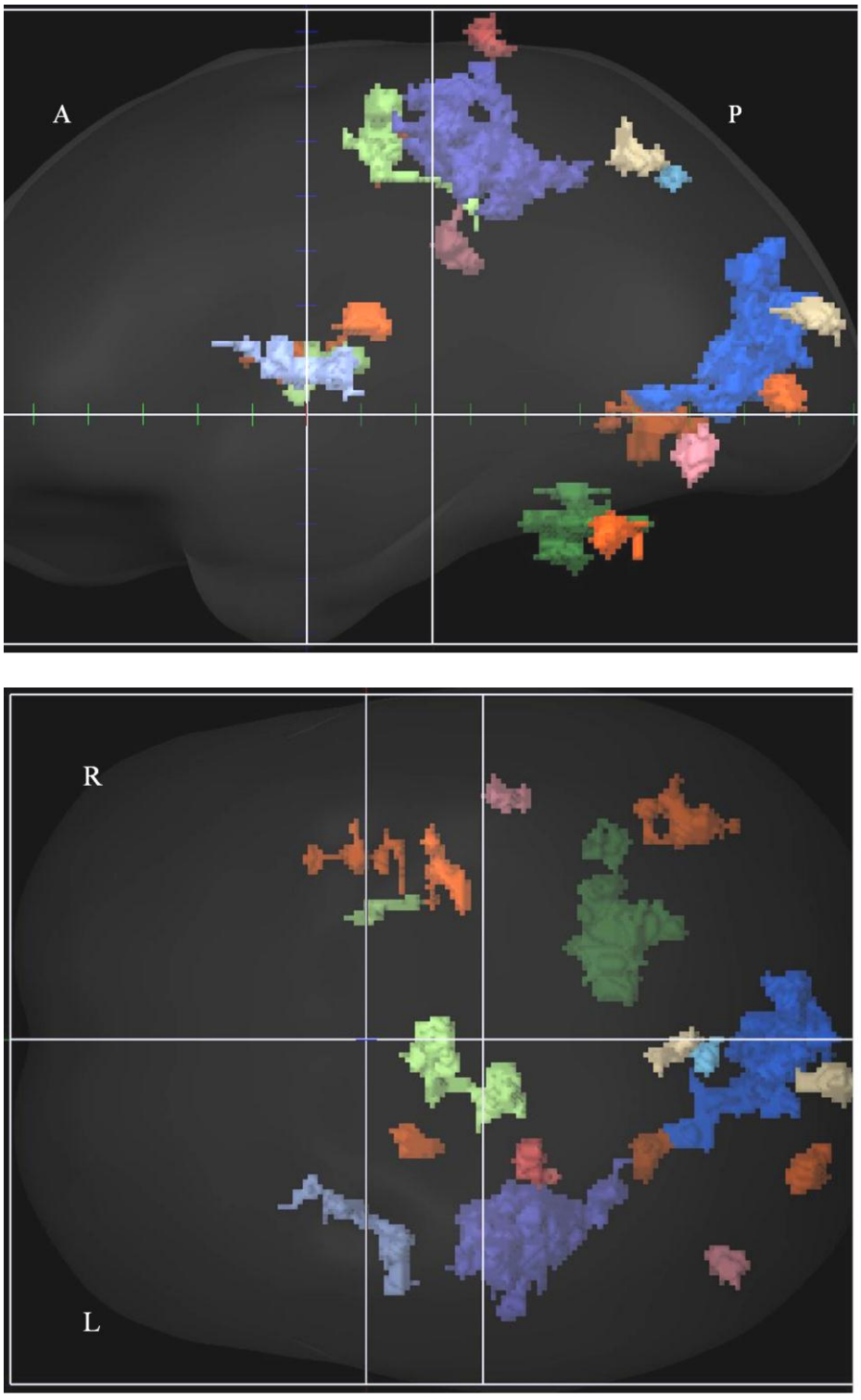

4.1.1.2 Tongue Press. As presented in Table 2 and Figure 8, thirteen clusters exceeded the threshold parameters for the group RFX GLM in the tongue press task. Positive activations occurred in the right S1, the right PMA/SMA, the right fusiform gyrus, the left putamen, and one portion of the left V3 (clusters 1, 2, 3, 12, and 13). Activations in the right putamen, left cingulate cortex, right caudate, another portion of left V3, left SA, left cingulate cortex, and left PMA/SMA were negative.

Table 2. *Volumes of Interest for Tongue Press.* Group mask at $p = 0.005$, minimum cluster size 5 voxels. BA = Brodmann's area, PMA/SMA = premotor/supplementary motor areas, S1 = primary somatosensory cortex, SA = somatosensory association cortex, V3 = visual association cortex

Cluster	Location	BA	Talairach Coordinates	# Voxels
1	R S1	2	52 -18 29	242
2	R PMA/SMA	6	52 -1 35	167
3	R fusiform	37	43 -67 1	151
4	R putamen	--	24 16 0	308
5	L posterior cingulate	30	-2 -61 7	362
6	R caudate	--	2 13 11	212
7	L V3	18	-2 -82 17	2167
8	L SA	7	-3 -66 31	247
9	L posterior cingulate	31	-4 -44 26	159
10	L anterior cingulate	32	-5 40 7	252
11	L PMA/SMA	6	-7 26 34	1454
12	L putamen	--	-29 -3 7	730
13	L V3	18	-29 -89 5	215

Figure 8. *Glass Brain of Tongue Press Volumes of Interest.* View from left side (upper) and top (lower) of brain illustrating the thirteen VOIs resulting from the group active > rest contrast at $p = 0.005$ and minimum cluster size 5 voxels.

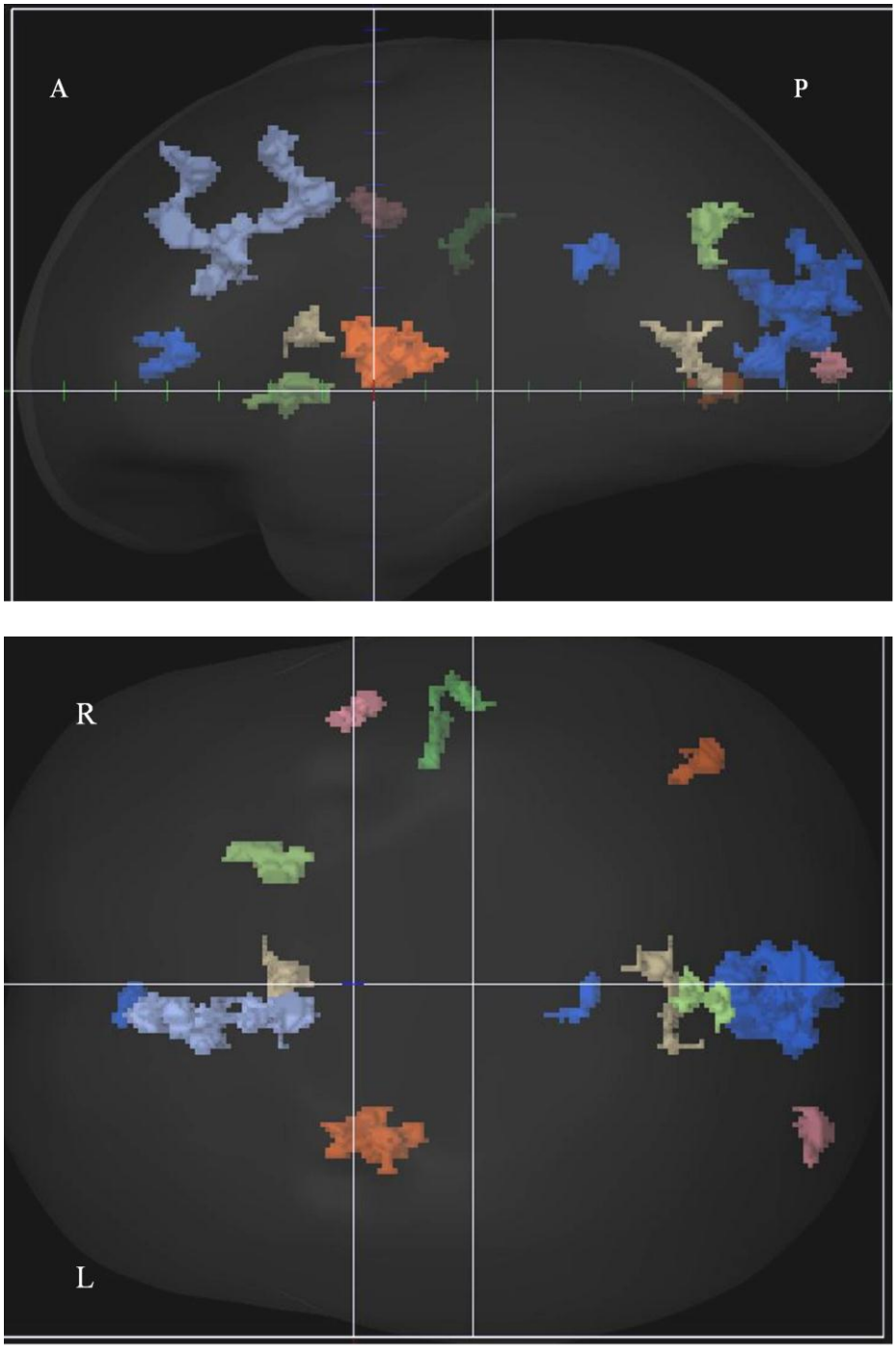

4.1.1.3 Syllable Repetition. The group RFX GLM for syllable repetition task yielded nineteen clusters of statistically significant activation shown in Table 3 and Figure 9. These included the right primary auditory and auditory association cortices (A1), bilateral PMA/SMA and CB, left somatosensory and cingulate cortices, left V3, and several areas within the frontal cortex. Activations in some left cingulate, V3, and left frontal regions were negative (clusters 8, 11, 12, 13, 14, 16, 17, and 18).

Table 3. *Volumes of Interest for Syllable Repetition.* Group mask at $p = 0.005$, minimum cluster size 5 voxels. A1 = primary auditory cortex, BA = Brodmann's area, CB = cerebellum, PMA/SMA = premotor/supplementary motor cortex, S1 = primary somatosensory cortex, V3 = visual association cortex

Cluster	Location	BA	Talairach Coordinates	# Voxels
1	R A1	41	56 -24 6	248
2	R A1	42	57 -31 15	187
3	R posterior parietal	43	52 -12 22	200
4	R PMA/SMA	6	44 -14 34	227
5	R fusiform	37	40 -63 1	139
6	R anterior CB	--	24 -56 -19	301
7	R anterior CB	--	11 -55 -22	171
8	L anterior cingulate	24	-5 33 14	4841
9	L posterior cingulate	30	-1 -50 17	171
10	L PMA/SMA	6	-1 -11 55	234
11	L posterior cingulate	31	-3 -42 41	355
12	L frontal	--	-4 -31 -36	566
13	L V3	18	-2 -84 15	143
14	L V3	18	-6 -80 26	191
15	L anterior CB	--	-20 -54 -21	146
16	L midfrontal	8	-25 25 42	189
17	L PMA/SMA	6	-27 8 47	419
18	L midfrontal	10	-32 48 20	189
19	L S1	2	-48 -19 27	451

Figure 9. *Glass Brain of Syllable Repetition Volumes of Interest.* View from left side (upper) and top (lower) of brain illustrating the nineteen VOIs resulting from the group active > rest contrast at $p = 0.005$ and minimum cluster size 5 voxels.

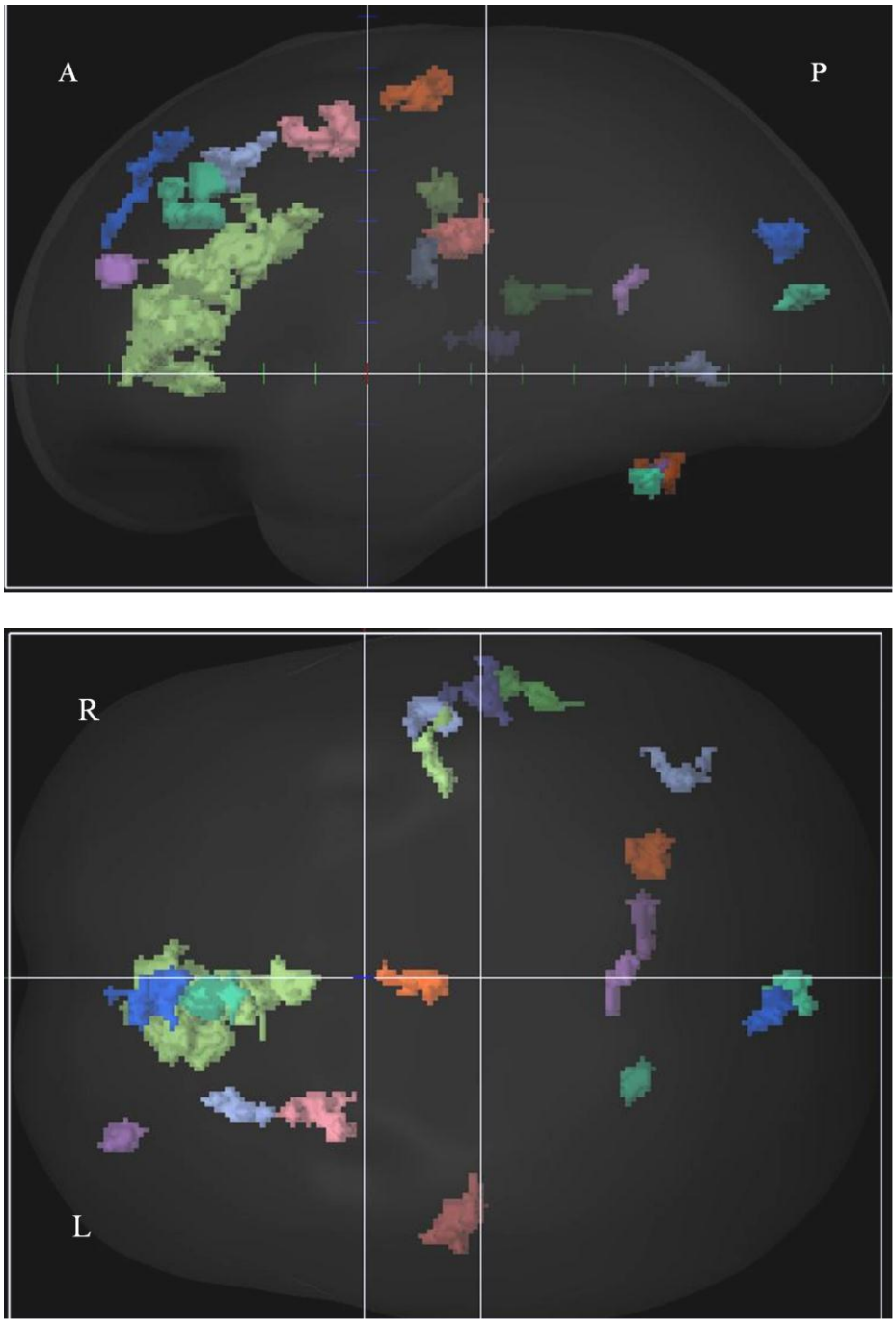

4.1.2 Individual Analysis

After the group masks were created from the unscaled data, each subject's scaled functional SPM was overlaid onto the Talairach-transformed model of his/her own brain. Data from the intersection of the individual's areas of activation and the group VOI mask were compiled for the group second-level analysis of scaling patterns (reported in Section 4.1.3). Within the study design, there were no hypotheses or planned statistical comparisons pertaining to the single-subject level. However, individual activation maps were reviewed for quality and preliminary impressions of patterns in the course of preparing data for the second level group analyses. This initial appraisal of the individual maps hinted at potential trends in the data, some of which were substantiated with the group-level statistics while others were not. The results in this section explore a few of these potential trends that were relevant to the study aims. The cases presented were chosen as the best exemplars of particular patterns or effects from the VOIs of interest. To avoid repetition in a topic that is not central to the specific aims of the study, patterns (or the absence thereof) that were repeated in a number of subjects' VOIs were only reviewed in one case. In addition, VOIs from the visual or auditory cortices were not considered since their activations were superfluous to the targeted study behavior.

4.1.2.1 Hand Squeeze. Review of individual SPMs revealed brain activity within some areas that were expected to be involved in hand squeeze but did not meet statistical thresholds for inclusion in the group mask. For example, the hand area of left M1was not part of the group mask but as shown in Figures 10, 11, and 12, there were robust activations in the region that correlates to hand M1 on the motor homunculus. There was variation across subjects in the precise site of this neural activity as shown in the selected images. This finding has been documented repeatedly in other studies (more details in Section 5.1.1) and that may have prevented any individual voxels in the region to achieve statistical significance in the group average in the current study (see

figure captions for additional information).

Figure 10. *Left Primary Motor Cortex Activity in Hand Squeeze (S001).* Statistical parametric maps for a single subject during hand squeeze; intersubject spatial differences in the precise area of activation in the left primary motor cortex (M1, circled) resulted in no left M1 VOI in the group mask. In subject 1, activation locus is on the superior surface of the precentral gyrus, extending into the sulcus. Additional activation is noted in the premotor region at the top of the circle.

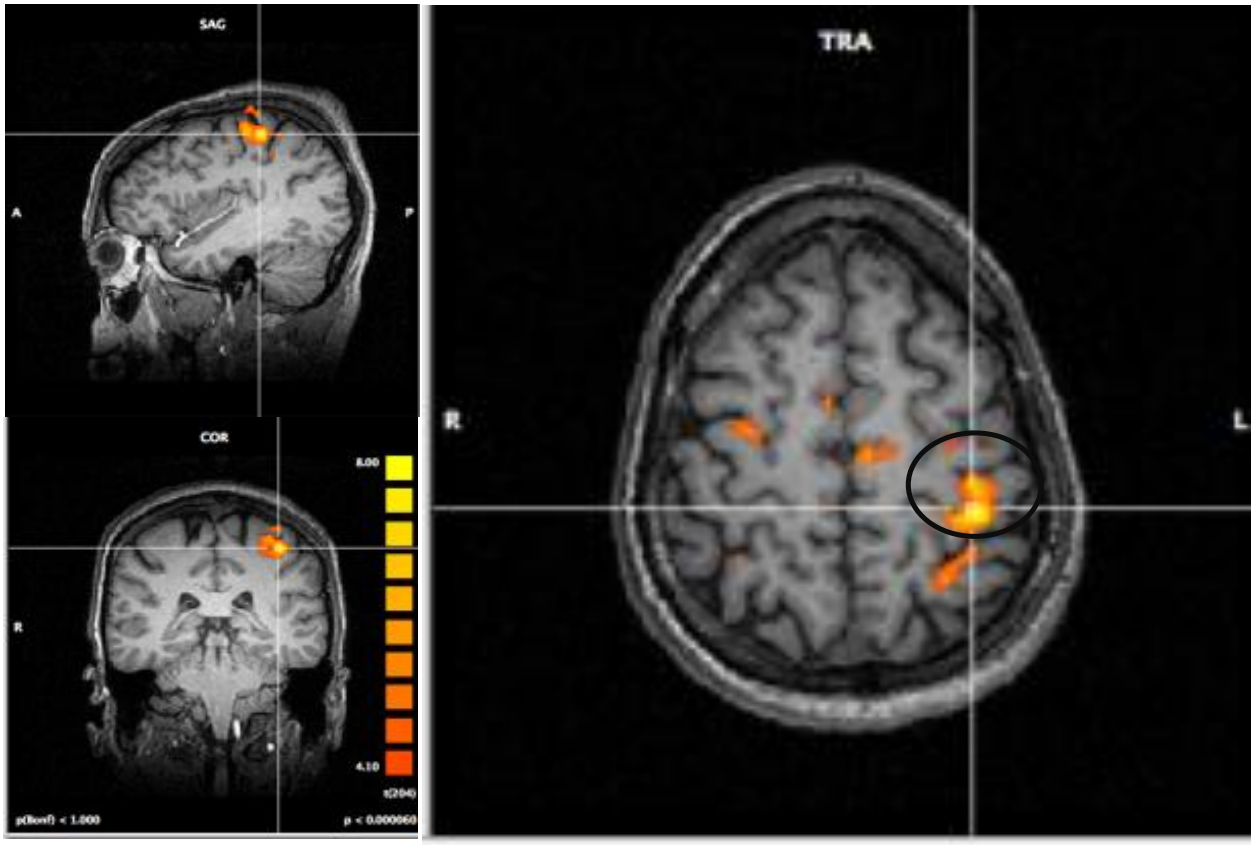

Figure 11. *Left Primary Motor Cortex Activity in Hand Squeeze (S002).* Statistical parametric maps for a single subject during hand squeeze; intersubject spatial differences in the precise area of activation in the left primary motor cortex (M1, circled) resulted in no left M1 VOI in the group mask. In subject 2, the most intense area of activation is on the frontal aspect of the central sulcus, with limited extension to the superior surface of the precentral gyrus (see sagittal view). BOLD signal for S1 is also visible, posterior to the circled area in the horizontal plane.

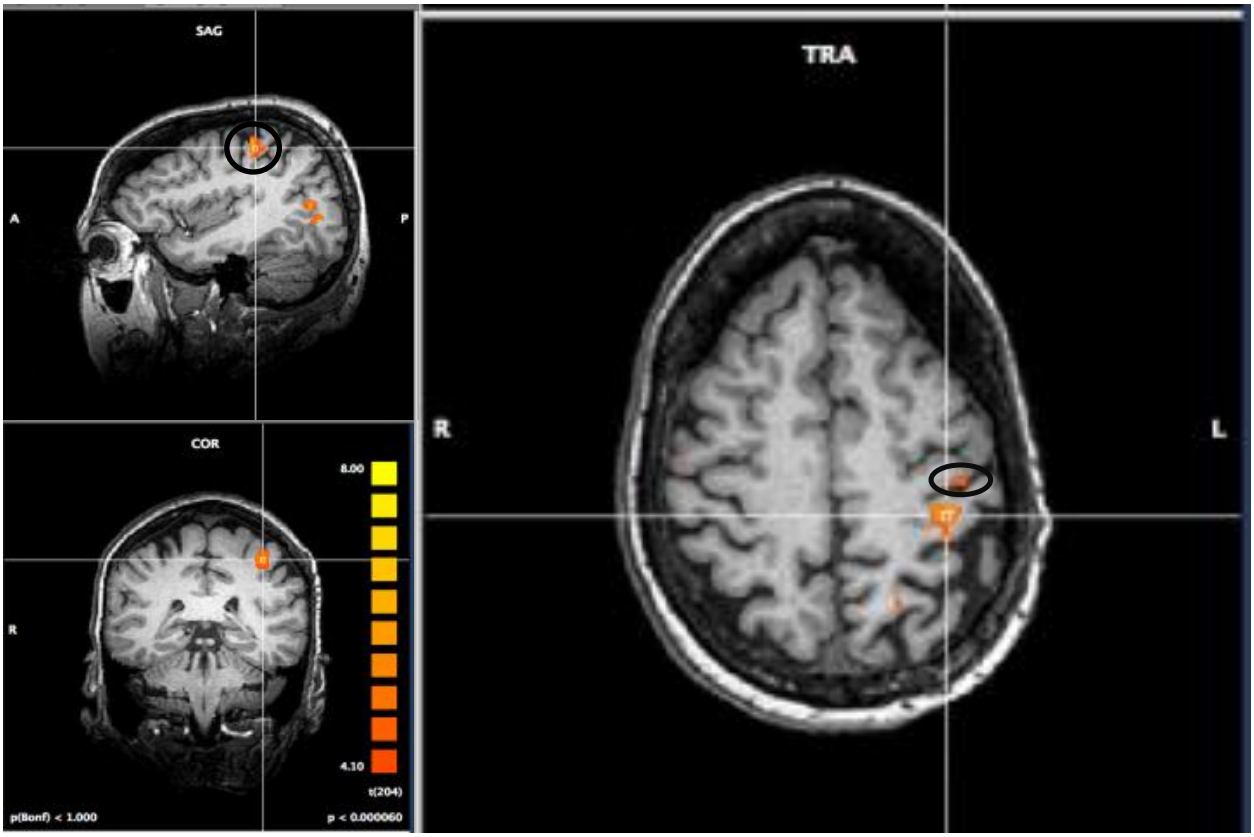

Figure 12. *Left Primary Motor Cortex Activity in Hand Squeeze (S005).* Statistical parametric maps for a single subject during hand squeeze; intersubject spatial differences in the precise area of activation in the left primary motor cortex (M1, circled) resulted in no left M1 VOI in the group mask. In subject 5, the locus of activation is closer to the lateral margin of the superior surface of the precentral gyrus and extends into the central sulcus.

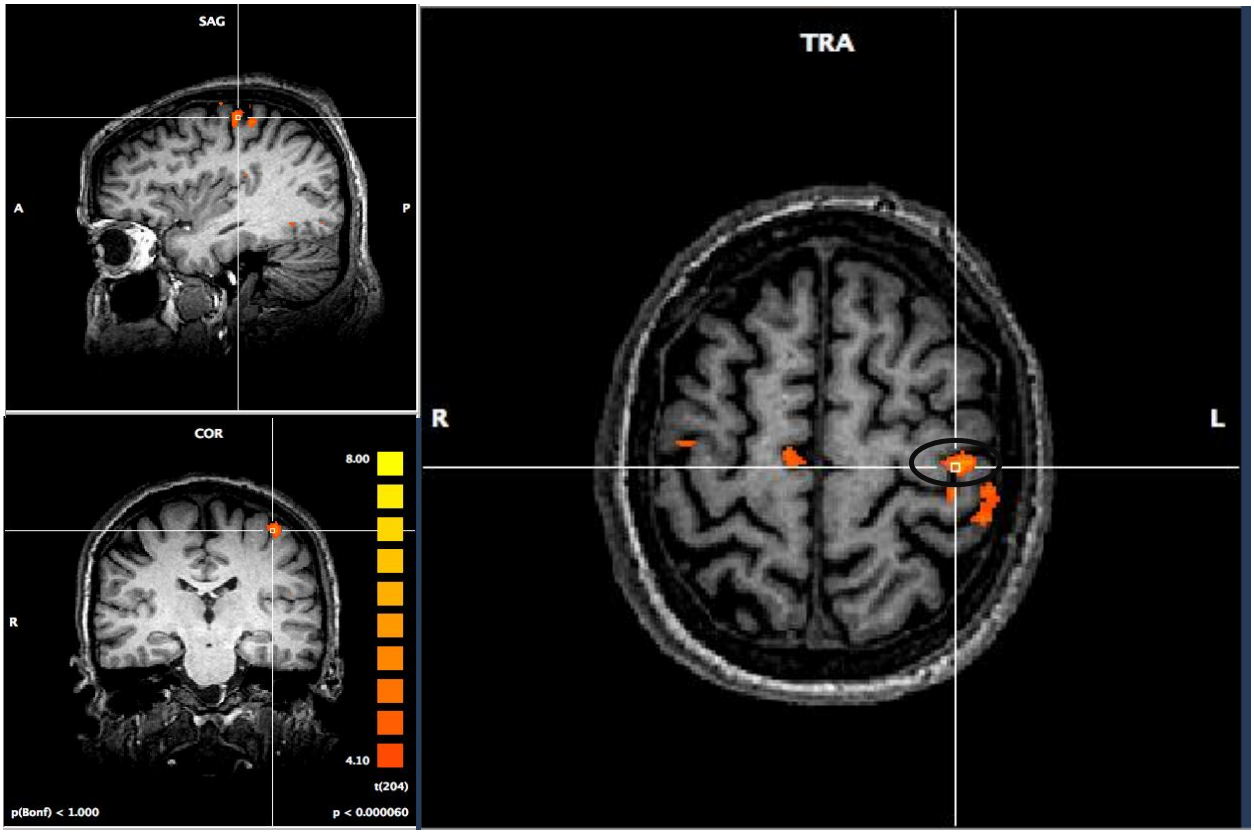

Spatial extent of activation and %SC values tended to change across effort levels in some regions at the individual level, although multiple patterns of change were evident. For example, in the right putamen, subjects 1, 3, 4, 5, 9, and 12 exhibited a decrease in %SC from 25% MVC to 75% MVC. Of these six subjects, half had a decrease in %SC in the interval from 25% MVC to 50% MVC (a continuous downward trend) while the other half had increased %SC (resulting

in a V-type profile). In contrast, subjects 2, 6, 7, 8, 10, and 11 had increases in % SC from 25% MVC to 75% but the 25% MVC to 50% MVC interval was split (Figure 13). These mixed results are likely to be the cause for the non-significant finding in the analysis at the group level that is evaluating scaled activation (Section 4.1.3). The individual data from left S1 (Figure 14) demonstrate that for seven of the twelve subjects, %SC values were lower at 50% MVC while both extremes elicited higher magnitudes of activation. As indicated by the %SC changes, average blood flow to these regions changed in response to the target tasks. However, very few voxels exceeded the threshold of $p = 0.05$ according to the spatial extent of activation data for these VOIs (shown in Figures 15 and 16). Although in theory this could be due to either a broad expanse of relatively moderate increases in CBF so that only a few voxels exceeded the threshold, review of the activation maps shows that these increases in blood flow were isolated to a relatively small area of focal activity in most subjects.

Figure 13. *Percent Signal Change in Right Putamen (Hand VOI 6).* The bar graph shows %SC for each effort level and subject at the volume of interest in the lentiform nucleus of the right putamen during the hand squeeze task.

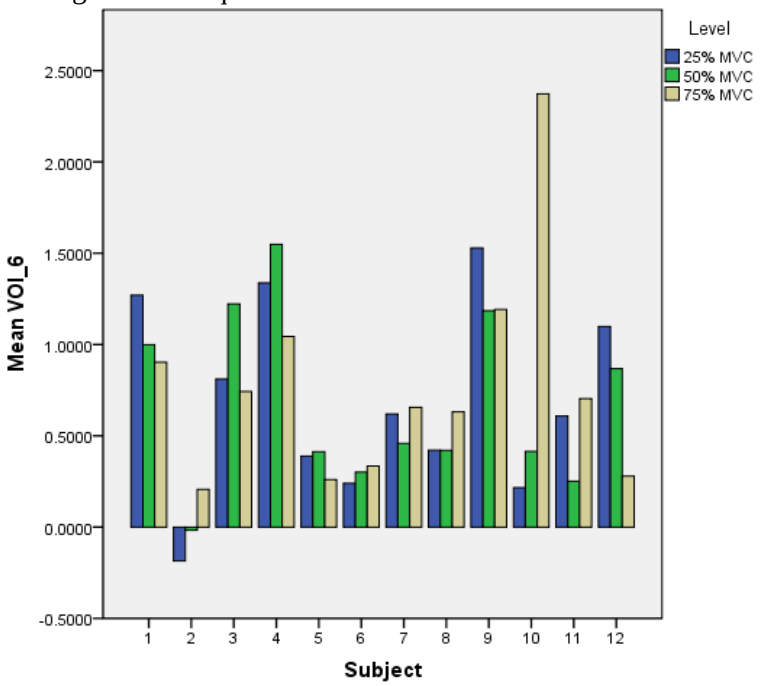

Figure 14. *Percent Signal Change in Left Primary Somatosensory Cortex (Hand VOI 13).* The bar graph shows %SC for each effort level and subject at the volume of interest in the left S1during the hand squeeze task.

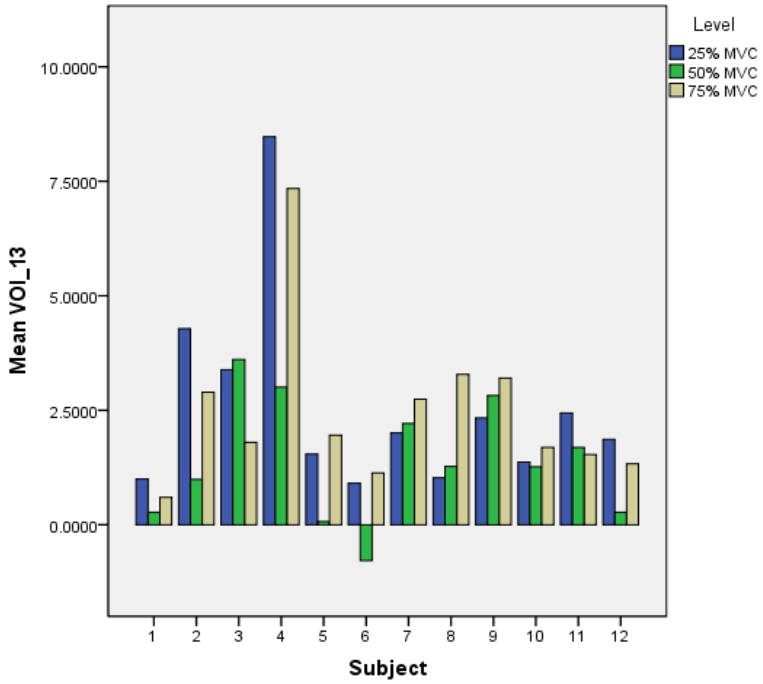

Figure 15. *Spatial Extent of Activation in Right Putamen (Hand VOI 6).* The bar graph shows spatial extent of activation for each effort level and subject at the volume of interest in the lentiform nucleus of the right putamen during the hand squeeze task.

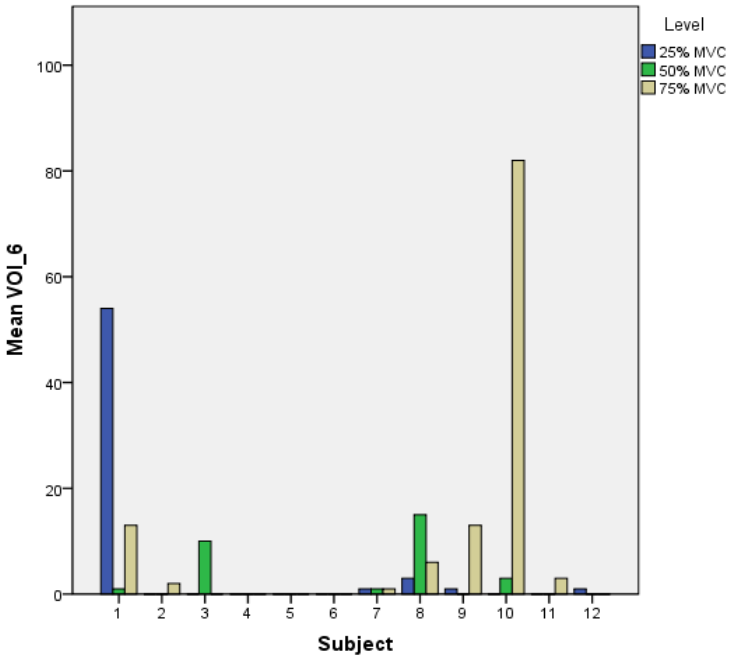

Figure 16. *Spatial Extent of Activation in Left Primary Somatosensory Cortex (Hand VOI 13).* The bar graph shows spatial extent of activation for each effort level and subject at the volume of interest in the left S1during the hand squeeze task.

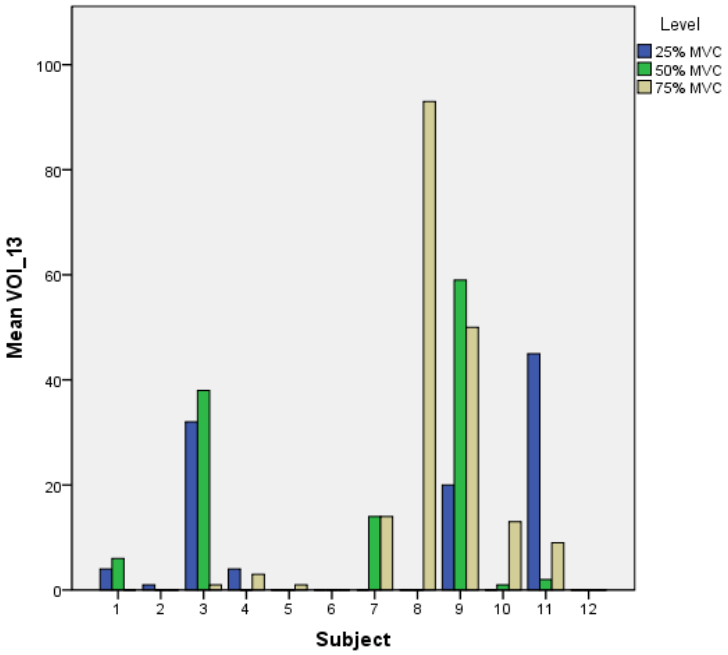

4.1.2.2 Tongue Press. Review of individual subjects' %SC and spatial extent data again revealed indications of scaling in some areas during tongue press. Increasing %SC was generally observed in right S1 and right PMA/SMA. In right S1, %SC was higher at 75% MVC than at 25% MVC in eleven of twelve subjects but the profiles followed different patterns (Figure 17). Values for %SC in right S1 increased across the three effort levels in subjects 7, 8, 9, 11, and 12. Subjects 1, 2, 5, and 10 had an intervening drop at 50% MVC before rising again at the 75% MVC, and subjects 3 and 6 spiked at the 50% level. Based on the consistent relationship between the 25% MVC and 75% MVC levels in the individual data, one could predict that group differences were statistically significant during the second-level analysis although the 50% MVC level may not be statistically different from either extreme.

In %SC for right PMA/SMA, eight of the twelve subjects had higher values at 75% MVC than at 25% MVC (Figure 18). Five of these subjects (3, 4, 5, 7, and 12) showed a progressive increase from 25% to 50% to 75% MVC; for the other three (subjects 1, 2, and 10), there was a spike (subject 1) or drop (subjects 2 and 10) at 50% MVC. Subjects 6, 8, 9, and 11 had decreasing intensities of activation from 25% MVC to 75% MVC with various configurations at the 50% level. The magnitude of activation for subjects 2, 3, 4, and 10 was two to four times greater than for any of the other subjects. This skewed the mean %SC values in the subsequent group analysis, but the intersubject variability in magnitude caused the group differences not to be statistically significant (see Section 4.1.3.2).

Figure 17. *Percent Signal Change in Right Primary Somatosensory Cortex (Tongue VOI 1).* The bar graph shows %SC for each effort level and subject for the volume of interest in the right S1during the tongue press task.

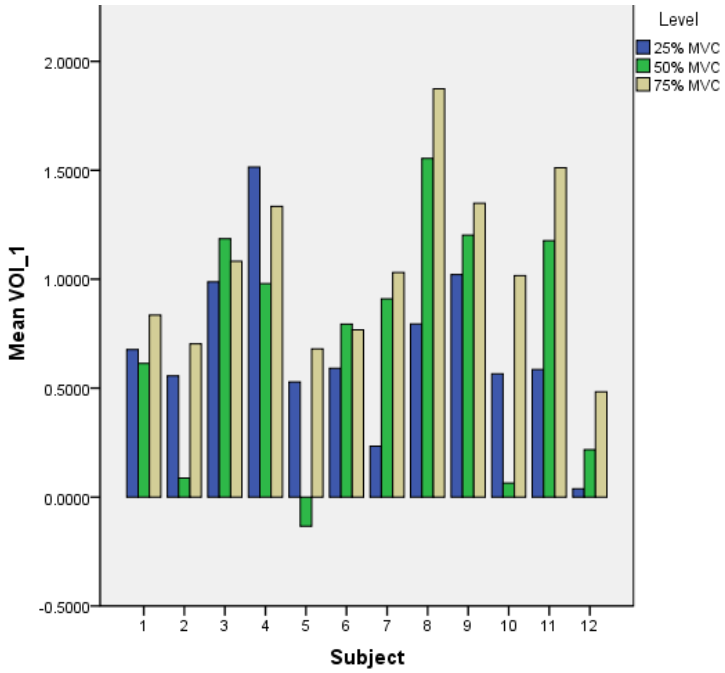

Figure 18. *Percent Signal Change in Right Premotor/Supplementary Motor Cortex (Tongue VOI 2).* The bar graph shows %SC for each effort level and subject for the volume of interest in the right PMA/SMA during the tongue press task.

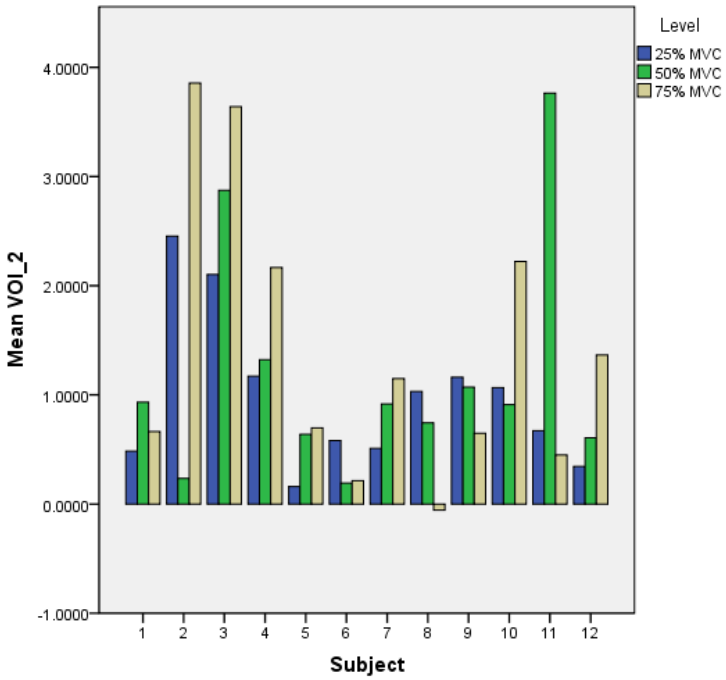

Two examples of spatial extent of activation data in the tongue press task were chosen to highlight the impact of overall volume magnitude. The VOI in left posterior cingulate (VOI 9) was the smallest VOI in the group mask at 159 voxels. Only five subjects' scaled data had any voxels that exceeded the statistical thresholds for this study and intersected with the group VOI generated by the unscaled data (Figure 19). In all five cases, these intersections occurred at only one effort level during tongue press and all of these were on a small scale with the largest extent at 11 voxels.

Compared to this left posterior cingulate region, the VOI in the left putamen (VOI 12) was considerably larger at 730 voxels (Figure 20). Even so, five subjects had zero voxels exceeding the study thresholds in at least two effort levels. In the other seven subjects, five different patterns of activation were noted across the three effort levels. This high degree of variability in the spatial extent of activation data reduced the probability of identifying any group differences at the second level analysis in this small sample population.

Figure 19. *Spatial Extent of Activation in Left Posterior Cingulate Cortex (Tongue VOI 9).* The bar graph shows spatial extent of activation for each effort level and subject at the volume of interest in the left dorsal posterior cingulate during the tongue press task.

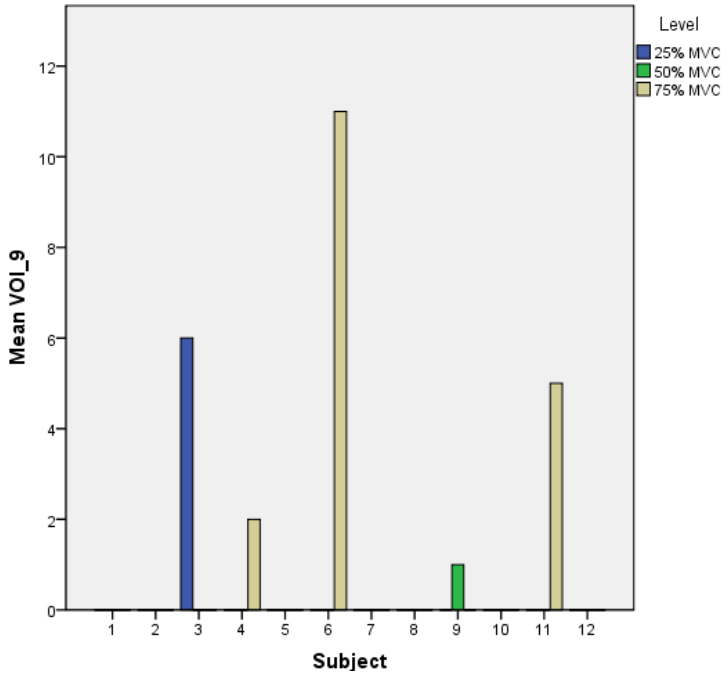

Figure 20. *Spatial Extent of Activation in Left Putamen (Tongue VOI 12).* The bar graph shows spatial extent of activation for each effort level and subject at the volume of interest in the left putamen during the tongue press task.

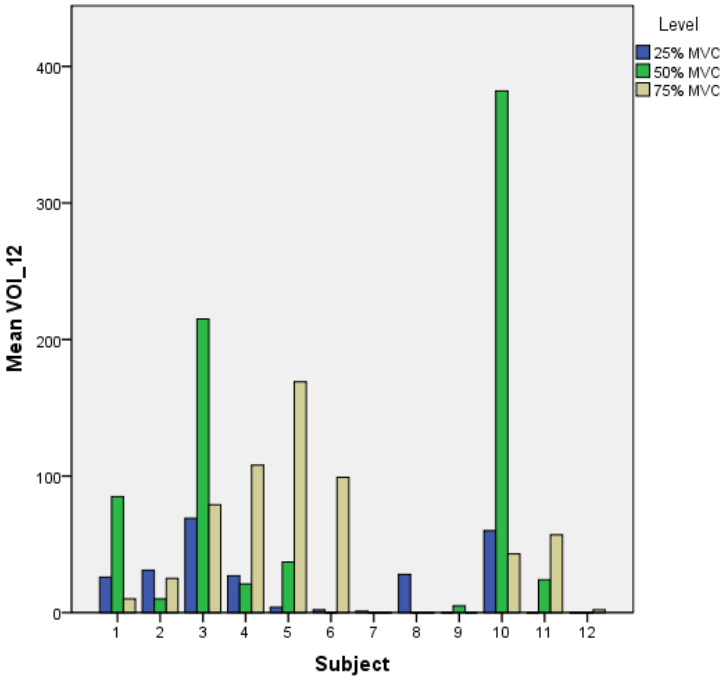

4.1.2.3 Syllable Repetition. The single largest VOI in this study was in left anterior cingulate cortex during the syllable repetition task (VOI 8, Figure 21). Comprised of 4841 voxels, this VOI's individual data demonstrated a trend toward increased spatial extent of activation at the 75% effort level even though four subjects (4, 5, 6, and 12) had minimal overlap with the group VOI mask. Seven of the other eight subjects had greater extents of activation at the 75% MVC level compared to 25% MVC. The only subject with decreasing extent at increased effort levels (subject 8) had much smaller overlap with the group VOI so this exception was unlikely to affect the group comparisons significantly in the second level analysis.

In three of the syllable VOIs, there was a tendency for spatial extent values to spike at the 75% MVC effort level with relatively few and smaller activations at the other effort levels (Figures 22, 23, and 24). Furthermore, spatial extent volumes for subjects 1, 3, 7, 9, 10, and 11 were considerably larger than those for other subjects across most tasks and VOIs. In particular, subject 10 had the largest data values in four of the eight spatial extent examples highlighted in this discussion as well as two of the four %SC examples (Figures 13, 15, 19, 21, 23, and 24). This may indicate that the location of these subjects' activations happened to overlap the group VOIs more than other subjects whose loci for particular brain functions deviated further from the group's average map. Also, the cerebral blood flow of these subjects may be such that they had more intense and voluminous activations than others in the sample, and their values skewed the first level group analysis on which the VOI maps were based. The examples offered from the individual analysis results were highlighted to illustrate important considerations for the group analysis; individual analysis of multiple other VOIs support differences across effort levels but these are not all explicitly discussed here in order to avoid redundancy.

Figure 21. *Spatial Extent of Activation in Left Anterior Cingulate Cortex (Syllable VOI 8).* The bar graph shows spatial extent of activation for each effort level and subject at the volume of interest in the left ventral anterior cingulate cortex during the syllable repetition task.

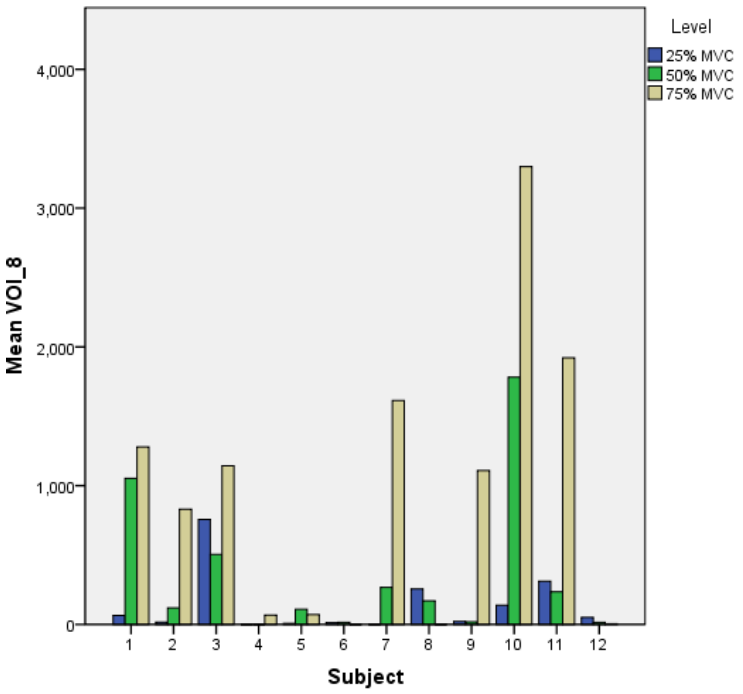

Figure 22. *Spatial Extent of Activation in Left Posterior Cingulate Cortex (Syllable VOI 11).* The bar graph shows spatial extent of activation for each effort level and subject at the volume of interest in the left dorsal posterior cingulate cortex during the syllable repetition task.

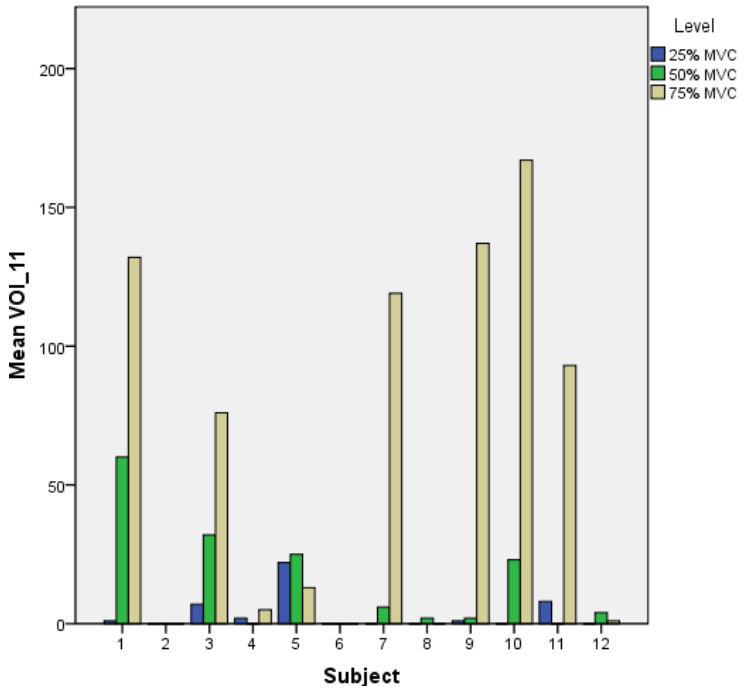

Figure 23. *Spatial Extent of Activation in Left Midfrontal Cortex (Syllable VOI 16).* The bar graph shows spatial extent of activation for each effort level and subject at a volume of interest in the left midfrontal cortex during the syllable repetition task.

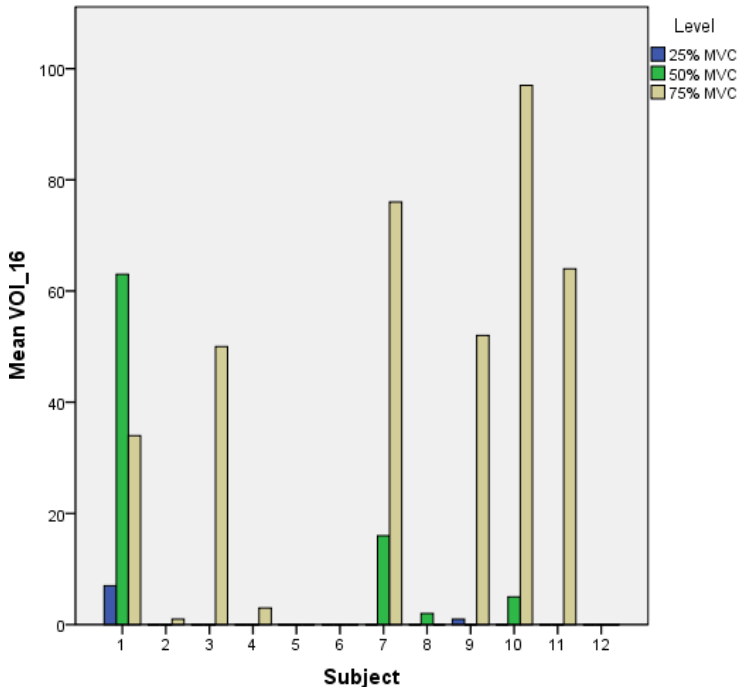

Figure 24. *Spatial Extent of Activation in Left Premotor/Supplementary Motor Cortex (Syllable VOI 17).* The bar graph shows spatial extent of activation for each effort level and subject at the volume of interest in the left PMA/SMA during the syllable repetition task.

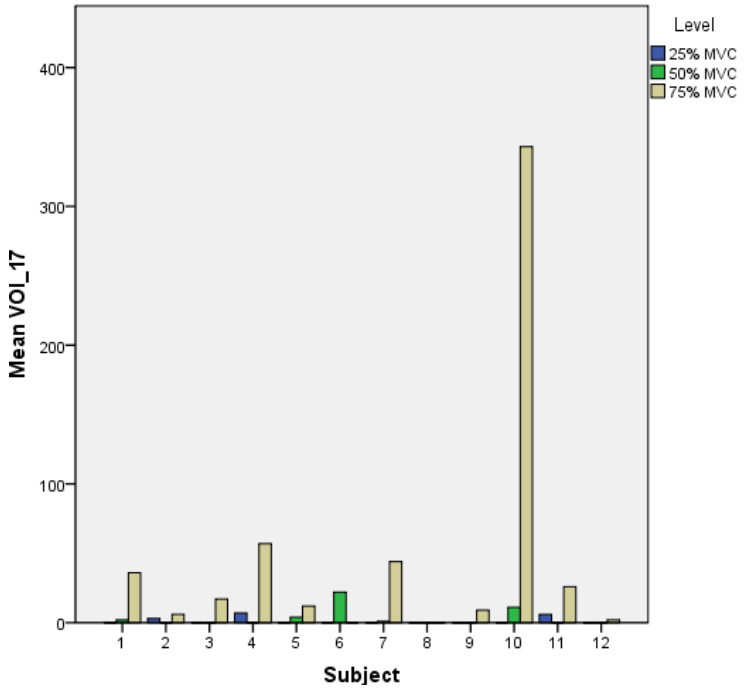

4.1.3 Group Analysis: Part II

4.1.3.1 Hand Squeeze. Data for average %SC and spatial extent of activation are displayed in Table 4. Mean values trended toward incremental increases (upward scaling) on one or both outcome measures (%SC and spatial extent) in the right and left S1, right CB, right M1, right putamen, left ventral lateral nucleus (VL) of the thalamus, left V3, left supramarginal gyrus, and left insula (VOI 1, 4, 5, 6, 11, 13, 14, 15, and 16). Results from the repeated measures ANOVA of effort levels for each VOI are reflected in the reported p-values. There were statistically significant differences between effort levels on one or both outcomes in the right and left CB, left posterior cingulate, left primary motor cortex, and left supramarginal gyrus (VOI 4, 8, 12, 13, and 15; Table 4, p-values bolded; Figures 25 and 26 for example). Interestingly, most of the statistically significant differences were in regions and outcomes where the means showed a drop in activation at 50% of MVC compared to the 25% effort and the 75% effort levels.

Table 4. *Scaled Activations for Right Hand Squeeze.* Mean reflects the average intersection between individual subjects' activation and the group mask (both at $p = 0.005$, minimum cluster size 5 voxels). The p-value is from the one-way ANOVA of effort levels.

			% Signal Change		Spatial Extent	
Cluster	Location	Effort Level	*Mean*	*p-value*	*Mean*	*p-value*
1	R S1	25%	0.631	0.796	18.67	0.917
		50%	0.660		21.08	
		75%	0.721		18.33	
2	R occipital	25%	0.937	0.505	91.33	0.546
		50%	0.906		125.67	
		75%	0.704		108.08	
3	R insular cortex	25%	0.514	0.689	21.17	0.705
		50%	0.613		28.42	
		75%	0.563		25.33	
4	R anterior CB	25%	0.562	0.100	74.58	**0.051***
		50%	0.716		132.92	
		75%	0.776		209.50	
5	R M1	25%	0.764	0.428	13.42	0.097
		50%	0.739		20.33	
		75%	0.884		27.25	
6	R putamen	25%	0.696	0.813	5.00	0.377
		50%	0.672		2.50	
		75%	0.777		10.00	
7	L V1	25%	1.081	0.719	866.00	0.758
		50%	1.145		937.33	
		75%	1.032		819.67	
8	L posterior cingulate	25%	0.922	**0.022**	179.08	0.134
		50%	0.695		149.75	
		75%	1.013		212.50	
9	L SA	25%	0.612	0.265	22.25	0.549
		50%	0.861		35.50	
		75%	0.744		20.42	*continued*

Table 4 continued. *Scaled Activations for Right Hand Squeeze.*

Cluster	Location	Effort Level	% Signal Change		Spatial Extent	
			Mean	*p-value*	*Mean*	*p-value*
10	L V3	25%	-1.185	0.623	37.00	0.699
		50%	-0.738		48.58	
		75%	-1.001		43.42	
11	L VL	25%	0.362	0.379	3.42	0.102
		50%	0.427		5.58	
		75%	0.476		7.42	
12	L anterior CB	25%	0.542	**0.040**	22.67	0.430
		50%	0.430		15.00	
		75%	0.580		29.50	
13	L S1	25%	2.552	**0.022**	8.83	0.691
		50%	1.392		10.00	
		75%	2.459		15.33	
14	L V3	25%	0.847	0.791	32.33	0.469
		50%	0.916		41.83	
		75%	0.934		47.17	
15	L supramarginal	25%	1.229	**0.014**	965.08	**0.018**
		50%	1.162		1084.25	
		75%	1.388		1253.50	
16	L insular cortex	25%	0.614	0.848	32.67	0.359
		50%	0.648		55.42	
		75%	0.688		66.50	
17	L V3	25%	1.123	0.451	45.42	0.834
		50%	0.912		44.92	
		75%	1.188		52.00	

* approximated p-value threshold

Figure 25. *Scaled Activations In Hand Task (VOI 4).* Statistical parametric maps of activation in the right anterior cerebellum reflect scaled increases in activation with increased effort levels at 25% of maximum voluntary contraction (MVC; top), 50% MVC (lower left), and 75% MVC (lower right).

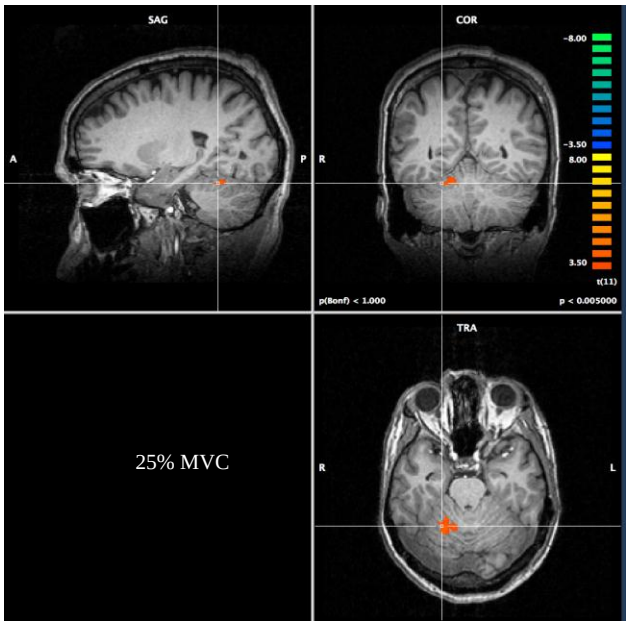

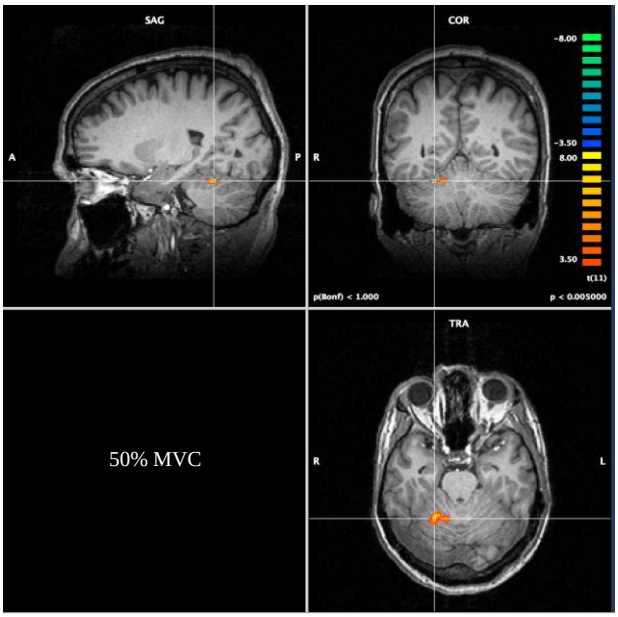

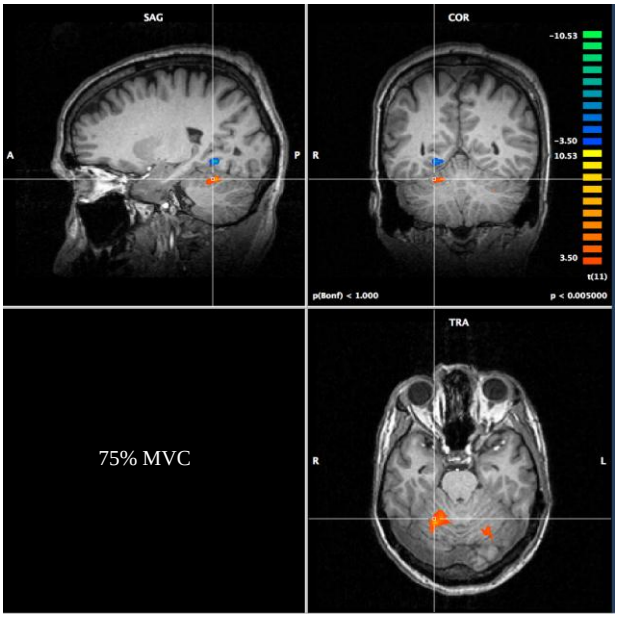

Figure 26. *Scaled Activations In Hand Task (VOI 15).* Statistical parametric maps of activation in the left supramarginal region reflect scaled increases in activation with increased effort levels at 25% of maximum voluntary contraction (MVC; top), 50% MVC (lower left), and 75% MVC (lower right).

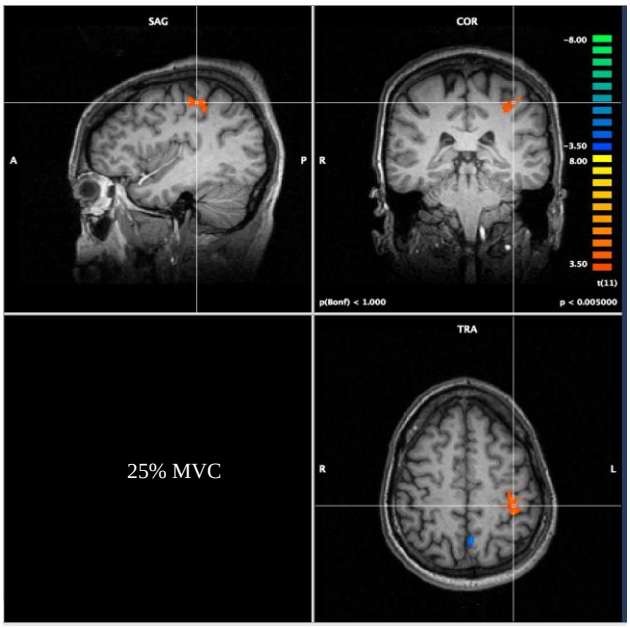

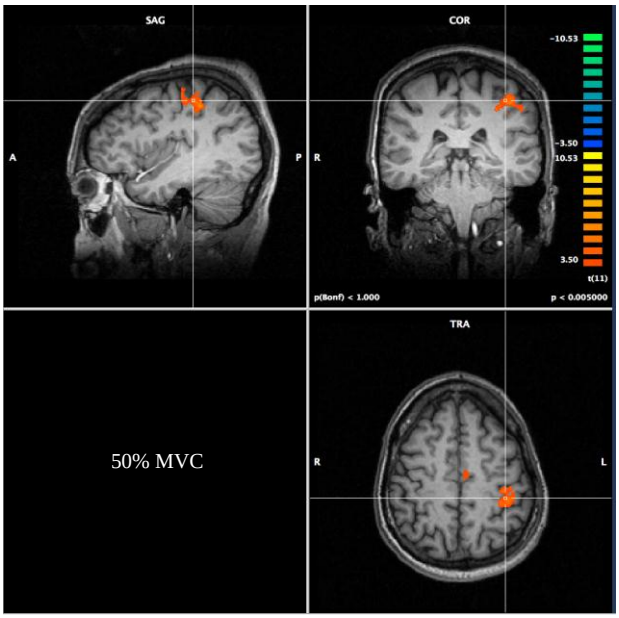

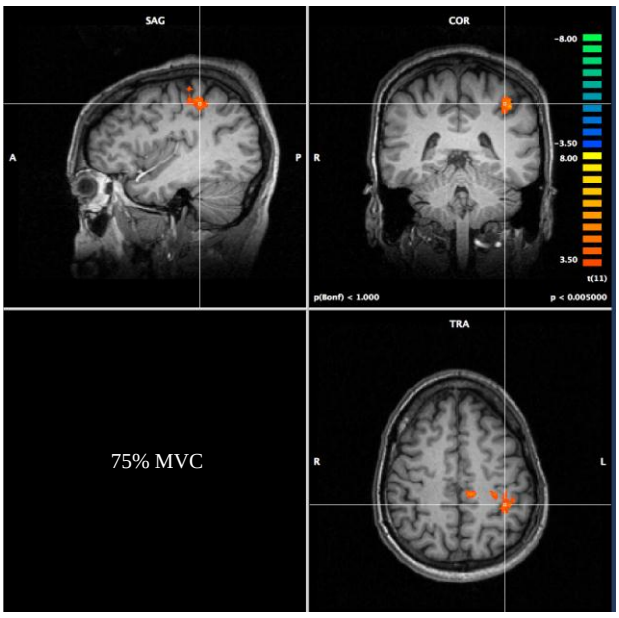

4.1.3.2 Tongue Press. Table 5 illustrates average %SC and spatial extent of activation across effort levels in each VOI for tongue press. Increasing BOLD activations across effort levels were noted in right S1 (%SC and spatial extent, VOI 1), right PMA/SMA (%SC, VOI 2), and an area within left cingulate (spatial extent, VOI 9). Decreasing activations across effort levels occurred in right putamen (spatial extent, cluster 4) and left SA (spatial extent, cluster 8). A number of areas, including bilateral putamen (spatial extent), right caudate (%SC and spatial extent), and left PMA/SMA (spatial extent) exhibited spikes in activation at the 50% MVC level compared to either extreme (VOI 4, 6, 11, and 12). Drops in activation occurred at the 50% level compared to 25 and 75% MVC in right fusiform (%SC and spatial extent, VOI 3), left SA (%SC, VOI 8), left anterior cingulate (spatial extent, VOI 10), and left PMA/SMA (spatial extent, VOI 11). However, results from the repeated measures ANOVA of effort levels for each VOI (reflected in the reported p-values) indicated that the only statistically significant difference was in right S1 (VOI 1). Here, increases in %SC with each advancing effort level were relatively small but consistent across subjects.

Table 5. *Scaled Activations for Tongue Press.* Mean reflects the average intersection between individual subjects' activation and the group mask (both at $p = 0.005$, minimum cluster size 5 voxels). The p-value is from the one-way ANOVA of effort levels.

			% Signal Change		Spatial Extent	
	Location	Effort Level	*Mean*	*p-value*	*Mean*	*p-value*
1	R S1	25%	0.67	**0.007**	6.00	0.226
		50%	0.72		13.33	
		75%	1.06		21.42	
2	R PMA/SMA	25%	0.98	0.501	2.75	0.294
		50%	1.18		12.58	
		75%	1.42		12.33	
3	R fusiform	25%	1.08	0.290	17.67	0.964
		50%	0.73		15.33	
		75%	1.16		15.25	
4	R putamen	25%	-1.73	0.282	31.42	0.787
		50%	-1.68		39.83	
		75%	-1.07		27.58	
5	L posterior cingulate	25%	-0.79	0.974	38.75	0.739
		50%	-0.80		34.25	
		75%	-0.83		29.92	
6	R caudate	25%	-1.64	0.495	8.17	0.923
		50%	-1.29		9.08	
		75%	-1.32		6.50	
7	L V3	25%	-1.28	0.869	544.92	0.667
		50%	-1.34		440.83	
		75%	-1.32		427.75	
8	L SA	25%	-0.54	0.376	8.67	0.429
		50%	-0.77		7.58	
		75%	-0.69		4.58	
9	L posterior cingulate	25%	-0.33	0.489	0.50	0.326
		50%	-0.43		0.08	
		75%	-0.46		1.50	
10	L anterior cingulate	25%	-0.65	0.285	25.00	0.497
		50%	-1.07		3.58	
		75%	-1.29		21.17	

continued

Table 5 continued. *Scaled Activations for Tongue Press.*

			% Signal Change		Spatial Extent	
	Location	Effort Level	*Mean*	*p-value*	*Mean*	*p-value*
11	L PMA/SMA	25%	-0.66	0.636	47.83	0.669
		50%	-0.78		72.92	
		75%	-0.76		55.92	
12	L putamen	25%	0.61	0.992	20.67	0.305
		50%	0.62		64.92	
		75%	0.60		49.33	
13	L V3	25%	1.05	0.991	24.00	0.435
		50%	1.07		31.17	
		75%	1.08		32.75	

4.1.3.3 Syllable Repetition. Group means for BOLD outcome measures during the syllable repetition task are shown in Table 6. BOLD signal increased across all three effort levels for at least one measure in right CB, left cingulate cortex, left midfrontal lobe, and one portion of the left PMA/SMA (VOI 7, 8, 11, 12, 16, 17, and 18). Decreasing spatial extent of activation across effort levels was noted in right CB, an area within the left PMA/SMA, and left SA (VOI 6, 10 and 19). Decreasing %SC across all three effort levels occurred in R posterior parietal cortex, left anterior and posterior cingulate, two regions of left PMA/SMA, and three areas in left frontal lobe (VOI 3, 8, 9, 10, 11, 12, 16, 17, and 18). Per the repeated measures ANOVA, differences across effort levels were statistically significant for one or both measures in multiple regions within left anterior and posterior cingulate, left PMA/SMA, and left frontal regions (Table 6, p-values bolded).

Table 6. *Scaled Activations for Syllable Repetition.* Mean reflects the average intersection

between individual subjects' activation and the group mask (both at $p = 0.005$, minimum cluster size 5 voxels). The p-value is from the one-way ANOVA of effort levels.

			% Signal Change		Spatial Extent	
Cluster	Location	Effort Level	*Mean*	*p-value*	*Mean*	*p-value*
1	R A1	25%	1.37	**0.014**	32.58	0.688
		50%	1.59		44.75	
		75%	0.86		35.33	
2	R A1	25%	1.28	0.533	23.17	0.411
		50%	1.60		19.50	
		75%	1.25		10.42	
3	R posterior parietal	25%	1.26	0.219	39.42	0.123
		50%	1.20		39.17	
		75%	0.92		19.67	
4	R PMA/SMA	25%	1.07	0.815	24.75	0.251
		50%	0.94		81.17	
		75%	0.94		23.50	
5	R fusiform	25%	0.92	0.067	11.25	0.389
		50%	1.01		12.67	
		75%	0.42		3.67	
6	R anterior CB	25%	1.06	0.131	55.17	0.520
		50%	1.33		53.67	
		75%	0.71		37.00	
7	R anterior CB	25%	0.74	0.612	24.25	0.939
		50%	0.87		28.67	
		75%	0.88		26.83	
8	L anterior cingulate	25%	-0.73	**<0.001**	136.42	**0.006**
		50%	-1.36		357.58	
		75%	-1.81		944.92	
9	L posterior cingulate	25%	-1.06	**0.022**	30.25	0.696
		50%	-1.55		22.75	
		75%	-1.78		38.50	
10	L PMA/SMA	25%	1.07	**0.003**	24.67	0.695
		50%	0.93		20.58	
		75%	0.34		8.75	*continued*

Table 6 continued. *Scaled Activations for Syllable Repetition.*

Cluster	Location	Effort Level	% Signal Change		Spatial Extent	
			Mean	*p-value*	*Mean*	*p-value*
11	L posterior cingulate	25%	-1.95	**0.017**	3.42	**0.002**
		50%	-2.58		12.83	
		75%	-3.23		61.92	
12	L frontal	25%	-0.29	**<0.001**	3.33	**0.001**
		50%	-1.11		20.92	
		75%	-1.52		102.67	
13	L V3	25%	-1.33	0.670	28.00	0.145
		50%	-1.27		27.50	
		75%	-1.47		42.67	
14	L V3	25%	-1.28	0.071	34.17	0.654
		50%	-1.32		30.50	
		75%	-2.38		39.58	
15	L anterior CB	25%	0.64	0.083	8.00	0.620
		50%	0.80		13.58	
		75%	0.52		12.08	
16	L midfrontal	25%	1.23	0.155	0.67	**0.002**
		50%	1.12		7.17	
		75%	0.85		31.42	
17	L PMA/SMA	25%	-0.88	0.104	1.33	**0.003**
		50%	-1.24		3.33	
		75%	-1.55		46.00	
18	L midfrontal	25%	-2.47	**0.018**	0.67	**0.036**
		50%	-3.17		8.83	
		75%	-5.00		19.67	
19	L S1	25%	1.23	0.155	90.42	0.352
		50%	1.12		72.00	
		75%	0.85		48.58	

4.2 *Behavioral Data*

Summary descriptive data for pressures obtained during all tasks are presented in Table 7. In order to locate the pressure transducer outside the magnetic field, tubing length was 65 feet from bulb to transducer. Small pressure changes generated by the 10 ml compression bulbs could go undetected in such a length of "dead space," so the bulb-tubing-transducer system had to be preloaded with air to approximately 1 psi. The resulting pressure values reflect the actual pressures produced above the baseline one-psi level, but this fundamental alteration to the system does not allow a direct comparison to hand and tongue pressure values obtained in other studies. A p-value of 0.05 was selected as the upper limit for statistically significant results, based on past studies of similar behaviors (Lafargue, et al., 2008; Solomon, et al., 2000; Somodi, et al., 1995).

Table 7. *Actual and Target Pressures for Hand Squeeze, Tongue Press, and Syllable Repetition Tasks.* Target pressures are derived as percentages of the actual MVC obtained.

			Actual Pressure (psi)		Target Pressure (psi)	
Task	Position	Effort Level	*Mean*	*SD*	*Mean*	*SD*
Hand	Upright	25% MVC	0.094	0.015	0.101	0.010
		50% MVC	0.162	0.024	0.202	0.020
		75% MVC	0.234	0.036	0.303	0.031
		MVC	0.403	0.040	--	--
	Supine	25% MVC	0.099	0.015	0.115	0.011
		50% MVC	0.180	0.025	0.231	0.022
		75% MVC	0.258	0.043	0.346	0.033
		MVC	0.462	0.044	--	--
Tongue	Upright	25% MVC	0.115	0.031	0.143	0.035
		50% MVC	0.208	0.061	0.285	0.069
		75% MVC	0.316	0.094	0.428	0.104
		MVC	0.571	0.138	--	--
	Supine	25% MVC	0.130	0.029	0.142	0.042
		50% MVC	0.226	0.074	0.287	0.074
		75% MVC	0.314	0.055	0.441	0.090
		MVC	0.574	0.106	--	--
Syllable	Upright	25% MVC	0.084	0.034	0.102	0.037
		50% MVC	0.118	0.047	0.204	0.074
		75% MVC	0.161	0.071	0.306	0.110
		MVC	0.408	0.147	--	--
	Supine	25% MVC	0.087	0.043	0.104	0.039
		50% MVC	0.132	0.068	0.209	0.077
		75% MVC	0.178	0.087	0.313	0.116
		MVC	0.418	0.188	--	--

4.2.1 Actual Pressures by Position and Effort Level

Two-way repeated measures ANOVA for actual pressures by effort level (25%, 50%, 75%, and MVC), and position (upright and supine) were completed for each task to address the Exploratory Aim. Table 8 presents ANOVA results for all three tasks. For all effort levels and all tasks, the pressures obtained in the supine position were higher than those from the upright position but not to a statistically significant degree.

Table 8. *Repeated Measures ANOVA for Actual Pressures.* The results of the two-way repeated measures ANOVAs for effort level by position are shown. Data for 25% MVC, 50% MVC, 75% MVC, and MVC were included in the calculations.

Source	*df*	*F-statistic*	*p-value*
Hand			
Effort Level x Position	3	2.989	**0.035**
Effort Level	3	475.713	< 0.001
Position	1	15.872	< 0.001
Tongue			
Effort Level x Position	3	0.190	0.903
Effort Level	3	142.789	**< 0.001**
Position	1	0.944	0.334
Syllable			
Effort Level x Position	3	0.023	0.995
Effort Level	3	61.147	**< 0.001**
Position	1	0.359	0.551

4.2.1.1 Hand Squeeze. For the hand squeeze behavior, the main effect of effort level *(F = 475.713, df = 3, p < 0.001)* and position (*F = 15.872, df = 1, p < 0.001*) were both statistically significant. Additionally, there was a statistically significant interaction between effort level and position (*F = 2.989, df = 3, p = 0.035*) so main effects were not considered in further detail. Based on the significant interaction effect, and as reflected in the summary data from Table 7 and illustrated in Figure 27, actual hand pressures were higher in the supine position at all effort levels, and the differences increased as the effort level increased. The supine pressure increased by 5% over the upright pressure when squeezing at the 25% effort level, 11% at the 50% effort level and 10% at the 75% effort level.

Figure 27. *Actual Pressures During Study Tasks.* Pressures in the supine position were consistently higher than those obtained while the subject was upright.

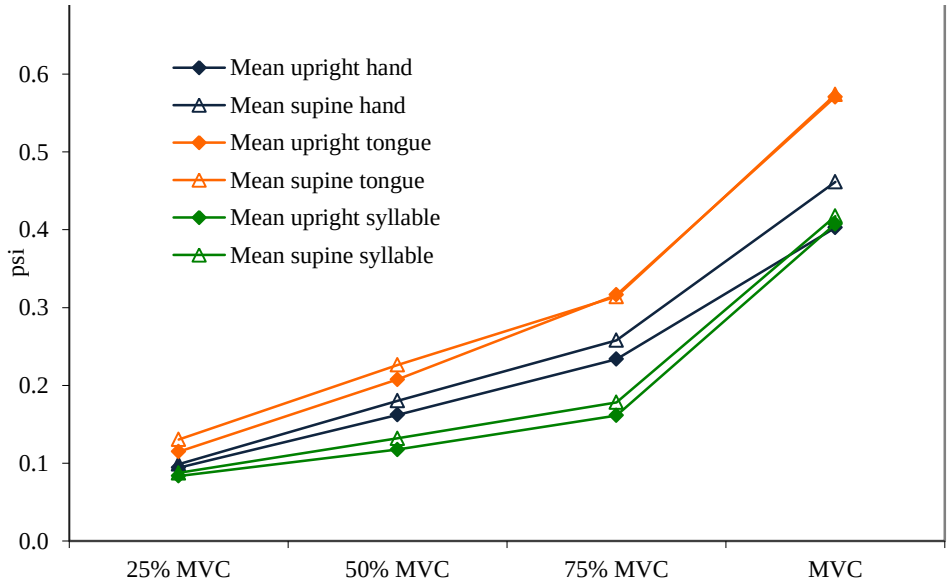

4.2.1.2 Tongue Press. There was no interaction effect for the tongue press task ($F = 0.190$, $df = 3$, $p = 0.903$), and main effects were significant for effort level ($F = 142.789$, $df = 3$, $p < 0.001$) but not position ($F = 0.944$, $df = 1$, $p = 0.334$). As shown in Table 7 and Figure 27, tongue pressures increased with higher effort levels, as expected. Combining data across positions, pressures increased by ~77% from the 25% effort level to the 50% effort level; pressures increased ~45% from the 50% effort level to the 75% effort level.

4.2.1.3 Syllable Repetition. Similar to the tongue press, there was no interaction effect for the syllable repetition task ($F = 0.023$, $df = 3$, $p = 0.995$), and main effects were significant for effort level ($F = 61.147$, $df = 3$, $p < 0.001$) but not position ($F = 0.359$, $df = 1$, $p = 0.551$). Again, tongue pressures increased with each increase in effort level (Tables 7 and 8). Combining data across positions, pressures increased ~46% from the 25% effort level to the 50% effort level; pressures increased ~36% from the 50% effort level to the 75% effort level.

4.2.2 Accuracy of Actual Pressures Compared to Target Levels

Three-way repeated measures ANOVA for pressures by accuracy (target and actual), effort level (25%, 50%, and 75%), and position (upright and supine) were completed for each task (Table 9). Subjects' mean actual pressures at each effort level were consistently lower than the target pressures derived from their individual MVCs. Summary statistics for target and actual pressures on all tasks are shown in Table 7.

Table 9. *Repeated Measures ANOVA for Accuracy of Pressures.* The results of the three-way repeated measures ANOVAs for accuracy by effort level by position are shown. Data for 25% MVC, 50% MVC, and 75% MVC were included in the calculations.

Source	*df*	*F-statistic*	*p-value*
Hand			
Effort Level x Position x Accuracy	2	0.122	0.885
Effort Level x Position	2	2.723	0.069
Position x Accuracy	1	2.475	0.118
Effort Level x Accuracy	2	20.263	**< 0.001**
Effort Level	2	605.728	< 0.001
Position	1	27.329	**< 0.001**
Accuracy	1	110.416	< 0.001
Tongue			
Effort Level x Position x Accuracy	2	0.232	0.793
Effort Level x Position	2	0.033	0.967
Position x Accuracy	1	0.068	0.794
Effort Level x Accuracy	2	6.947	**0.001**
Effort Level	2	160.987	< 0.001
Position	1	1.494	0.224
Accuracy	1	71.842	< 0.001
Syllable			
Effort Level x Position x Accuracy	2	0.012	0.988
Effort Level x Position	2	0.050	0.951
Position x Accuracy	1	0.077	0.781
Effort Level x Accuracy	2	8.616	**< 0.001**
Effort Level	2	48.850	< 0.001
Position	1	0.483	0.488
Accuracy	1	44.041	< 0.001

4.2.2.1 Hand Squeeze. The three-way interaction between effort level, position, and accuracy was not statistically significant level *(F = 0.122, df = 2, p = 0.885)* , nor were the secondary interactions for effort level x position (*F = 2.723, df = 2, p = 0.069)* or position x accuracy (*F = 2.475, df = 1, p = 0.118).* The interaction of effort level and accuracy was significant (*F = 20.263, df = 2, p < 0.001)* with a larger gap between target and actual pressures at higher effort levels as illustrated in Figure 28. All main effects were significant at *p < 0.001*, though only position was considered due to the interaction of effort level and accuracy. Hand pressures were higher in the supine position at all effort levels.

Figure 28. *Accuracy of Pressures During Hand Squeeze Task.* Actual pressures were consistently lower than targets derived from each subject's MVC data, with greater disparity at higher effort levels. Hand pressures were consistently higher when subjects were supine versus upright.

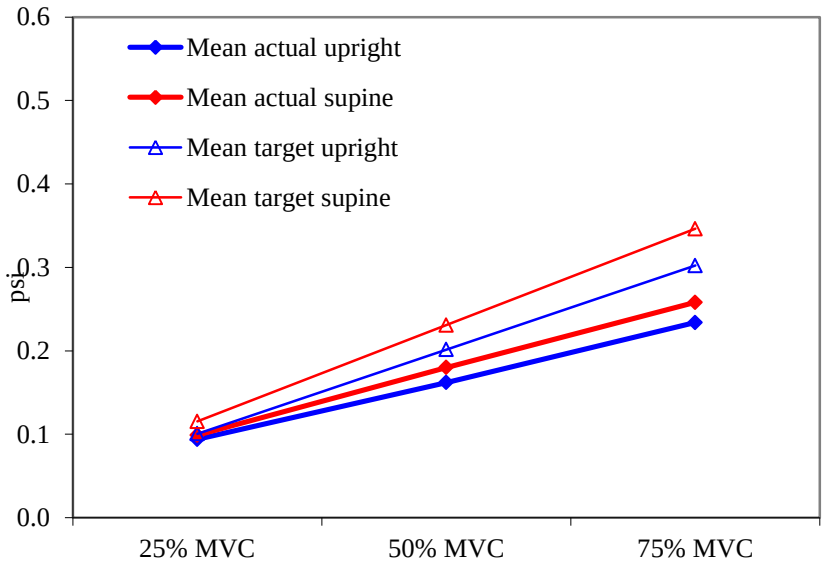

4.2.2.2 Tongue Press. The three-way interaction between accuracy, effort level, and position was not significant (*F = 0.232, df = 2, p = 0.871).* There was a statistically significant interaction effect for effort level x accuracy during the tongue press task (*F = 6.947, df = 2, p = 0.001),* with subjects becoming less accurate at matching their targets as effort level increased regardless of body position (Figure 29). Interactions for effort level x position and position x accuracy were not statistically significant (*F = 0.033, df = 2, p = 0.967* and *F = 0.068, df = 1, p = 0.794*, respectively), nor were main effects for position (*F = 1.494, df = 1, p = 0.224*). Main effects for accuracy and effort level were not considered despite significance levels of *p < 0.001* for both given the presence of interaction effects. Tongue pressures increased as expected with higher effort levels.

Figure 29. *Accuracy of Pressures During Tongue Press Task.* Actual pressures were lower than targets derived from each subject's MVC data, with larger discrepancies at higher effort levels. There were no significant positional differences in tongue pressures.

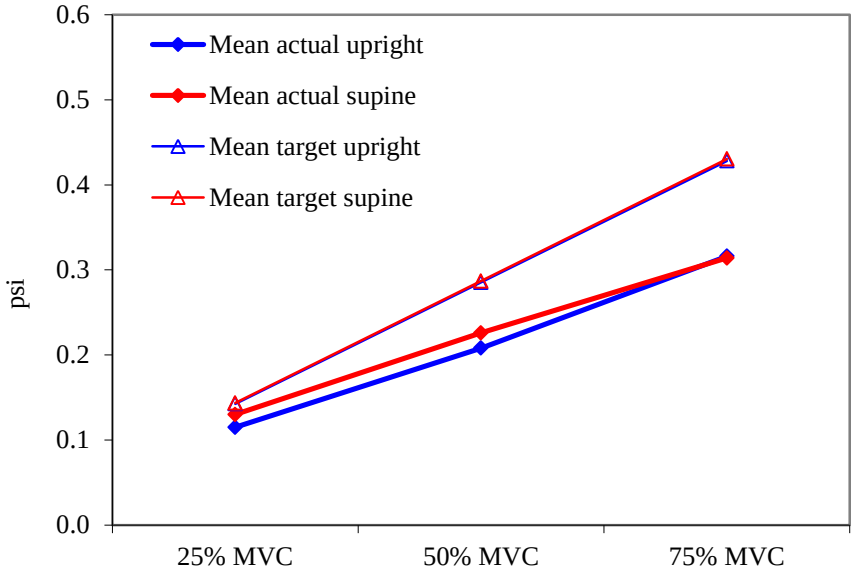

4.2.2.3 Syllable Repetition. The three-way interaction was not significant (*F = 0.012, df = 2, p = 0.988*). The interaction for effort level x accuracy was significant during syllable repetition (*F = 8.616, df = 2, p < 0.001*), with less accurate pressures at higher effort levels. Interactions for position x accuracy and effort level x position were not statistically significant (*F = 0.077, df = 1, p = 0.781* and *F = 0.050, df = 2, p = 0.951*, respectively). Main effects for position were not significant (*F = 0.483, df = 1, p = 0.488*). Accuracy and effort level main effects were not considered because of their interaction, though *p < 0.001* for both. Figure 30 illustrates the relationship between target and actual pressures during syllable repetition.

Figure 30. *Accuracy of Pressures During Syllable Repetition Task.* Subjects consistently undershot the targets derived from their MVC data, and accuracy was lower as effort levels increased.

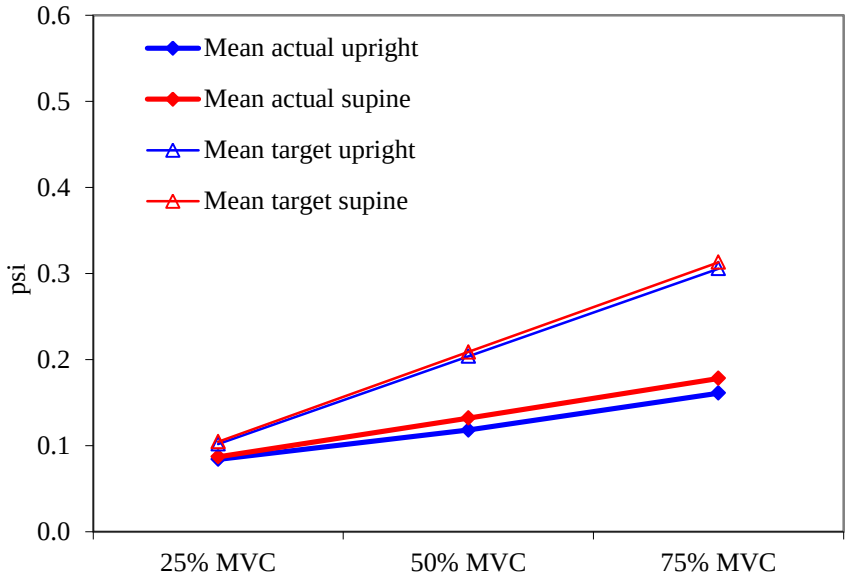

5.0 DISCUSSION

The results of this investigation provide a quantitative description of the location, magnitude, and spatial extent of BOLD signals associated with modulated force production tasks by the hand and tongue. Pressures generated during the hand squeeze, tongue press, and syllable repetition tasks by the healthy older adults also were evaluated in terms of accuracy at matching target effort levels (as a percent of MVC). Finally, the influence of body position (upright vs. supine) on hand and tongue pressure generation at various effort levels was analyzed.

The primary interest was in describing neural substrates and scaled activations for the tongue behaviors given the paucity of available research in this area. Ultimately, more detailed information about tongue force control is expected to (i) further the understanding of mechanisms by which speech is produced normally, (ii) yield insight into the speech deficits associated with diseases that affect the brain, and (iii) stimulate development or refinement of interventions to treat articulation deficits in dysarthria associated with neurological disease. The current study is a first attempt at delineating neural control of tongue movements in nondisordered speakers. The tongue press and syllable repetition behaviors were selected because they have been studied in non-imaging research of aged and disease populations, and because they minimize confounding factors such as auditory feedback during vocalization. The hand squeeze task was included for comparative purposes and also has been studied in imagining and non-imagining research of aged and disease populations.

The discussion that follows first provides a summation of the neural substrates for each task from the hand and tongue. Scaled activations for each task are considered next. Lastly, the behavioral data regarding accuracy of pressure generation at specified target effort levels, and the impact of body position are considered. Overall, fMRI patterns of activation revealed some

overlap in the cortical and subcortical substrates of hand, lingual nonspeech, and lingual speech control, and suggested differing contributions to scaled force control in the brain for these three tasks. Pressure measures from the behavioral tasks showed a direct relationship between effort level and accuracy of force production, which is consistent with previous studies and has implications for future clinical assessment and research.

5.1 *Neural Bases of Hand and Tongue Control*

Both positive and negative neural activations were included in the RFX analysis. Activations are generally assumed to be positive unless otherwise stated, and to represent an increase in blood flow to a particular brain region. This change in CBF results from increased neural activity, but any speculation as to whether this activity is excitatory or inhibitory cannot be verified through fMRI studies alone. Negative activation, characterized by negative %SC values, indicates a decrease in BOLD signal intensity compared to the rest condition. The long-standing supposition that this represents a local decrease in neural activity has recently been confirmed by a multi-echo high-resolution fMRI study of known inhibitory regions during active tasks (Bianciardi, Fukunaga, van Gelderen, de Zwart, & Duyn, 2011). Again, the nature of the decreased activity as either excitatory or inhibitory is based on other knowledge about the particular brain area, such as through lesion studies. For example, M1 has been widely accepted as the source of excitatory signals that trigger motor activity in the body. A positive activation in M1 is expected during the hand squeeze task, and increased activity at higher effort levels would be a reasonable probability even if other studies had not already shown this. Conversely, some areas in the medial prefrontal cortex are believed to be part of the default mode network, a collection of brain regions that activate when the brain is in a wakeful rest state (Miller & Cohen,

2001). During a goal-directed active study condition, neural activity and thus CBF and BOLD signal in this area are expected to decrease because it is no longer working to maintain that wakeful rest state. Since %SC is calculated by subtracting the active BOLD signal from that of the rest condition, the decrease in inhibitory activity is reported as a negative value.

5.1.1 Neural Substrates of Hand Control

Whole-brain group RFX analysis outlined a network of bi-hemispheric cortical and subcortical substrates for the hand squeeze task that was generally consistent with those described in other functional imaging studies of hand control (Allison, et al., 2000; Ehrsson, et al., 2000; Keisker, et al., 2009; Spraker, et al., 2007; Wasson, et al., 2010). This study detected regions of consistent neural activity in the right putamen, bilateral CB, left VL, bilateral S1, and left SA (VOI 1, 4, 6, 9, 11, 12, and 13). These are components of the feedback loops that are expected to contribute to force adjustments in the hand (Kandel, et al., 2000; Mink, 2003). All of these activations were positive except left SA, which is involved in gauging where objects are in relation to the body (Kandel, et al., 2000). A negative %SC here is expected since sensory feedback during the hand squeeze makes it unnecessary to approximate the bulb's location.

In addition to the activations noted above, the whole-brain group RFX analysis revealed other areas of activation during the hand squeeze task. Activations noted in the left posterior cingulate cortex (VOI 8) are described in prior fMRI hand-control studies and may be related to its input from the also-active left thalamus and its functions related to the processing of visual-spatial information for motor tasks (Ehrsson, et al., 2000; Keisker, et al., 2009; Spraker, et al., 2007; Zwicker, Missiuna, Harris, & Boyd, 2010). Activations in the bilateral insular and left supramarginal cortices (VOI 3, 15, and 16) are consistent with their roles as identified in other studies. The insula has been implicated in motor control and the perception of exertion in studies

of fine motor tasks and general exercise (Ackermann & Riecker, 2004; Fink, et al., 1997; Williamson, et al., 1999; Williamson, et al., 2001). The supramarginal region appears to function as an integration center related to proprioception and kinesthesia (Bodegard, et al., 2003; de Vries, et al., 2009). A small area of activation within the right motor cortex was consistent with findings from other fMRI studies of hand grip behavior (Ehrsson, et al., 2000; Spraker, et al., 2007; Wasson, et al., 2010). Results were generally consistent with those anticipated in the hypothesis (H_{1A}) for Specific Aim #1.

Additional areas of activation in left M1 and bilateral PMA/SMA were expected based on previous research, but were not part of the group VOI mask at the chosen statistical parameters. A number of the individual subjects' SPMs showed activation in the left superior-lateral area of M1 (as expected for a right-handed behavior) but no such VOI emerged in the group analysis, most likely resulting from intersubject variability in the precise location of hand representation and associated activation within M1. Research regarding the locus of peak hand M1 BOLD signal has shown differences of up to 19 mm in each of three planes (Alkadhi et al., 2002; Rademacher et al., 2001). Depending on the statistical thresholds chosen, this may encompass the entire area of activation for a subject, such that the activation area for one individual shares no common voxels with that of another individual. In this scenario, it is entirely possible that the process of averaging would cause no voxels in that area to be statistically active at the group level even when all subjects had neural activity in some portion of the region.

Previous fMRI studies of hand grip emphasizing contraction versus relaxation (Spraker, Corcos, & Vaillancourt, 2009) and precision versus power (Ehrsson, et al., 2000; Keisker, et al., 2009; Toma et al., 1999) suggest that the SMA may be particularly active in the relaxation phase of quick isometric-like contractions regardless of force level. Thus, the event-related design of

this study may have captured peak HDR and associated BOLD response related to SMA's relaxation role during the intended "rest" phase of the sequence. If relaxation triggered HDR and BOLD peak in the SMA, each "active" image might reflect an early phase of that HDR and each "rest" image could reflect peak or recovery phases of the HDR. In this case, the activation and %SC values would be very similar across the two conditions, and when the "rest"/baseline SPM mask was subtracted from the "active" SPM mask, the negligible difference would be interpreted as an absence of activation.

Some research also has reported BOLD signaling in the bilateral GP with hand grip tasks. Activations in the putamen (VOI 6) were identified in this study, whereas other BG activity was not captured at the group level. This could result from slight inconsistencies across subjects in the location of this small area within the total brain volume. Also of note, although the values of the detection parameters selected for this study were more liberal than would be typically accepted for either the p-value or minimum cluster size on its own, the combination of the two parameters set a stricter detection threshold than the single-factor strategy used by some other studies. Consequently, it is possible that a less conservative p-value or minimum cluster size could have resulted in the inclusion of some or all of these areas of expected activation though this would also have increased the risk of Type I error. Probes into less stringent thresholds on either parameter in this study resulted in noisy SPM maps for some tasks, whereas the levels chosen yielded results that were most consistent with anticipated VOIs across the three study behaviors.

5.1.2 Neural Substrates of Lingual Control

This study identified overlapping but slightly different patterns of activation for lingual nonspeech (tongue press) and speech (syllable repetition) behaviors, partially supporting the

hypothesis regarding the neural network for such tasks (H_{1B}). Common areas of neural activity included bilateral PMA/SMA, left cingulate, right fusiform, and S1 though hemisphere demonstrating activity differed by task for S1 (tongue VOI 1, 2, 3, 5, 9, 10, and 11; syllable VOI 4, 5, 8, 9, 10, 11, 17, and 19). All of these areas were consistently active in other fMRI studies of orolingual behaviors (Chang, Kenney, Loucks, Poletto, et al., 2009; Estep, 2009; Malandraki, et al., 2009; Riecker, et al., 2005; Soros, et al., 2006). Past studies also noted greater left-sided activations in cortical, thalamic, and BG regions. Both the overall VOI configurations and the spatial extent of activations within VOIs (as measured by the number of active voxels in each VOI, see Tables 2 and 3) in the current study confirmed a left lateralization component across most neural substrates for both lingual tasks, though the effect was stronger in the speech task. Other researchers have reported a similar effect, and hypothesize that speech-specific regions in the left frontal lobe may drive the lateralization of other neural activity during speech tasks (Ghosh, et al., 2008; Malandraki, et al., 2009; Simonyan, et al., 2009). Further research into the functional connectivity and white matter tracts of the brain could elucidate whether the left-hemisphere-dominant language components of speech and stronger intra- versus inter-hemispheric connectivity contribute to this phenomenon.

Activations in the right putamen and caudate during tongue press (VOI 4 and 6) and in the left cingulate and left PMA/SMA during both tongue press (VOI 5, 9, 10, and 11) and syllable repetition (VOI 8, 11, and 17) were negative. The caudate and putamen provide inhibitory input to the GP and STN, so a decrease in this inhibitory neural activity in the right putamen paired with an increase on the left could support the left-dominant control of orolingual movements evidenced in the cortical and thalamic activity. The posterior cingulate is theorized to contribute to the default mode network that maintains homeostasis at rest via inhibitory signals,

and this area deactivates during goal-directed tasks (Delaveau et al., 2010). Negative %SC here points toward cessation of the "rest" network during the active orolingual behaviors. For both the tongue press and syllable repetition tasks, PMA/SMA activations were positive on the right and negative on the left (tongue VOI 2 and 11; syllable VOI 4 and 17). These areas appear to be involved in the selection and planning of appropriate movements (PMA) and integration of bilateral movements (SMA; Kandel, et al., 2000). The relationship between PMA, SMA, and M1 is complex, but some research indicates the PMA/SMA exerts inhibitory control over M1 and overactivation of PMA/SMA results in an imbalance between agonist and antagonist muscles that interfere with the execution of fine motor tasks (Buch, Mars, Boorman, & Rushworth, 2010; Cuny et al., 2008; Murase et al., 2005). The polarized activations in the PMA/SMA in the current study are not readily explainable based on results from the current study. Although speculative, it may be that the polarized activations in the PMA/SMA are an accommodation to the left laterality of the rest of the sensorimotor integration network.

Nonspeech tongue press has been widely studied in kinematic research, but no published neuroimaging investigations of similar tongue force tasks exist for comparison. In this study, tongue press elicited fewer VOIs than the speech task but included some areas of BOLD signal beyond the shared ones described above. These additional areas were located in the right S1, left SA, right caudate, and bilateral putamen (tongue VOI 1, 4, 6, 8, and 12). The negative activation in the left SA likely signaled the termination of proprioceptive monitoring related to tongue bulb location during the actual press behavior (similar to the hand squeeze data). Caudate activation has not been reported in studies of nonspeech orolingual behavior, but has been noted in studies of multisyllabic and scaled hand force (Dresel, et al., 2005; Soros, et al., 2006; Spraker, et al., 2007; Ward, et al., 2008; Wasson, et al., 2010). This structure within the BG may only be

engaged in control of motor tasks that require high levels of force or precision of movement. No areas within the CB exceeded the established statistical parameters for the group RFX analysis during the tongue press. These results suggest that the relatively gross lingual elevation movement involved in this task did not require as much CB regulation as the more complex speech-like behaviors included in other studies.

The syllable repetition task yielded a greater number of VOIs overall, and a larger proportion of negative activations than the tongue press and the hand squeeze tasks. Syllable repetition is more dynamic in that it requires many contacts and releases throughout each five-second active block as opposed to the more static tongue press and hand squeeze. The relatively higher complexity of the speech movements could necessitate a larger network of excitatory and inhibitory inputs for accurate execution. Activations in the bilateral CB, the right subcentral parietal region, and the left midfrontal gyrus were identified in the speech task but not during the tongue press. The CB activations (syllable VOI 6, 7, and 15) are typical of findings in other speech-related studies, particularly when multi-syllable utterances are involved (Chang, Kenney, Loucks, Poletto, et al., 2009; Riecker, et al., 2006; Riecker, et al., 2005; Soros, et al., 2006). The subcentral parietal area (syllable VOI 3, BA 43) is associated with gustatory sensation; its involvement in this task is unclear and inconsistent with other speech neuroimaging research.

An area of midfrontal negative activation corresponding to Brodmann's area (BA) 10 (syllable VOI 18 in this study) has been implicated in high level sensory integration and executive functions via inhibitory control (Gilbert, Spengler, Simons, Frith, & Burgess, 2006; Petrides & Pandya, 2007; Simons, Scholvinck, Gilbert, Frith, & Burgess, 2006). This region has also been implicated as a key area for speech sound mapping (Ghosh, et al., 2008). Another center of midfrontal neural activity (syllable VOI 16, BA 8) is commonly linked to control of eye

movements and has recently been identified as the key area of inhibitory activity in an "go/no-go" paradigm (Nakata et al., 2009; Volz, Schubotz, & von Cramon, 2005). Activation of both of these midfrontal regions during the syllable repetition task but not the tongue press task is consistent with the roles specified in these earlier studies. That is, the syllable task demands more sensory integration of proprioceptive (and possibly auditory) signals in order to meet the articulatory contact point for /t/ repetition accurately and repeatedly. These speech movements also require precise accelerations and decelerations of the articulators, control of which may be mediated by co-activation of excitatory and inhibitory regions within the "go/no go" network.

Although the left anterior cingulate was active in both orolingual tasks, there was a much larger spatial extent of negative activation during speech repetition compared to tongue press. The anterior cingulate has been shown to use inhibitory signals to contribute to error detection. Because the syllable repetition task is more complex than tongue press, there is a greater potential for errors, thereby accounting for the increase in anterior cingulate activity.

The combined results for the tongue press and syllable repetition tasks were generally supportive of Hypothesis 1_B which predicted neural activity that included M1/S1, PMA/SMA, and cingulate cortices. However, this hypothesis also included an expectation of bilateral BG and CB activation for both tasks. This expectation was based on findings from previous neuroimaging studies of orolingual movements during speech and swallowing (Bohland & Guenther, 2006; Estep, 2009; Malandraki, et al., 2009; Riecker, et al., 2005). In the current study, no BG VOIs were detected during syllable repetition and no CB VOIs were detected during tongue press. The body of literature offers no comparable fMRI studies using lingual movements for power versus precision tasks, such as the tongue press versus syllable repetition. Studies of hand movements comparing sustained force and precise grip behaviors report greater

CB activations during the precision tasks without mention of BG activity (Ehrsson, et al., 2000; Keisker, Hepp-Reymond, Blickenstorfer, & Kollias, 2010; Keisker, et al., 2009; Kuhtz-Buschbeck, et al., 2001). Some studies have suggested that the BG are more correlated to changes in force production and externally-paced timing whereas CB seems to be responsible for internal rate coordination (Aparicio, Diedrichsen, & Ivry, 2005; Fellows, Ernst, Schwarz, Topper, & Noth, 2001; Teki, Grube, Kumar, & Griffiths, 2011). This theory is consistent with the differential findings regarding BG and CB activity in the nonspeech and speech tasks. There was evidence of putamen activation during syllables and CB activation during tongue press in some individuals' scans, so failure to meet group VOI thresholds as described above could also be related to the limited power of this study or intersubject variability in the precise location of activation.

Activations were expected in M1 but were not detected in either lingual task. A previous study of the location of the primary motor tongue area revealed intersubject variability up to several centimeters within the inferolateral central sulcus (Fesl et al., 2003). This inconsistent locus of activation across subjects and the limited statistical power of the small sample size may have prevented activations from being detected during the group analysis.

5.2 *Scaled Magnitude of Activations in Hand and Tongue Movements*

Statistically significant differences in activation intensity or volume across effort levels were identified in specific brain areas through the repeated measures ANOVAs for each of the three tasks. It should be noted that changes in intensity of activation (%SC) and volume of activation across effort levels did not always occur together for a given brain area. That is, as effort level changed, volume of activation might change significantly in a given area, but

intensity of activation might remain constant for that area. The fact that some brain areas exhibited statistically significant changes in effort-correlated activations in one measure but not the other (or different patterns of change across the two measures) may appear counterintuitive, but this is a relatively common finding in neuroimaging research. There are multiple reasonable explanations that have been offered. Brain volume and CBF both tend to decrease with age, but not necessarily to the same extent in an individual because of mitigating factors such as genetics, exercise, and disease process (Bangen, et al., 2009; Colcombe, et al., 2003; Honea, et al., 2009; Pereira, et al., 2007). Smoking, certain medications, and even internal adjustments to ambient temperature also can influence CBF but do not have immediate consequences for brain volume. Within an individual, CBF can be different from one brain region to another based on proximity to larger vessels and vascular compliance/occlusion. It is well-documented that spatial extent of neural activity for a given task tends to decrease with age (Buckner, et al., 2000; Hesselmann et al., 2001; Huettel, Singerman, & McCarthy, 2001; Ross et al., 1997). Other studies, however, have found increased activation volume in some areas and some tasks (D'Esposito, et al., 1999; Malandraki, et al., 2009; Riecker, et al., 2003). These results may reflect compensatory mechanisms in the older brain, wherein motor control plans are expanded to accommodate changes in the neuromuscular system. Within one cohort of older subjects, some brains could be undergoing this compensatory effect while others follow the more typical pattern of activation volume reduction. This would result in elevated variability across subjects and increased likelihood of nonsignificant findings. Finally, the variations in localization and vascularization for different anatomical and functional brain regions across and within subjects could account for discrepancies between the intensities of activations and their extents.

For each task, there were some areas where scaling was expected but not detected. Changes in BOLD signaling represent the totality of excitatory and inhibitory activations within a region, but the relative proportion of each of these two types of activation cannot be determined from the fMRI data. Researchers have theorized that differences in force execution are the result of shifts in the balance between excitatory and inhibitory activity within the various sensorimotor areas of the brain (Buccolieri, Abbruzzese, & Rothwell, 2004; Buccolieri et al., 2004; Spraker, et al., 2009). In this case, a region's activation at 25% MVC might be mostly inhibitory but at 75% MVC becomes mostly excitatory. If the *sum* of the excitatory and inhibitory activations within the region do not change from one effort level to another, no scaling effect is detected even though meaningful and real shifts in neural activity are occurring.

5.2.1 Scaled Magnitude in Hand Control

The hypothesis regarding the scaling of activations during hand squeeze (H_{2A}) was partially confirmed in the analysis of %SC and spatial extent of activation data. Two different patterns of effort-related differences in activation were predominant. First, a relationship wherein the activation measure increased across all effort levels was statistically significant in right CB (%SC and spatial extent, VOI 4) and left supramarginal (spatial extent, VOI 15) regions. The CB exhibited similar scaling effects in other hand-force studies (Keisker, et al., 2009; Spraker, et al., 2007; Ward, et al., 2008; Wasson, et al., 2010). Increases in activation of the supramarginal region have been inconsistently reported, but are reasonable given its role in sensorimotor feedback. Activations in right M1 (spatial extent, VOI 5), left thalamus (%SC and spatial extent, VOI 11) and left S1 regions (spatial extent, VOI 13) also were trending toward an increase across all effort levels but the changes were not statistically significant. Increasing activation in thalamus and S1 as effort level increased likely represents increased sensorimotor feedback at

the higher effort levels. The integration of this feedback to facilitate proprioception and kinesthesia is the primary role of the supramarginal area (Bohland & Guenther, 2006; de Vries, et al., 2009).

A second pattern of effort-correlated activations occurred in the %SC data from the right putamen, left posterior cingulate, left SA, left CB, left S1, and left supramarginal areas (VOI 6, 8, 9, 12, 13, and 15). In these regions, the intensity of the BOLD signal dropped from 25% MVC to 50% MVC, and then increased at 75% MVC to levels exceeding the 25% MVC signal. A similar pattern was detected in the spatial extent of activation data for the right putamen and left posterior cingulate (VOI 6 and 8). This V-shaped configuration indicates that mid-range force levels elicited less neural activity in these areas than either effort extreme. Spraker and colleagues (2007) reported a similar sigmoid-shaped scaling effect in their fMRI study of five incrementally increasing effort levels for hand grip. Perhaps this pattern indicates that the relative equilibrium of the motor control program is in this middle range, and higher or lower effort levels require additional accommodations by the neuromuscular system. This seems inconsistent with the decreased pressure matching accuracy in the middle of an individual's pressure range noted in behavioral studies, however (Crow & Ship, 1996; Lafargue, et al., 2008; O'Day, et al., 2005; Solomon, et al., 2000; Somodi, et al., 1995). Lower accuracy at these ranges in the pressure studies despite a linear relationship between perceived effort and actual force and a decrease in neural activity in these key areas at the middle ranges appears more suggestive of a failure of the motor plan to adjust to the demands of the middle effort range.

The positively correlated relationships between activation and effort level in S1, M1, thalamus, and CB were predicted in the study hypothesis, though not all activations or scaling trends were bilateral. The BG was the only other area expected to exhibit scaled activations, and

the V-configured upward trend partially met this projection. Previously described confounds to neuroimaging such as altered neurovascularity and brain volume, intersubject variability in locus of activation, and reciprocity in excitatory and inhibitory activations could account for the failure of all predicted areas to exhibit scaling activations bilaterally.

5.2.2 Scaled Magnitude in Lingual Control

Taken together, the changes in activation volume and intensity for tongue press and syllable repetition tasks were generally reflective of those predicted in the hypothesis (H_{2B}). For the tongue press, scaling was statistically significant only in right S1 (%SC, VOI 1), where it increased proportionally to effort level. Nonsignificant trends toward increased activation were also noted in right S1 (spatial extent, VOI 1), right PMA/SMA (%SC, VOI 2), and right putamen (%SC, VOI 4). Spatial extent of activation measures in the bilateral putamen (VOI 4 and 12) followed the V-shaped pattern previously noted in hand scaling, but did not reach statistically significant levels due at least in part to high intersubject variability. In addition to the detected scaling trends in S1 and BG, it was hypothesized that scaled activation would be evident in M1, thalamus, and CB. However, the absence of VOIs in M1, thalamus, and CB during tongue press precluded assessment of scaling for these regions. It may be that, in fact, these areas are not significantly involved in regulating force of tongue press. High intersubject variability, lack of power, or other factors affecting the detection of statistically significant group activations also may have compromised the assessment of scaling during tongue press.

Through analysis of the syllable repetition scaling, several interesting trends emerged. In multiple foci within the left cingulate (VOI 8, 9, and 11), %SC exhibited negative activations that increased in magnitude with higher effort levels. At the same time, spatial extent of activation increased to a statistically significant degree in two of the three VOIs. Given the

cingulate's previously-discussed role in error detection and the increased demands on the speech system at higher percentages of MVC, this scaling behavior is logical. This scaling supports motor control theory in that equilibrium, as measured by typical effort levels for speech, exists at the lower end of the force range and higher effort requires greater adjustments to the stable motor control pattern. Scaling also was noted in four separate foci within the left midfrontal gyrus and the left PMA/SMA (VOI 12, 16, 17, and 18). The pattern was statistically significant for spatial activation measures and approached or exceeded significance for %SC across all four areas. Less inhibitory control by these regions is likely to facilitate more effortful sensorimotor behaviors, though further studies of orolingual force control are necessary to confirm this hypothesis. Finally, both the right and left CB exhibited an inverted V pattern of %SC that approached statistical significance (VOI 6 and 15). The BOLD signal was highest at 50% MVC and lower at both extremes. This result could indicate that the motor control system is struggling to correct the lower accuracy levels detected at middle ranges during behavioral force control studies. The hypothesis of scaling during syllable repetition was partially supported for CB but not for M1, thalamus, or BG due to a failure to detect VOIs in these predicted areas.

5.3 *Positional Effects on Force Magnitude and Accuracy of Pressures*

5.3.1 Positional Effects on Hand Force Control

Results from the repeated measures ANOVAs are equivocal in supporting the hypothesis that pressure magnitude and target accuracy would be similar across positions for hand squeeze (H_{EX}). In terms of pressure magnitude, the interaction between position and effort level for actual pressures in the two-way ANOVA reflected statistically significant differences in actual hand squeeze pressures in upright versus supine positions across effort levels. Review of the raw data

indicates that the values were similar at 25% MVC but became more disparate at the higher effort levels. There were inadequate degrees of freedom for formal post hoc testing of this trend. The supine position yielded a higher MVC and higher pressure values across effort levels compared to upright. This could be a result of increased muscle recruitment and stability when the arm was extended at the reclined subject's side versus when the elbow was bent as the hand rested on the table in the seated position.

In terms of generating a specified pressure target (%MVC), the three-way ANOVA revealed a significant interaction between effort level and accuracy. The ability to match pressures reliably decreased as effort level increased, regardless of position. The effect of position on hand squeeze pressures was confirmed in this analysis, with lower pressures in the upright position compared to supine. The same supplementary muscle activity that was speculated to underlie higher supine hand pressures could have made fine control of the task more complex in the supine position, particularly since subjects are probably less accustomed to performing such tasks in that plane. No other studies directly comparing hand pressure in different body positions were identified, and the hand was used only for comparative purposes in this study. If the positional differences are confirmed in subsequent studies, researchers will have to be mindful of this effect when attempting to extrapolate findings acquired in fMRI scanners to execution of those same movements in upright positions.

5.3.2 Positional Effects on Orolingual Force Control

For tongue press and syllable repetition behaviors, position had no effect on actual pressures or accuracy of pressure matching, supporting the exploratory hypothesis. In fact, the pattern of actual and targeted pressures for the upright and supine positions was virtually identical in both of the orolingual tasks, though pressures were higher in the tongue press than in

the syllable repetition. The lack of a position effect on magnitude and accuracy of tongue pressure production is not overly surprising given that resting tongue position was unchanged in upright versus supine position in several ultrasound studies (Stone, Parthasarathy, et al., 2002; Stone, Sutton, & Crouse, 2002; Stone, Sutton, et al., 2002). Even though the gravitational influences on tongue movements when upright versus supine are different, they apparently are not sufficient to tax motor control plans or pressure generation capabilities in the tasks included here. The interaction between accuracy and effort level was significant in both tasks, with greater difficulty matching pressures at the higher percentages of MVC. This effect is similar to that documented by other researchers who identified lower accuracies in the middle of the physiological range (Somodi, et al., 1995). The fact that this accuracy-effort interaction was significant in all three study tasks could suggest that increased effort levels constrain the degrees of freedom of the motor control plan beyond its stable range, and the plan has not been adequately practiced within the new constraints to maintain accuracy in its execution. The absence of positional differences in orolingual force magnitude and accuracy measures offers reassurance for the validity of future neuroimaging studies. Although speech typically occurs while the speaker is upright, inferences about results obtained when subjects are reclined in the scanner may not be significantly undermined.

6.0 STUDY LIMITATIONS AND CONCLUSIONS

6.1 Limitations

Several limitations are inherent to this investigation into the neural bases of scaled orolingual movements. Statistical power was limited by small sample size as well as a novel methodology paradigm. A total of twelve subjects were included; a review of relevant neuroimaging literature that focuses on speech production indicates that small N studies are fairly common and the current sample size is commensurate with or even greater than other similar studies. However, it is increasingly clear that there can be substantial individual variability in the anatomical location of functional brain regions activated for a particular task. As such, it is important that future work strive for ever increasing the subject pool. As it stands, individual variability within the relatively small group of participants could have undermined the recognition of statistically significant BOLD signal changes at the group level.

An event-related design was selected to minimize motion artifact from orolingual movements. The ten-second epoch time with five seconds between task initiation and image acquisition was based on other sparse temporal sampling or clustered volume fMRI studies of orolingual behaviors (Bohland & Guenther, 2006; Dresel, et al., 2005; Estep, 2009). It is possible that this timing interval did not capture peak HDR, causing some signal loss of the BOLD response. The inclusion of jitter within the scanner sequence would have staggered the pause between task onset and image acquisition. Using this strategy, the BOLD signal is captured across the full evolution of the HDR, ensuring that peak BOLD is obtained in at least some of the fMRI volumes. This comes at the sacrifice of statistical power, since there are fewer trials of

each behavior at each phase of the HDR. Future studies could include jittered intervals on a more powerful scanner to address these issues.

Scanner limitations present another limitation to the neuroimaging of orolingual behaviors. Scanner fields of view are not unlimited and distortions increase at the edges of the field, so investigators are often forced to exclude tissue at the superior or inferior margins of the skull. Cortical activations were central to the specific aims of this study. In order to include the full expanse of the cortex, however, brainstem views had to be sacrificed. In addition to cranial nerve roots throughout the brainstem that might manifest important information, data regarding central pattern generators in the brainstem could contribute to our understanding of neural control of orolingual movements. Preliminary studies such as this offer researchers the opportunity to make more informed choices about how to select the most relevant neural areas of interest (and thus focus the scanner field of view) for future studies. Advancements in scanner technology also may expand the range of high-quality imaging dimensions, reducing the need to exclude brain regions from the imaged field.

The methodological paradigm utilized in this study also may have limited statistical power. The chosen approach was discussed in more detail in Section 3.4.2. In order to expose activations in anticipated areas of neural activity, data analysis incorporated statistical thresholds that were not subjected to traditional methods of multiple comparison correction. While these methods have been shown to control Type I error as effectively as the traditional methods, they also decrease the risk of Type II error. Even so, thousands of calculations were involved in fMRI processing and it is likely that at least some of the voxels considered active were falsely positive.

Additional limitations are related to generalization of results and replication of the approach with other populations of interest. The sample population was comprised of middle-

aged adults who were free from neurological disease by self-report. Future studies involving patient populations may be more complex because disease progression and the corresponding alternations in brain tissue may introduce further intersubject variability. Additional confounds of neuroimaging research in aged and diseased populations and potential solutions were reviewed in Section 2.4. Larger sample size in future studies could attenuate all of these factors during group analysis.

The length of tubing necessary to accommodate the distance from the subject to the pressure transducer distorted the actual pressure values obtained. This prevented the data from being directly compared to that from previous behavioral studies of hand and tongue force control. Using pressures referenced to maximum within each subject was sufficient for the purposes of this study focused on scaled activations; however, it precludes confirmation that the subjects were generating expected pressures with the hand and tongue. Currently, the equipment configuration requires the hand bulb and tongue bulb to be exchanged on the single tubing-transducer line multiple times over the course of the study session. Some of these switches occur while the subject is in the scanner and all are done in the presence of the subject, so it would be cumbersome to recalibrate the entire system to a standard baseline pressure at each exchange. In the future, the use of multiple transducers could allow the bulb-tubing-transducer system to remain closed throughout the experiment. This way, baseline pressures could be matched to a consistent standard once during the equipment setup that precedes each subject session. Known pressures could be applied to this MRI-compatible setup as well as the short-tubed IOPI configuration that has been used in a number of behavioral studies and a corrective algorithm could be developed. This formula could be applied to the data obtained with the MR-compatible arrangement, converting the raw pressure data to the scale of other studies using IOPI bulbs.

6.2 Conclusions

This study is the first to outline the neural substrates of orolingual force control and to demonstrate scaling of neural activations in speech and nonspeech behaviors. As hypothesized, the hand squeeze task elicited activations in M1/S1, thalamus, putamen, and CB, with scaling in S1 and CB. Additional areas of neural activity that scaled with effort during hand squeeze included the left cingulate and supramarginal cortices. Tongue press and syllable production tasks shared areas of group activation in bilateral PMA/SMA, left cingulate, and right fusiform. BG activations were noted during tongue press but not syllable repetition, whereas CB activations occurred during syllable repetition but not tongue press. Several areas of midfrontal activation were only active during syllable repetition, suggesting that an intricate network of inhibitory and excitatory controls modulates the more complex speech task. Scaling was observed in S1 for the tongue press and in cingulate, PMA/SMA, and midfrontal regions of the left hemisphere during syllable repetition. This left lateralization during motor speech behavior has been observed in other studies. Pressure data indicated that accuracy of pressure matching decreased at higher effort levels for all study tasks regardless of position. Hand squeeze pressures were lower in the upright position compared to supine, but position did not affect tongue press or syllable repetition pressures. These findings give preliminary evidence of modulated neural activity in brain regions that contribute to the control of orolingual speech and nonspeech tasks and offer further insights into the accommodation of perturbations to motor control plans. These results inform future studies of healthy and disease populations, and may help elucidate differences in neural control that contribute to dysarthria and other motor speech disorders.

Literature Citations

Ackermann, H. (2008). Cerebellar contributions to speech production and speech perception: psycholinguistic and neurobiological perspectives. *Trends Neurosci, 31*(6), 265-272.

Ackermann, H., & Riecker, A. (2004). The contribution of the insula to motor aspects of speech production: a review and a hypothesis. *Brain Lang, 89*(2), 320-328.

Alkadhi, H., Crelier, G. R., Boendermaker, S. H., Golay, X., Hepp-Reymond, M. C., & Kollias, S. S. (2002). Reproducibility of primary motor cortex somatotopy under controlled conditions. *AJNR Am J Neuroradiol, 23*(9), 1524-1532.

Allison, J. D., Meador, K. J., Loring, D. W., Figueroa, R. E., & Wright, J. C. (2000). Functional MRI cerebral activation and deactivation during finger movement. *Neurology, 54*(1), 135-142.

Amerman, J. D., & Parnell, M. M. (1990). Auditory impressions of the speech of normal elderly adults. *Br J Disord Commun, 25*(1), 35-43.

Aparicio, P., Diedrichsen, J., & Ivry, R. B. (2005). Effects of focal basal ganglia lesions on timing and force control. *Brain Cogn, 58*(1), 62-74.

Arima, T., Yanagi, Y., Niddam, D. M., Ohata, N., Arendt-Nielsen, L., Minagi, S., et al. (2011). Corticomotor plasticity induced by tongue-task training in humans: a longitudinal fMRI study. *Exp Brain Res, 212*(2), 199-212.

Bangen, K. J., Restom, K., Liu, T. T., Jak, A. J., Wierenga, C. E., Salmon, D. P., et al. (2009). Differential age effects on cerebral blood flow and BOLD response to encoding: associations with cognition and stroke risk. *Neurobiol Aging, 30*(8), 1276-1287.

Baweja, H. S., Patel, B. K., Martinkewiz, J. D., Vu, J., & Christou, E. A. (2009). Removal of visual feedback alters muscle activity and reduces force variability during constant isometric contractions. *Exp Brain Res, 197*(1), 35-47.

Benjamin, B. J. (1982). Phonological performance in gerontological speech. *J Psycholinguist Res, 11*(2), 159-167.

Benjamin, B. J. (1997). Speech production of normally aging adults. *Semin Speech Lang, 18*(2), 135-141.

Bethel-Brown, C. S., Morris, J. K., & Stanford, J. A. (2011). Young and middle-aged rats exhibit isometric forelimb force control deficits in a model of early-stage Parkinson's disease. *Behav Brain Res, 225*(1), 97-103.

Bianciardi, M., Fukunaga, M., van Gelderen, P., de Zwart, J. A., & Duyn, J. H. (2011). Negative BOLD-fMRI signals in large cerebral veins. *J Cereb Blood Flow Metab, 31*(2), 401-412.

Birn, R. M., Bandettini, P. A., Cox, R. W., & Shaker, R. (1999). Event-related fMRI of tasks involving brief motion. *Hum Brain Mapp, 7*(2), 106-114.

Birn, R. M., Cox, R. W., & Bandettini, P. A. (2004). Experimental designs and processing strategies for fMRI studies involving overt verbal responses. *Neuroimage, 23*(3), 1046-1058.

Bodegard, A., Geyer, S., Herath, P., Grefkes, C., Zilles, K., & Roland, P. E. (2003). Somatosensory areas engaged during discrimination of steady pressure, spring strength, and kinesthesia. *Hum Brain Mapp, 20*(2), 103-115.

Bohland, J. W., & Guenther, F. H. (2006). An fMRI investigation of syllable sequence production. *Neuroimage, 32*(2), 821-841.

Brown, S., Laird, A. R., Pfordresher, P. Q., Thelen, S. M., Turkeltaub, P., & Liotti, M. (2009). The somatotopy of speech: phonation and articulation in the human motor cortex. *Brain Cogn, 70*(1), 31-41.

Buccolieri, A., Abbruzzese, G., & Rothwell, J. C. (2004). Relaxation from a voluntary contraction is preceded by increased excitability of motor cortical inhibitory circuits. *J Physiol, 558*(Pt 2), 685-695.

Buccolieri, A., Avanzino, L., Marinelli, L., Trompetto, C., Marchese, R., & Abbruzzese, G. (2004). Muscle relaxation is impaired in dystonia: a reaction time study. *Mov Disord, 19*(6), 681-687.

Buch, E. R., Mars, R. B., Boorman, E. D., & Rushworth, M. F. (2010). A network centered on ventral premotor cortex exerts both facilitatory and inhibitory control over primary motor cortex during action reprogramming. *J Neurosci, 30*(4), 1395-1401.

Buckner, R. L., Snyder, A. Z., Sanders, A. L., Raichle, M. E., & Morris, J. C. (2000). Functional brain imaging of young, nondemented, and demented older adults. *J Cogn Neurosci, 12 Suppl 2*, 24-34.

Carroll, E., & Sanchez-Ramos, J. (2011). Hyperkinetic movement disorders associated with HIV and other viral infections. *Handb Clin Neurol, 100*, 323-334.

Caruso, A. J., McClowry, M. T., & Max, L. (1997). Age-related effects on speech fluency. *Semin Speech Lang, 18*(2), 171-179; quiz 179-180.

Chang, S. E., Kenney, M. K., Loucks, T. M., & Ludlow, C. L. (2009). Brain activation abnormalities during speech and non-speech in stuttering speakers. *Neuroimage, 46*(1), 201-212.

Chang, S. E., Kenney, M. K., Loucks, T. M., Poletto, C. J., & Ludlow, C. L. (2009). Common neural substrates support speech and non-speech vocal tract gestures. *Neuroimage, 47*(1), 314-325.

Ciucci, M. R., & Connor, N. P. (2009). Dopaminergic influence on rat tongue function and limb movement initiation. *Exp Brain Res, 194*(4), 587-596.

Colcombe, S. J., Erickson, K. I., Raz, N., Webb, A. G., Cohen, N. J., McAuley, E., et al. (2003). Aerobic fitness reduces brain tissue loss in aging humans. *J Gerontol A Biol Sci Med Sci, 58*(2), 176-180.

Cools, R., Miyakawa, A., Sheridan, M., & D'Esposito, M. (2010). Enhanced frontal function in Parkinson's disease. *Brain, 133*(Pt 1), 225-233.

Costagli, M., Waggoner, R. A., Ueno, K., Tanaka, K., & Cheng, K. (2009). Correction of 3D rigid body motion in fMRI time series by independent estimation of rotational and translational effects in k-space. *Neuroimage, 45*(3), 749-757.

Crow, H. C., & Ship, J. A. (1996). Tongue strength and endurance in different aged individuals. *J Gerontol A Biol Sci Med Sci, 51*(5), M247-250.

Cuny, E., Ghorayeb, I., Guehl, D., Escola, L., Bioulac, B., & Burbaud, P. (2008). Sensory motor mismatch within the supplementary motor area in the dystonic monkey. *Neurobiol Dis, 30*(2), 151-161.

D'Esposito, M., Deouell, L. Y., & Gazzaley, A. (2003). Alterations in the BOLD fMRI signal with ageing and disease: a challenge for neuroimaging. *Nat Rev Neurosci, 4*(11), 863-872.

D'Esposito, M., Zarahn, E., Aguirre, G. K., & Rypma, B. (1999). The effect of normal aging on the coupling of neural activity to the bold hemodynamic response. *Neuroimage, 10*(1), 6-14.

de Graaf, J. B., Gallea, C., Pailhous, J., Anton, J. L., Roth, M., & Bonnard, M. (2004). Awareness of muscular force during movement production: an fMRI study. *Neuroimage, 21*(4), 1357-1367.

de Vries, P. M., de Jong, B. M., Bohning, D. E., Walker, J. A., George, M. S., & Leenders, K. L. (2009). Changes in cerebral activations during movement execution and imagery after parietal cortex TMS interleaved with 3T MRI. *Brain Res, 1285*, 58-68.

Delaveau, P., Salgado-Pineda, P., Fossati, P., Witjas, T., Azulay, J. P., & Blin, O. (2010). Dopaminergic modulation of the default mode network in Parkinson's disease. *Eur Neuropsychopharmacol, 20*(11), 784-792.

Dickerson, C. R., Martin, B. J., & Chaffin, D. B. (2007). Predictors of perceived effort in the shoulder during load transfer tasks. *Ergonomics, 50*(7), 1004-1016.

Dresel, C., Castrop, F., Haslinger, B., Wohlschlaeger, A. M., Hennenlotter, A., & Ceballos-Baumann, A. O. (2005). The functional neuroanatomy of coordinated orofacial movements: sparse sampling fMRI of whistling. *Neuroimage, 28*(3), 588-597.

Edmister, W. B., Talavage, T. M., Ledden, P. J., & Weisskoff, R. M. (1999). Improved auditory cortex imaging using clustered volume acquisitions. *Hum Brain Mapp, 7*(2), 89-97.

Ehrsson, H. H., Fagergren, A., Jonsson, T., Westling, G., Johansson, R. S., & Forssberg, H. (2000). Cortical activity in precision- versus power-grip tasks: an fMRI study. *J Neurophysiol, 83*(1), 528-536.

Estep, M. E. (2009). Cortical and subcortical corelates of ororhythmic behaviors. Unpublished Dissertation. University of Kansas.

Feldman, A. G. (2008). New insights into action-perception coupling. *Exp Brain Res*.

Fellows, S. J., Ernst, J., Schwarz, M., Topper, R., & Noth, J. (2001). Precision grip deficits in cerebellar disorders in man. *Clin Neurophysiol, 112*(10), 1793-1802.

Fesl, G., Moriggl, B., Schmid, U. D., Naidich, T. P., Herholz, K., & Yousry, T. A. (2003). Inferior central sulcus: variations of anatomy and function on the example of the motor tongue area. *Neuroimage, 20*(1), 601-610.

Field, A. S., Yen, Y. F., Burdette, J. H., & Elster, A. D. (2000). False cerebral activation on BOLD functional MR images: study of low-amplitude motion weakly correlated to stimulus. *AJNR Am J Neuroradiol, 21*(8), 1388-1396.

Fink, G. R., Frackowiak, R. S., Pietrzyk, U., & Passingham, R. E. (1997). Multiple nonprimary motor areas in the human cortex. *J Neurophysiol, 77*(4), 2164-2174.

Forman, S. D., Cohen, J. D., Fitzgerald, M., Eddy, W. F., Mintun, M. A., & Noll, D. C. (1995). Improved assessment of significant activation in functional magnetic resonance imaging (fMRI): use of a cluster-size threshold. *Magn Reson Med, 33*(5), 636-647.

Friston, K. J., Holmes, A. P., Price, C. J., Buchel, C., & Worsley, K. J. (1999). Multisubject fMRI studies and conjunction analyses. *Neuroimage, 10*(4), 385-396.

Gentil, M., & Tournier, C. L. (1998). Differences in fine control of forces generated by the tongue, lips and fingers in humans. *Arch Oral Biol, 43*(7), 517-523.

Ghosh, S. S., Tourville, J. A., & Guenther, F. H. (2008). A neuroimaging study of premotor lateralization and cerebellar involvement in the production of phonemes and syllables. *J Speech Lang Hear Res, 51*(5), 1183-1202.

Giannakopoulou, D., Armata, I., Mitsacos, A., Shashidharan, P., & Giompres, P. (2010). Modulation of the basal ganglia dopaminergic system in a transgenic mouse exhibiting dystonia-like features. *J Neural Transm, 117*(12), 1401-1409.

Gilbert, S. J., Spengler, S., Simons, J. S., Frith, C. D., & Burgess, P. W. (2006). Differential functions of lateral and medial rostral prefrontal cortex (area 10) revealed by brain-behavior associations. *Cereb Cortex, 16*(12), 1783-1789.

Goozee, J. V., Stephenson, D. K., Murdoch, B. E., Darnell, R. E., & Lapointe, L. L. (2005). Lingual kinematic strategies used to increase speech rate: comparison between younger and older adults. *Clin Linguist Phon, 19*(4), 319-334.

Gracco, V. L., Tremblay, P., & Pike, B. (2005). Imaging speech production using fMRI. *Neuroimage, 26*(1), 294-301.

Hall, D. A., Haggard, M. P., Akeroyd, M. A., Palmer, A. R., Summerfield, A. Q., Elliott, M. R., et al. (1999). "Sparse" temporal sampling in auditory fMRI. *Hum Brain Mapp, 7*(3), 213-223.

Handwerker, D. A., Ollinger, J. M., & D'Esposito, M. (2004). Variation of BOLD hemodynamic responses across subjects and brain regions and their effects on statistical analyses. *Neuroimage, 21*(4), 1639-1651.

Hesselmann, V., Zaro Weber, O., Wedekind, C., Krings, T., Schulte, O., Kugel, H., et al. (2001). Age related signal decrease in functional magnetic resonance imaging during motor stimulation in humans. *Neurosci Lett, 308*(3), 141-144.

Hewitt, A., Hind, J., Kays, S., Nicosia, M., Doyle, J., Tompkins, W., et al. (2008). Standardized instrument for lingual pressure measurement. *Dysphagia, 23*(1), 16-25.

Hikosaka, O. (2007). GABAergic output of the basal ganglia. *Prog Brain Res, 160*, 209-226.

Ho, A. K., Iansek, R., Marigliani, C., Bradshaw, J. L., & Gates, S. (1998). Speech impairment in a large sample of patients with Parkinson's disease. *Behav Neurol, 11*(3), 131-137.

Honea, R. A., Thomas, G. P., Harsha, A., Anderson, H. S., Donnelly, J. E., Brooks, W. M., et al. (2009). Cardiorespiratory fitness and preserved medial temporal lobe volume in Alzheimer disease. *Alzheimer Dis Assoc Disord, 23*(3), 188-197.

Huang, J., Carr, T. H., & Cao, Y. (2002). Comparing cortical activations for silent and overt speech using event-related fMRI. *Hum Brain Mapp, 15*(1), 39-53.

Huettel, S. A., Singerman, J. D., & McCarthy, G. (2001). The effects of aging upon the hemodynamic response measured by functional MRI. *Neuroimage, 13*(1), 161-175.

Huettel, S. A., Song, A. W., & McCarthy, G. (2004). *Functional Magnetic Resonance Imaging*. Sunderland, Masachusetts: Sinauer Associates, Inc.

Hughes, L. E., Barker, R. A., Owen, A. M., & Rowe, J. B. (2010). Parkinson's disease and healthy aging: Independent and interacting effects on action selection. *Hum Brain Mapp*.

Jones, T. B., Bandettini, P. A., & Birn, R. M. (2008). Integration of motion correction and physiological noise regression in fMRI. *Neuroimage, 42*(2), 582-590.

Kandel, E. R., Schwartz, J. H., & Jessell, T. M. (Eds.). (2000). *Principles of Neural Science* (4th ed.). New York: McGraw-Hill.

Kannurpatti, S. S., Motes, M. A., Rypma, B., & Biswal, B. B. (2010). Neural and vascular variability and the fMRI-BOLD response in normal aging. *Magn Reson Imaging*.

Keisker, B., Hepp-Reymond, M. C., Blickenstorfer, A., & Kollias, S. S. (2010). Differential representation of dynamic and static power grip force in the sensorimotor network. *Eur J Neurosci, 31*(8), 1483-1491.

Keisker, B., Hepp-Reymond, M. C., Blickenstorfer, A., Meyer, M., & Kollias, S. S. (2009). Differential force scaling of fine-graded power grip force in the sensorimotor network. *Hum Brain Mapp, 30*(8), 2453-2465.

Kelchner, L. N., Toner, M. M., & Lee, L. (2006). Effects of prolonged loud reading on normal adolescent male voices. *Lang Speech Hear Serv Sch, 37*(2), 96-103.

Kemeny, S., Ye, F. Q., Birn, R., & Braun, A. R. (2005). Comparison of continuous overt speech fMRI using BOLD and arterial spin labeling. *Hum Brain Mapp, 24*(3), 173-183.

Kent, R. D., Duffy, J. R., Slama, A., Kent, J. F., & Clift, A. (2001). Clinicoanatomic studies in dysarthria: review, critique, and directions for research. *J Speech Lang Hear Res, 44*(3), 535-551.

Kent, R. D., Kent, J. F., & Rosenbek, J. C. (1987). Maximum performance tests of speech production. *J Speech Hear Disord, 52*(4), 367-387.

Koch, W., Teipel, S., Mueller, S., Buerger, K., Bokde, A. L., Hampel, H., et al. (2010). Effects of aging on default mode network activity in resting state fMRI: does the method of analysis matter? *Neuroimage, 51*(1), 280-287.

Kuhtz-Buschbeck, J. P., Ehrsson, H. H., & Forssberg, H. (2001). Human brain activity in the control of fine static precision grip forces: an fMRI study. *Eur J Neurosci, 14*(2), 382-390.

Lafargue, G., D'Amico, A., Thobois, S., Broussolle, E., & Sirigu, A. (2008). The ability to assess muscular force in asymmetrical Parkinson's disease. *Cortex, 44*(1), 82-89.

Lam, Y. W., & Sherman, S. M. (2010). Functional organization of the somatosensory cortical layer 6 feedback to the thalamus. *Cereb Cortex, 20*(1), 13-24.

Latash, M. L., Levin, M. F., Scholz, J. P., & Schoner, G. (2010). Motor control theories and their applications. *Medicina (Kaunas), 46*(6), 382-392.

Laukkanen, A. M., Ilomaki, I., Leppanen, K., & Vilkman, E. (2008). Acoustic measures and self-reports of vocal fatigue by female teachers. *J Voice, 22*(3), 283-289.

Leenders, K. L., Perani, D., Lammertsma, A. A., Heather, J. D., Buckingham, P., Healy, M. J., et al. (1990). Cerebral blood flow, blood volume and oxygen utilization. Normal values and effect of age. *Brain, 113 (Pt 1)*, 27-47.

Lieberman, M. D., & Cunningham, W. A. (2009). Type I and Type II error concerns in fMRI research: re-balancing the scale. *Soc Cogn Affect Neurosci, 4*(4), 423-428.

Lindquist, M. A. (2008). The statistical analysis of fMRI data. *Statistical Science, 23*(4), 439-464.

Liss, J. M., Weismer, G., & Rosenbek, J. C. (1990). Selected acoustic characteristics of speech production in very old males. *J Gerontol, 45*(2), P35-45.

Lu, T., Pan, Y., Kao, S. Y., Li, C., Kohane, I., Chan, J., et al. (2004). Gene regulation and DNA damage in the ageing human brain. *Nature, 429*(6994), 883-891.

Luschei, E. S. (1991). Development of objective standards of nonspeech oral strength and performance: An advocate's view. In C. A. Moore, K. Yorkston & D. R. Beukelman (Eds.), *Dysarthria and apraxia of speech: Perspectives on Management* (pp. 3-14). Baltimore: Paul H Brookes Publishing Co.

Luschei, E. S. (2009). IOPI User's Manual: Iowa Oral Performance Instrument Model 2.1. In L. IOPI™ Northwest Co. (Ed.). Carnation, WA: IOPI™ Northwest Co., LLC.

Malandraki, G. A., Sutton, B. P., Perlman, A. L., & Karampinos, D. C. (2009). Age-Related Differences in Laterality of Cortical Activations in Swallowing. *Dysphagia*.

Marchal, G., Rioux, P., Petit-Taboue, M. C., Sette, G., Travere, J. M., Le Poec, C., et al. (1992). Regional cerebral oxygen consumption, blood flow, and blood volume in healthy human aging. *Arch Neurol, 49*(10), 1013-1020.

Martin, A. J., Friston, K. J., Colebatch, J. G., & Frackowiak, R. S. (1991). Decreases in regional cerebral blood flow with normal aging. *J Cereb Blood Flow Metab, 11*(4), 684-689.

McAuliffe, M. J., Ward, E. C., Murdoch, B. E., & Farrell, A. M. (2005). A nonspeech investigation of tongue function in Parkinson's disease. *J Gerontol A Biol Sci Med Sci, 60*(5), 667-674.

Mehta, Verber, M. D., Wieser, J. A., Schmit, B. D., & Schindler-Ivens, S. M. (2009). A novel technique for examining human brain activity associated with pedaling using fMRI. *J Neurosci Methods, 179*(2), 230-239.

Mehta, S., Grabowski, T. J., Razavi, M., Eaton, B., & Bolinger, L. (2006). Analysis of speech-related variance in rapid event-related fMRI using a time-aware acquisition system. *Neuroimage, 29*(4), 1278-1293.

Miller, E. K., & Cohen, J. D. (2001). An integrative theory of prefrontal cortex function. *Annu Rev Neurosci, 24*, 167-202.

Min, B. K. (2010). A thalamic reticular networking model of consciousness. *Theor Biol Med Model, 7*, 10.

Mink, J. W. (Ed.). (2003). *The Basal Ganglia*. Amsterdam: Academic Press.

Muellbacher, W., Artner, C., & Mamoli, B. (1999). The role of the intact hemisphere in recovery of midline muscles after recent monohemispheric stroke. *J Neurol, 246*(4), 250-256.

Murase, N., Rothwell, J. C., Kaji, R., Urushihara, R., Nakamura, K., Murayama, N., et al. (2005). Subthreshold low-frequency repetitive transcranial magnetic stimulation over the premotor cortex modulates writer's cramp. *Brain, 128*(Pt 1), 104-115.

Murphy, K., Corfield, D. R., Guz, A., Fink, G. R., Wise, R. J., Harrison, J., et al. (1997). Cerebral areas associated with motor control of speech in humans. *J Appl Physiol, 83*(5), 1438-1447.

Nakata, H., Sakamoto, K., Ferretti, A., Gianni Perrucci, M., Del Gratta, C., Kakigi, R., et al. (2009). Negative BOLD effect on somato-motor inhibitory processing: an fMRI study. *Neurosci Lett, 462*(2), 101-104.

Nebel, K., Stude, P., Wiese, H., Muller, B., de Greiff, A., Forsting, M., et al. (2005). Sparse imaging and continuous event-related fMRI in the visual domain: a systematic comparison. *Hum Brain Mapp, 24*(2), 130-143.

Nunes, E. J., Randall, P. A., Santerre, J. L., Given, A. B., Sager, T. N., Correa, M., et al. (2010). Differential effects of selective adenosine antagonists on the effort-related impairments induced by dopamine D1 and D2 antagonism. *Neuroscience, 170*(1), 268-280.

O'Day, C., Frank, E., Montgomery, A., Nichols, M., & McDade, H. (2005). Repeated tongue and hand strength measurements in normal adults and individuals with Parkinson's disease. *Int J Orofacial Myology, 31*, 15-25.

Okada, T., & Nakai, T. (2003). Silent fMRI acquisition methods for large acoustic noise during scan. *Magn Reson Med Sci, 2*(4), 181-187.

Oldfield, R. C. (1971). The assessment and analysis of handedness: the Edinburgh inventory. *Neuropsychologia, 9*(1), 97-113.

Pereira, A. C., Huddleston, D. E., Brickman, A. M., Sosunov, A. A., Hen, R., McKhann, G. M., et al. (2007). An in vivo correlate of exercise-induced neurogenesis in the adult dentate gyrus. *Proc Natl Acad Sci U S A, 104*(13), 5638-5643.

Petrides, M., & Pandya, D. N. (2007). Efferent association pathways from the rostral prefrontal cortex in the macaque monkey. *J Neurosci, 27*(43), 11573-11586.

Poldrack, R. A., & Mumford, J. A. (2009). Independence in ROI analysis: where is the voodoo? *Soc Cogn Affect Neurosci, 4*(2), 208-213.

Potter, N. L., & Short, R. (2009). Maximal tongue strength in typically developing children and adolescents. *Dysphagia, 24*(4), 391-397.

Rademacher, J., Burgel, U., Geyer, S., Schormann, T., Schleicher, A., Freund, H. J., et al. (2001). Variability and asymmetry in the human precentral motor system. A cytoarchitectonic and myeloarchitectonic brain mapping study. *Brain, 124*(Pt 11), 2232-2258.

Rajah, M. N., & D'Esposito, M. (2005). Region-specific changes in prefrontal function with age: a review of PET and fMRI studies on working and episodic memory. *Brain, 128*(Pt 9), 1964-1983.

Ramig, L. O., Fox, C., & Sapir, S. (2008). Speech treatment for Parkinson's disease. *Expert Rev Neurother, 8*(2), 297-309.

Raz, N., Lindenberger, U., Rodrigue, K. M., Kennedy, K. M., Head, D., Williamson, A., et al. (2005). Regional brain changes in aging healthy adults: general trends, individual differences and modifiers. *Cereb Cortex, 15*(11), 1676-1689.

Riecker, A., Grodd, W., Klose, U., Schulz, J. B., Groschel, K., Erb, M., et al. (2003). Relation between regional functional MRI activation and vascular reactivity to carbon dioxide during normal aging. *J Cereb Blood Flow Metab, 23*(5), 565-573.

Riecker, A., Kassubek, J., Groschel, K., Grodd, W., & Ackermann, H. (2006). The cerebral control of speech tempo: opposite relationship between speaking rate and BOLD signal changes at striatal and cerebellar structures. *Neuroimage, 29*(1), 46-53.

Riecker, A., Mathiak, K., Wildgruber, D., Erb, M., Hertrich, I., Grodd, W., et al. (2005). fMRI reveals two distinct cerebral networks subserving speech motor control. *Neurology, 64*(4), 700-706.

Robin, D. A., Goel, A., Somodi, L. B., & Luschei, E. S. (1992). Tongue strength and endurance: relation to highly skilled movements. *J Speech Hear Res, 35*(6), 1239-1245.

Robin, D. A., Somodi, L. B., & Luschei, E. (1991). Measurement of tongue strength and endurance in normal and articulation disordered subjects. In C. A. Moore, K. M. Yorkston & D. R. Beukelman (Eds.), *Dysarthria and Apraxia of Speech* (pp. 173-184). Baltimore: Paul H Brookes Publishing Co.

Ross, M. H., Yurgelun-Todd, D. A., Renshaw, P. F., Maas, L. C., Mendelson, J. H., Mello, N. K., et al. (1997). Age-related reduction in functional MRI response to photic stimulation. *Neurology, 48*(1), 173-176.

Salamone, J. D. (2009). Dopamine, effort, and decision making: theoretical comment on Bardgett et al. (2009). *Behav Neurosci, 123*(2), 463-467.

Salamone, J. D., Correa, M., Farrar, A. M., Nunes, E. J., & Pardo, M. (2009). Dopamine, behavioral economics, and effort. *Front Behav Neurosci, 3*, 13.

Salamone, J. D., Farrar, A. M., Font, L., Patel, V., Schlar, D. E., Nunes, E. J., et al. (2009). Differential actions of adenosine A1 and A2A antagonists on the effort-related effects of dopamine D2 antagonism. *Behav Brain Res, 201*(1), 216-222.

Searl, J. (2007). Bilabial contact pressure and oral air pressure during tracheoesophageal speech. *Ann Otol Rhinol Laryngol, 116*(4), 304-311.

Simons, J. S., Scholvinck, M. L., Gilbert, S. J., Frith, C. D., & Burgess, P. W. (2006). Differential components of prospective memory? Evidence from fMRI. *Neuropsychologia, 44*(8), 1388-1397.

Simonyan, K., Ostuni, J., Ludlow, C. L., & Horwitz, B. (2009). Functional but not structural networks of the human laryngeal motor cortex show left hemispheric lateralization during syllable but not breathing production. *J Neurosci, 29*(47), 14912-14923.

Skitek, E. B., Fowler, S. C., & Tessel, R. E. (1999). Effects of unilateral striatal dopamine depletion on tongue force and rhythm during licking in rats. *Behav Neurosci, 113*(3), 567-573.

Slifkin, A. B., Vaillancourt, D. E., & Newell, K. M. (2000). Intermittency in the control of continuous force production. *J Neurophysiol, 84*(4), 1708-1718.

Solomon, N. P., Drager, K. D., & Luschei, E. S. (2002). Sustaining a constant effort by the tongue and hand: effects of acute fatigue. *J Speech Lang Hear Res, 45*(4), 613-624.

Solomon, N. P., & Munson, B. (2004). The effect of jaw position on measures of tongue strength and endurance. *J Speech Lang Hear Res, 47*(3), 584-594.

Solomon, N. P., & Robin, D. A. (2005). Perceptions of effort during handgrip and tongue elevation in Parkinson's disease. *Parkinsonism Relat Disord, 11*(6), 353-361.

Solomon, N. P., Robin, D. A., & Luschei, E. S. (2000). Strength, endurance, and stability of the tongue and hand in Parkinson disease. *J Speech Lang Hear Res, 43*(1), 256-267.

Solomon, N. P., Robin, D. A., Mitchinson, S. I., VanDaele, D. J., & Luschei, E. S. (1996). Sense of effort and the effects of fatigue in the tongue and hand. *J Speech Hear Res, 39*(1), 114-125.

Soltysik, D. A., & Hyde, J. S. (2008). High spatial resolution increases the specificity of block-design BOLD fMRI studies of overt vowel production. *Neuroimage, 41*(2), 389-397.

Somodi, L. B., Robin, D. A., & Luschei, E. S. (1995). A model of "sense of effort" during maximal and submaximal contractions of the tongue. *Brain Lang, 51*(3), 371-382.

Soros, P., Lalone, E., Smith, R., Stevens, T., Theurer, J., Menon, R. S., et al. (2008). Functional MRI of oropharyngeal air-pulse stimulation. *Neuroscience, 153*(4), 1300-1308.

Soros, P., Sokoloff, L. G., Bose, A., McIntosh, A. R., Graham, S. J., & Stuss, D. T. (2006). Clustered functional MRI of overt speech production. *Neuroimage, 32*(1), 376-387.

Spraker, M. B., Corcos, D. M., & Vaillancourt, D. E. (2009). Cortical and subcortical mechanisms for precisely controlled force generation and force relaxation. *Cereb Cortex, 19*(11), 2640-2650.

Spraker, M. B., Yu, H., Corcos, D. M., & Vaillancourt, D. E. (2007). Role of individual basal ganglia nuclei in force amplitude generation. *J Neurophysiol, 98*(2), 821-834.

Sterr, A., Shen, S., Kranczioch, C., Szameitat, A. J., Hou, W., & Sorger, B. (2009). fMRI effects of task demand and feedback accuracy on grip force tracking. *Neurosci Lett, 457*(2), 61-65.

Talairach, J., & Tornoux, P. (1988). *Co-planar stereotaxic atlas of the human brain : 3-dimensional proportional system : an approach to cerebral imaging*. Stuttgart: Georg Thieme.

Teki, S., Grube, M., Kumar, S., & Griffiths, T. D. (2011). Distinct neural substrates of duration-based and beat-based auditory timing. *J Neurosci, 31*(10), 3805-3812.

Toma, K., Honda, M., Hanakawa, T., Okada, T., Fukuyama, H., Ikeda, A., et al. (1999). Activities of the primary and supplementary motor areas increase in preparation and execution of voluntary muscle relaxation: an event-related fMRI study. *J Neurosci, 19*(9), 3527-3534.

Torre, P., 3rd, & Barlow, J. A. (2009). Age-related changes in acoustic characteristics of adult speech. *J Commun Disord, 42*(5), 324-333.

Vaillancourt, D. E., Mayka, M. A., Thulborn, K. R., & Corcos, D. M. (2004). Subthalamic nucleus and internal globus pallidus scale with the rate of change of force production in humans. *Neuroimage, 23*(1), 175-186.

Volz, K. G., Schubotz, R. I., & von Cramon, D. Y. (2005). Variants of uncertainty in decision-making and their neural correlates. *Brain Res Bull, 67*(5), 403-412.

Vul, E., Harris, C., Winkielman, P., & Pashler, H. (2009). Puzzlingly high correlations in fMRI studies of emotion, personality, and social cognition. *Perspectives on Psychological Science, 4*, 274-290.

Vul, E., & Kanwisher, N. (2010). Begging the question: The non-independence error in fMRI data analysis. In S. J. Hanson & M. Bunzl (Eds.), *Foundational issues for human brain mapping*. Cambridge: The MIT Press.

Wang, Q., Webber, R. M., & Stanley, G. B. (2010). Thalamic synchrony and the adaptive gating of information flow to cortex. *Nat Neurosci, 13*(12), 1534-1541.

Ward, N. S., Swayne, O. B., & Newton, J. M. (2008). Age-dependent changes in the neural correlates of force modulation: an fMRI study. *Neurobiol Aging, 29*(9), 1434-1446.

Warren, W. H. (2006). The dynamics of perception and action. *Psychol Rev, 113*(2), 358-389.

Wasson, P., Prodoehl, J., Coombes, S. A., Corcos, D. M., & Vaillancourt, D. E. (2010). Predicting grip force amplitude involves circuits in the anterior basal ganglia. *Neuroimage, 49*(4), 3230-3238.

Williamson, J. W., McColl, R., Mathews, D., Ginsburg, M., & Mitchell, J. H. (1999). Activation of the insular cortex is affected by the intensity of exercise. *J Appl Physiol, 87*(3), 1213-1219.

Williamson, J. W., McColl, R., Mathews, D., Mitchell, J. H., Raven, P. B., & Morgan, W. P. (2001). Hypnotic manipulation of effort sense during dynamic exercise: cardiovascular responses and brain activation. *J Appl Physiol, 90*(4), 1392-1399.

Wise, R. J., Greene, J., Buchel, C., & Scott, S. K. (1999). Brain regions involved in articulation. *Lancet, 353*(9158), 1057-1061.

Youmans, S. R., Youmans, G. L., & Stierwalt, J. A. (2009). Differences in tongue strength across age and gender: is there a diminished strength reserve? *Dysphagia, 24*(1), 57-65.

Zaehle, T., Schmidt, C. F., Meyer, M., Baumann, S., Baltes, C., Boesiger, P., et al. (2007). Comparison of "silent" clustered and sparse temporal fMRI acquisitions in tonal and speech perception tasks. *Neuroimage, 37*(4), 1195-1204.

Zwicker, J. G., Missiuna, C., Harris, S. R., & Boyd, L. A. (2010). Brain activation of children with developmental coordination disorder is different than peers. *Pediatrics, 126*(3), 678-686.